AIM OF THE WORK

The aim of this study is to develop theoretical and numerical tools to model interactions of x-rays with nanoparticles and to investigate the x-ray response of nanoparticles contrast agents for the purpose of enhancing imaging quality. Image contrast enhancement using nanoparticles will be compared to iodinated contrast media (CM) in different diagnostic investigations, x-ray, computed tomography (CT), ultrasound and magnetic resonance imaging.

MATERIALS AND METHODS

1- Radiological Instrumentations

1.1. X-ray Machine

A diagnostic radiography/fluoroscopy (R/F) (Philips duo-diagnost) x-ray machine with power (850 milliamp/second – 150 Kilovolt) which consists of the examination unit and the control room unit, was used to image all phantoms. At different powers for evaluation of the hounsienfield unit (HU) for each nanoparticle materials used in the study (GNPs, Fe_3O_4NP, Titanium NP, Cobalt NP, Nickel Oxide NP).

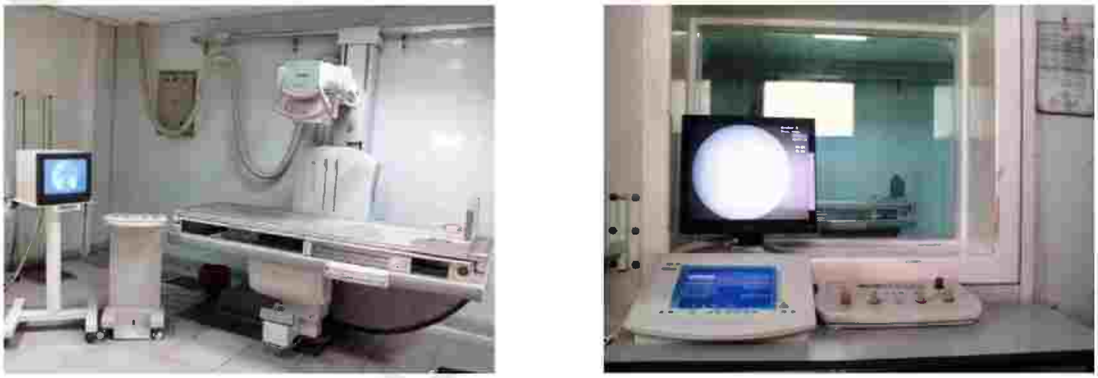

A B

Figure (13): Diagnostic radiography/fluoroscopy (R/F) (Philips duo-diagnost), A. scanning unit containing x-rat tube, movable table and a monitor, B. Control room unit containing computer, control board, computer and monitor

1.2. Computed Tomography (CT)

A Computed Tomography CT (GE high speed model zx/i) axial cuts was performed to all phantoms, for evaluation of the hounsienfield unit (HU) for each nanoparticle materials used in the study (GNPs, Fe_3O_4NP, Titanium NP, Cobalt NP, Nickel Oxide NP) the basic principle behind CT is that the internal structure of an object can be reconstructed from multiple projections of the object. It consists of gantry that contains (x-ray tube and detectors) table Figure 14, computer, operating console and automatic developer Figure 15.

Figure (14): Gantry and Table of the CT

Figure (15): Computer, operating system and automatic developer

1.2.1. Duel energy CT (GE) specifications

The general gantry specifications for a helical scanner is, aperture 65cm, tilt +/- 20 degree, tilt speed 1 degree/second, height to isocenter 90 cm, rotation speed 360 in 1.5,2,3,5 seconds.

The table specification for a single slice helical scanner, vertical range 40 to 90 cm, vertical elevation speed 17 mm/sec, maximum cradle travel 152 cm, cradle travel speed 20 to 100 mm/sec, table load capacity 205 kg. The operators console contains 1 monitor for patient information and technique selection, the control methods are mouse, trackball, Keyboard.

1.3. Ultrasound Machine

An ultrasound machine (Siemens Acuson x300), is used to image the different nanoparticles with different concentrations using 3.5 MHZ probe, this X300 system is a portable, digital diagnostic ultrasound imaging system. The system utilizes advanced imaging processing and transducer technology. The operating system is based on Windows technology. The system software supports standard applications, exam-specific imaging presets, measurements, pictograms, annotations, reports, worksheets, and system diagnostics. Operating modes for the system include: 2D-mode, Split mode, Dual-mode, 4B-mode, 2D/M-mode, M-mode. The system is equipped with a DIMAQ-IP integrated workstation. The workstation provides capabilities for digital acquisition, storage, and review of ultrasound studies. Additional system options provide integration into a networking environment.

A

B

Figure (16): A, B Siemens Acuson x300 ultrasound machine and its main components

1.4. Magnetic Resonance Imaging Machine (MRI)

The scanning procedure was done at Bright Scan Radiology Center, 6october city, the axis eighth district in front of metro market. A Neusoft Superstar 0.35T MRI machine model, the MRI knee coil was used in this study.

Superstar 0.35T MRI combines Philips' advanced technology with Neusoft Permanent Open Magnet. The Multi-Channel RF system and strong gradient configurations ensure advanced imaging capabilities, supporting a wide range of clinical applications.

Figure (17): Neusoft Superstar MRI machine model which contains 0.35Tesla magnet, knee coil and a movable table during the study

2. Nanoparticles

2.1. Gold Nanoparticles

Product name: PVP functionalized Gold Nanoparticles Brand: NT-Au NP Supplier: Nanotech Egypt for Photo-Electronics Communication Center.

2.1.1. Gold Nanoparticles Preparation

A gold nanoparticle has been prepared by chemical reduction method as reported by Turkevich. A solution of $HAuCl4$ has been used as $Au3+$ ions precursor, while sodium citrate has been used as both of mild reducing and stabilizing agent, the color of the solution slowly turned into faint pink color, indicating the reduction of the $Au3+$ ions to Au nanoparticles.

Figure (18): Colloidal gold with concentrations (0.1, 0.05, 0.025, 0.0125 and 0.00625 mg/ml)

2.1.2. Nanoparticles Characterization

Optical Properties: UV-Vis absorption spectra were obtained on an Ocean Optics USB2000+VIS-NIR Fiber optics spectrophotometer.

Particle diameter was carried out using electron microscope JEOL JEM-2100 high resolution transmission electron microscope at an accelerating voltage of 200 kV.

2.2. Iron Oxide Nanoparticles (Fe_3O_4)

Product name: Magnetite Iron (III) Oxide Nanoparticles Brand: NT- Fe_3O_4NP Supplier: NanoTech Egypt for Photo-Electronics Communication Center.

2.2.1. Iron Oxide Nanoparticles Preparation

Fe_3O_4 nanoparticles have been synthesized via co-precipitation method. This method based on alkaline co-precipitation of ferric and ferrous salts in aqueous solution. Briefly, two solutions containing Fe II and Fe III at a pre-determined concentration ratio were mixed followed by the addition of a base. Subsequently, the pH of the solution was carefully adjusted and a dispersing element was used to stabilize the particles. Figure (19)

Figure (19): Iron Oxide Nanoparticles (Fe_3O_4) with concentrations (0.2, 0.1, 0.05, 0.025, 0.0125, 0.00625 and 0.003125mg/ml)

2.2.2. Nanoparticles Characterization

Particle diameter was carried out using electron microscope JEOL JEM-2100 high resolution transmission electron microscope at an accelerating voltage of 200 kV.

2.3. Cobalt Oxide Nanoparticles

Product name: Cobalt Nanoparticles Brand: NT-Co NPs Supplier: NanoTech Egypt for Photo-Electronics Communication Center.

2.3.1. Cobalt Nanoparticles Preparation

Cobalt nanoparticles were prepared by the thermolysis of Co2 (CO) in hot toluene solutions using dichloro benzene as a reducing and capping agents, and dispersed in toluene.

2.3.2 Nanoparticles Characterization

Particle diameter was carried out using electron microscope JEOL JEM-2100 high resolution transmission electron microscope at an accelerating voltage of 200 kV, respectively.

2.4. Titanium Oxide Nanoparticles

Product name: Titanium Dioxide Nanoparticles Brand: NT-TD-NP Supplier: NanoTech Egypt for Photo-Electronics Communication Center.

2.4.1. Titanium Oxide Nanoparticles Preparation

Titanium Dioxide nanoparticles has been prepared by wet chemical method, they were successfully synthesized via sol–gel method using. Nanocrystalline titania powders were synthesized at room temperature (22 C) by a sol-gel method and using TiCl4 as a precursor with ethanol solution. After mixing for a specific duration, the gel solution was formed followed by aging. Then the sol-gel dried and calcined in a known temperature.

2.4.2. Nanoparticles Characterization

Particle diameter was carried out using electron microscope JEOL JEM-2100 high resolution transmission electron microscope at an accelerating voltage of 200 kV, respectively.

2.5. Nickel Nanoparticles

Product name: Nickel Nanoparticles Brand: NT-Ni NPs Supplier: NanoTech Egypt for Photo-Electronics Communication Center.

2.5.1. Nickel Nanoparticles Preparation

Nickel nanoparticles were prepared via chemical reduction method using a mild reducing agent (i.e. Sodium borohydride NaBH4), and sodium citrate as a capping agent.

2.5.3. Nanoparticles Characterization

Particle diameter was carried out using electron microscope JEOL JEM-2100 high resolution transmission electron microscope at an accelerating voltage of 200 kV, respectively.

3- Phantoms

3.1. Phantom One

To verify the ability of the nanoparticles (GNPs, Fe_3O_4NPs, Cobalt NPs, nickel and titanium) and conventional contrast media (ultravest) as an X-ray contrast agent, we constructed a phantom made of Plexiglas rectangle in shape with dimensions 14 X 18 cm and 1cm height, 70 cylindrical wells with dimensions 1 cm height and 1 cm diameter. (5 wells for each nanomaterial) were machined on this phantom. Each different concentrations of nanoparticles (0.11 mg/ml -0.051 mg/ml -0.0251 mg/ml -0.01251 mg/ml -0.006251 mg/ml) were embedded (Fig. 20).

The phantom imaged with radiological modalities (x-ray and CT). The Hounsfield unit where measured for each of these nanoparticles concentrations.

A B

Figure (20): A, Plexiglas rectangle, B, Plexiglas wells containing nanoparticles

3.2. Phantom Two

To verify the ability of the nanoparticles (GNPs, Fe_3O_4NPs) as an X-ray contrast agent, we constructed a phantom made of a plastic tubes which are represented as blood vessels with length 30 cm and diameter 3mm where filled with blood an then injected with gold and iron oxide nanoparticles during imaging using CT and conventional x-ray the HU unit where measured using X-ray Line and Millensys software figure (21).

Figure (21): Phantom 2, Plastic tubes filled with blood and injected with nanoparticles

3.3. Phantom Three

To verify the ability of the nanoparticles as a conventional x-ray, CT and MRI, we constructed a phantom made of 1 ml of the different nanoparticles used (Gold, Fe_3O_4, Cobalt, Nickel and Titanium) with different concentrations and mixed with 1ml of human blood and injected in aplastic tube with 1 cm diameter and 5cm height.

Figure (22): demonstrates the different nanoparticles mixed with blood

3.4. Phantom 4

To verify the ability of the nanoparticles as an CT and MRI we constructed a phantom made of 1 ml of nickel and titanium nanoparticles with different concentrations was mixed with 1 ml gel material in a plastic tube with 1 cm diameter and 5cm height.

A B

Figure (23): A,B demonstrates 1ml titanium and nickel nanoparticles with different concentrations (0.1,0.05,0.025,0.0125 and 0.00625 mg/ml) was mixed with 1ml gel material in a plastic tube with 1 cm diameter and 5 cm height.

3.5. Phantom Five

To verify the ability of the nanoparticles as an Ultrasound contrast agent, we constructed a phantom made of a plastic container which is filled with 350 ml of gel material and the test tube which containing the nanoparticles were placed at the bottom of this container figure (24) then imaged using linear ultrasound probe with power 7.5 MHZ in Longitudinal and transverse positions.

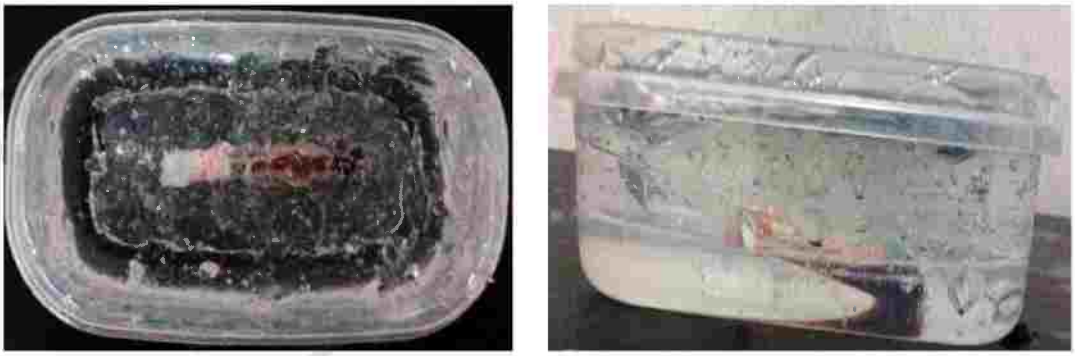

A B

Figure (24): A, B phantom 5 made up of a plastic container filled with gel material and the imaged nanomaterial were placed at its bottom

4- Pre Filling and Filling of Nanoparticles Protocol

1. Preparation of the contrast agent (nanomaterial's & conventional contrast agent.
2. Preparation of the phantom.
3. Fill the phantom with the contrast agent with different concentrations.
4. The phantom will be imaged under full scatter conditions in conventional x-ray, CT, MRI and ultrasound.
5. Evaluation of x-ray images, CT, MRI and ultrasound.
6. Create a full model using CST MICROWAVE STUDIO® (CST STUDIO) program to calculate the electric field distribution, effect of electromagnetic waves on nanomaterial's.

5. Theoretical Simulation

5.1. CST Microwave Studio

CST promotes Complete Technology for 3D EM, gives a great flexibility in tackling a wide application range through the variety of available solver technologies. Beside the flagship module, the broadly applicable Time Domain solver and the Frequency Domain solver, CST MWS offers further solver modules for our theoretical applications on nanoparticles.

RESULTS

1. Characterization of Nanoparticles

1.1. Gold Nanoparticles

1.1.1. TEM Transmission Electron Microscope

TEM analysis allows accurate measurement of particles average diameter results are shown in figure (25)

1.1.1.1. Absorption Spectra:

UV – Spectroscopy was used in the characterization of AuNPs. The results shown in figure (25)

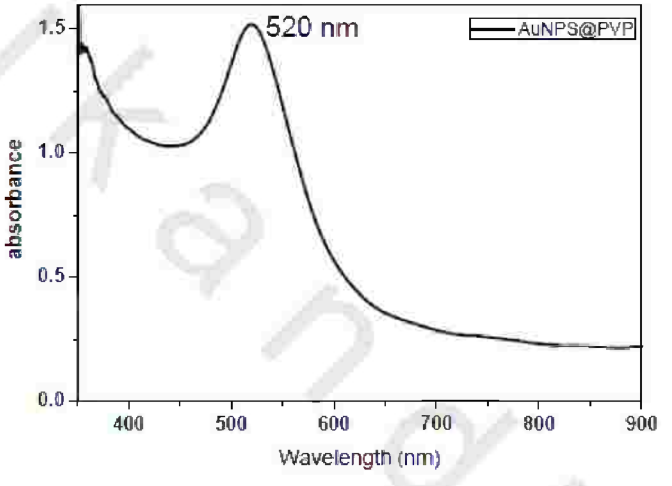

Figure (25): Absorption Spectrum of Au NPs

The prepared gold NPs show that UV-Vis absorption spectrum exhibited a single plasmon band at ~ 520 nm, indicative to formation of spherical gold NPs.

1.1.1.2. TEM micrographs

The TEM micrograph had been imaged by Nanotech Egypt for Photo-Electronics clearly and shows that, the prepared gold NPs has spherical diameter is ranging between 16 ± 5 nm.

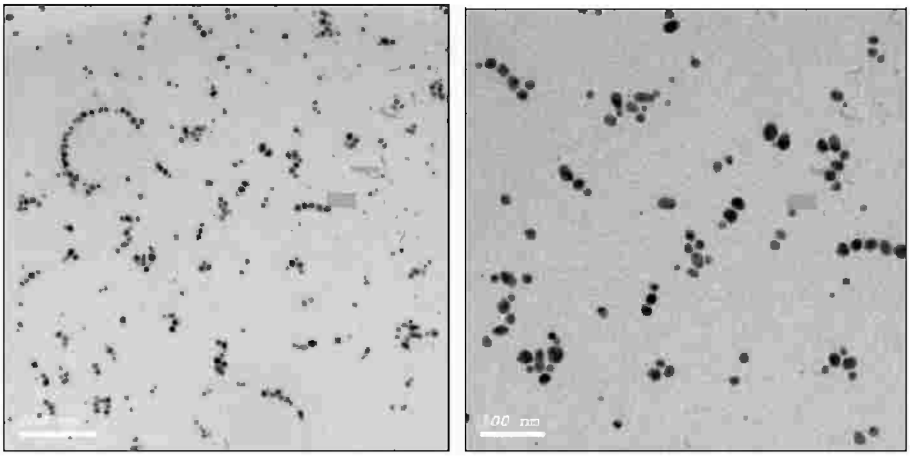

Figure (26): TEM micrograph of Au NPs

1.2. Iron Oxide Nanoparticles

1.2.1. TEM Transmission Electron Microscope

TEM analysis allows accurate measurement of particles average diameter results are shown in figure (27)

1.2.1.1. TEM micrographs

The TEM micrograph had been imaged by Nanotech Egypt for Photo-Electronics clearly and shows that, the prepared magnetite NPs has cubic-like shape and diameter is ranging between 17 ± 6 nm.

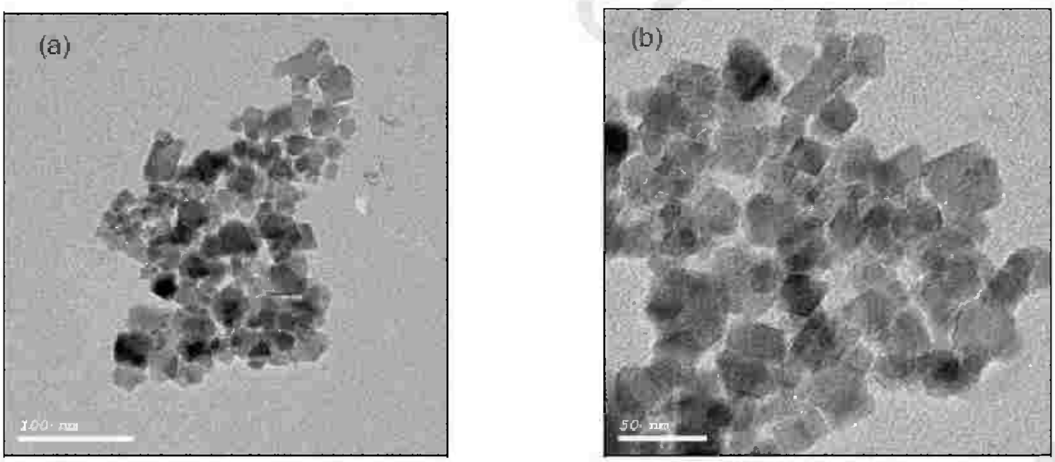

Figure (27): TEM micrograph of Magnetite Nanoparticles

1.3. Cobalt Oxide Nanoparticles

1.3.1. TEM Transmission Electron Microscope

TEM analysis allows accurate measurement of particles average diameter results are shown in figure (28)

1.3.1.1. TEM micrographs:

The TEM micrographs micrograph had been imaged by Nanotech Egypt for Photo-Electronics clearly and shows that, the as-prepared Co NPs has spherical-like shape and the average diameter was about 10 ± 5 nm

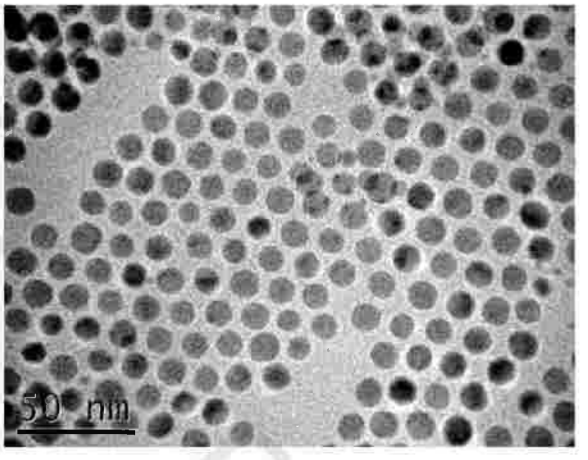

Figure (28): TEM micrograph of Co NPs

1.4. Titanium Oxide Nanoparticles

1.4.1. TEM Transmission Electron Microscope

TEM analysis allows accurate measurement of particles average diameter results are shown in figure (29)

2.4.1. TEM micrographs:

The TEM micrograph had been imaged by Nanotech Egypt for Photo-Electronics clearly and shows that, the prepared TiO2 NPs has mixture from spherical and hexagonal shapes and their diameter is about 33.7±10 nm.

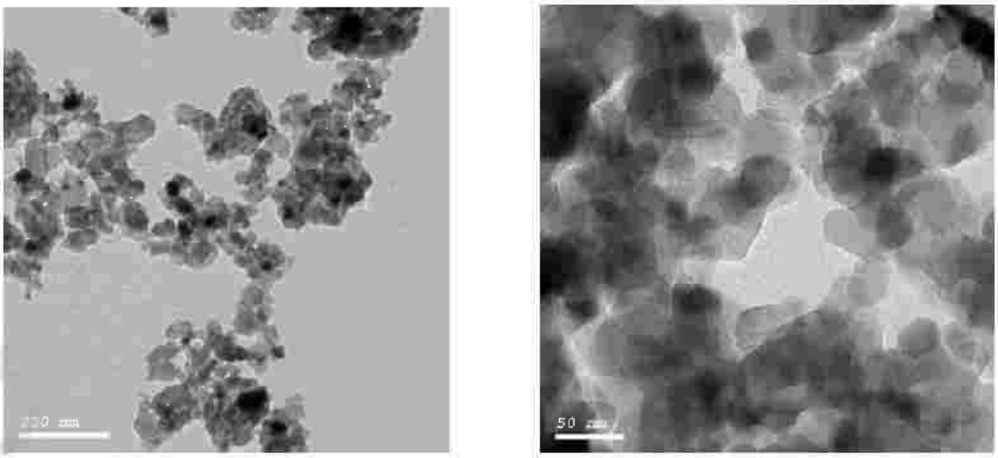

Figure (29): TEM micrograph of TiO2 NPs

1.5. Nickel Nanoparticles

1.5.1. TEM Transmission Electron Microscope

TEM analysis allows accurate measurement of particles average diameter results are shown in figure (30)

2.5.1. TEM micrographs:

The TEM micrograph had been imaged by Nanotech Egypt for Photo-Electronics clearly and shows that, the prepared NT-Ni NPs has mixture from Spherical-like shape and their diameter is up to 28 nm.

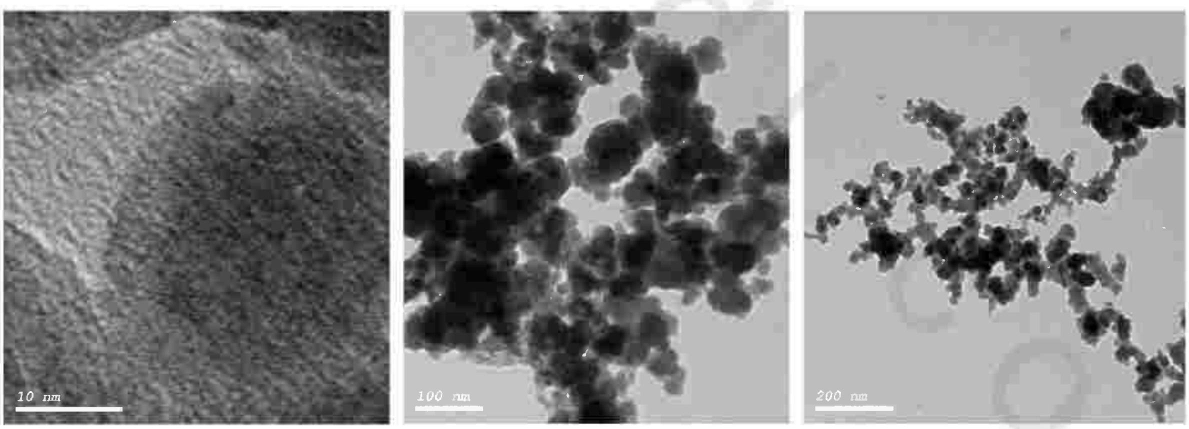

A B C

Figure (30): A,B,C, TEM micrograph of NT-Ni NPs

2. Experiment One

2.1. Phantom one

It is made up of Plexiglas rectangle in shape with dimensions 14 X 18 cm and 1cm height, 70 cylindrical wells with dimensions 1 cm height and 1 cm diameter. (5 wells for each nanomaterial) were machined on this phantom. Each different concentrations of nanoparticles (0.11 mg/ml -0.051 mg/ml -0.0251 mg/ml -0.01251 mg/ml -0.006251 mg/ml) were embedded then scanned in October 6 university, radiology department using (GE high speed model zx/i) Computed tomography (CT) machine with power 120 KV and 100 mAs with slice thickness 2 mm, zooming 1.25X, DFOV: 20.0x 20.0 cm and the Hounsfield unit (HU) had been measured.

2.2. CT Examination

2.2.1. CT imaging of Gold & Iron oxide nanoparticles

A CT axial cuts was performed for the phantom that contains nanoparticles diluted with water and the Hounsfield unit (HU) was measured for each of them.

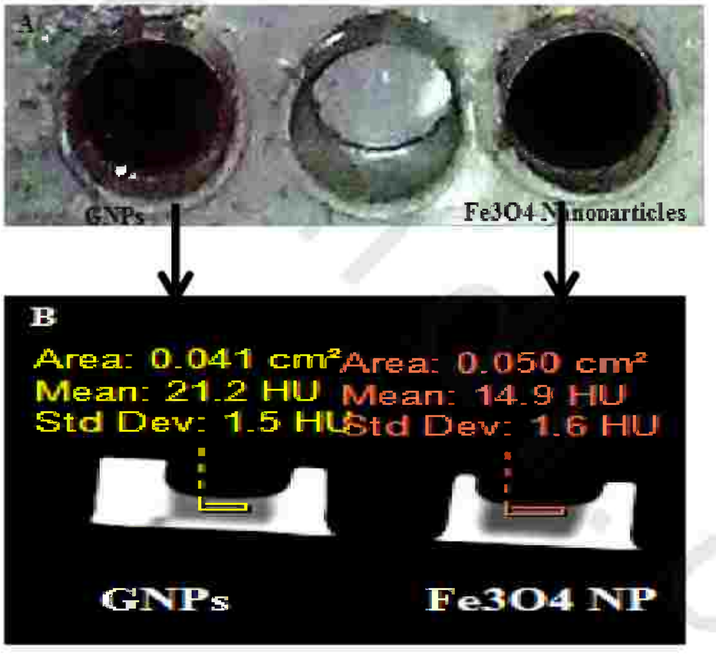

Figure (31): (A) demonstrates Phantom one: made up of Pyrex material, (B) shows the hounsienfield measurements in CT axial image of GNPs & Fe_3O_4 with concentration 0.1 mg/ml

Figure (32): (A) demonstrates Phantom one: made up of Pyrex material, (B) shows the hounsienfield measurements in CT axial image of GNPs & Fe_3O_4 with concentration 0.05mg/m.L

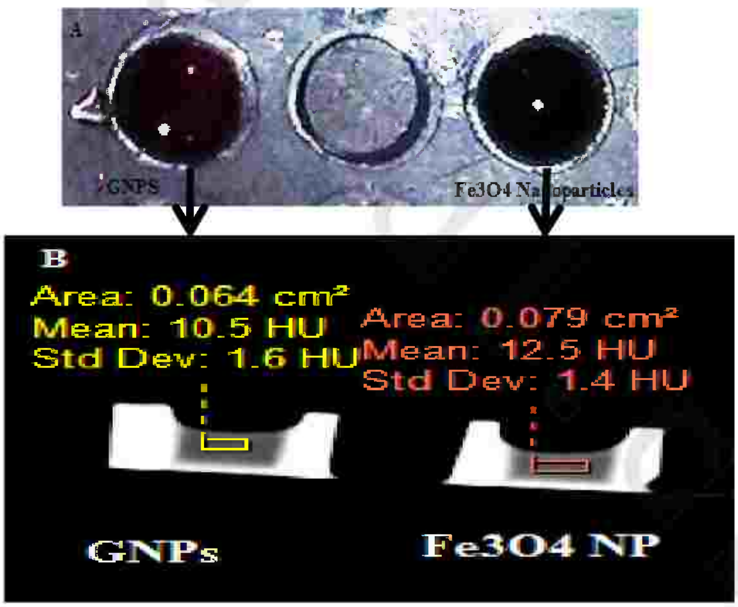

Figure (33): (A) demonstrates Phantom one: made up of Pyrex material, (B) shows the hounsienfield measurements in CT axial image of GNPs & Fe_3O_4 with concentration 0.025 mg/ml

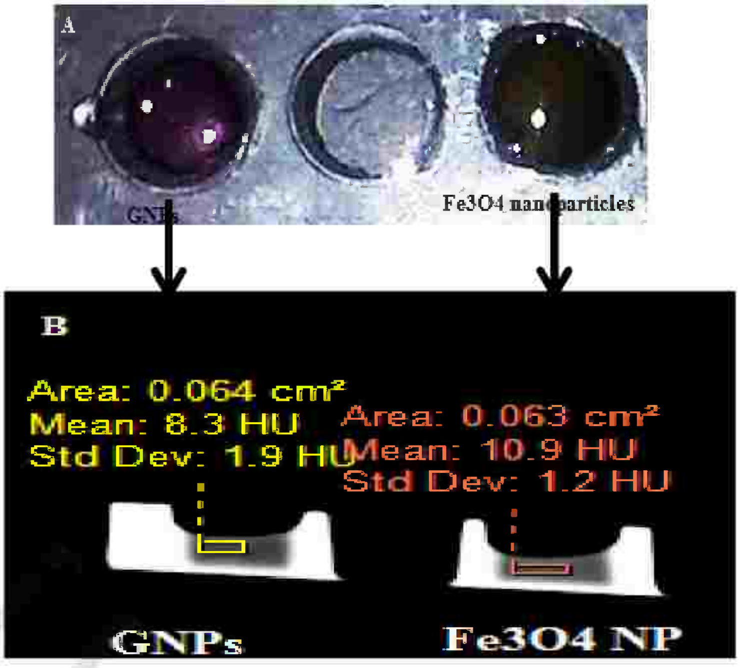

Figure (34): (A) demonstrates Phantom one: made up of Pyrex material, (B) shows the hounsienfield measurements in CT axial image of GNPs & Fe_3O_4 with concentration 0.0125 mg/ml

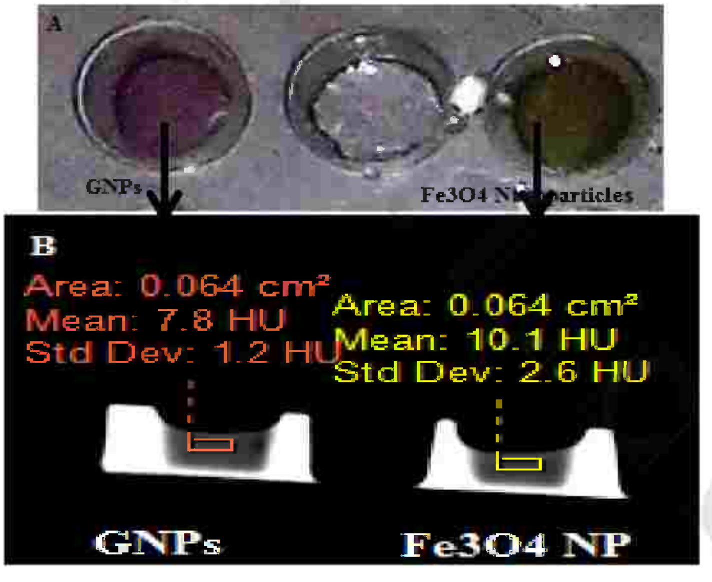

Figure (35): (A) demonstrates Phantom one: made up of Pyrex material, (B) shows the hounsienfield measurements in CT axial image of GNPs & Fe_3O_4 with concentration 0.0625 mg/ml

Table (2): Hounsfield units (HU) measured for different concentrations of gold and iron oxide nanoparticles in CT images

Concentration (mg/ml)	HU of GNPs	HU of Fe_3O_4
0.10000	21.2	14.9
0.05000	13.6	13.8
0.02500	10.5	12.5
0.01250	8.3	10.9
0.00625	7.8	8.5

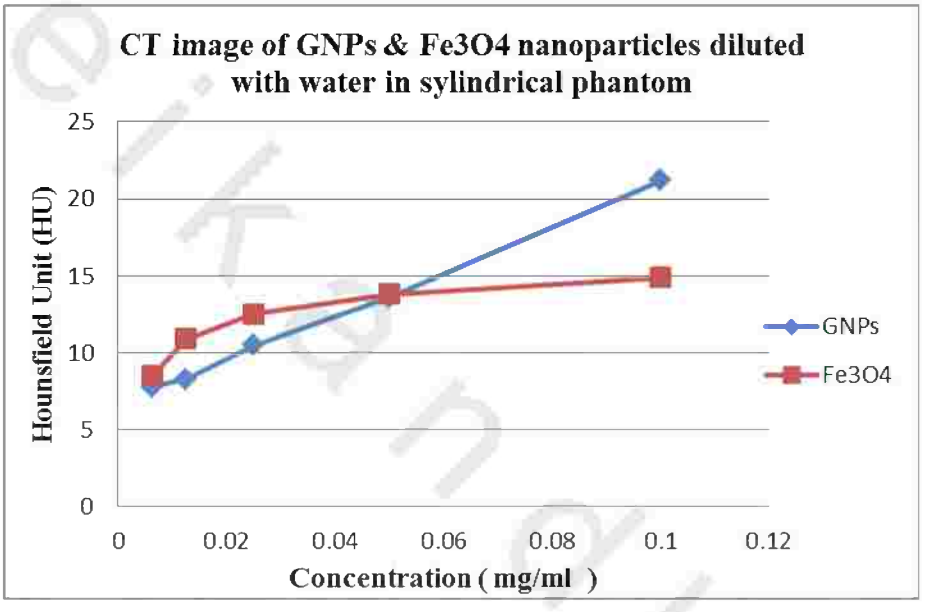

Figure (36): Variations in measured HU with different concentration of GNPs& Fe_3O_4 nanoparticles in CT images

2.2.2. CT imaging of Cobalt nanoparticles

The cobalt NPs imaged was diluted in distal water

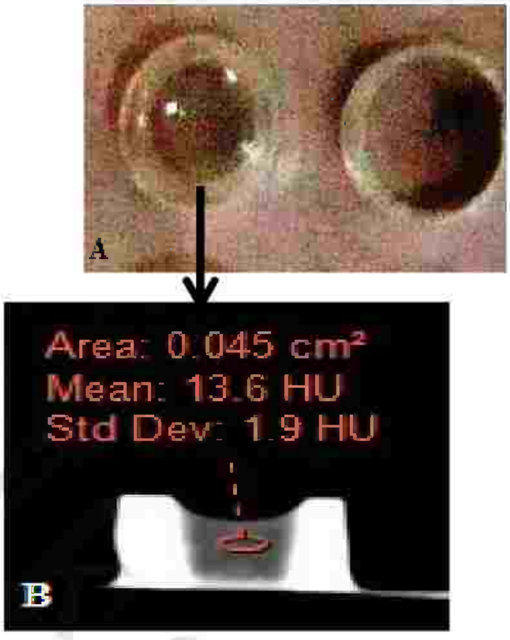

Figure (37): (A) demonstrates Phantom one: made up of Pyrex material filled with cobalt NPs, (B) shows the hounsienfield measurements in CT axial image of cobalt NPs with concentration 0.1 mg/ml

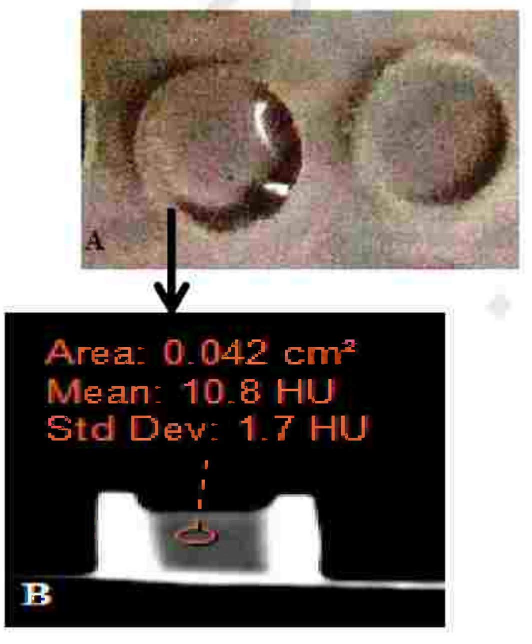

Figure (38): (A) demonstrates Phantom one: made up of Pyrex material filled with cobalt NPs, (B) shows the hounsienfield measurements in CT axial image of cobalt NPs with concentration 0.05 mg/ml

Figure (39): (A) demonstrates Phantom one: made up of Pyrex material filled with cobalt NPs, (B) shows the hounsienfield measurements in CT axial image of cobalt NPs with concentration 0.025 mg/ml

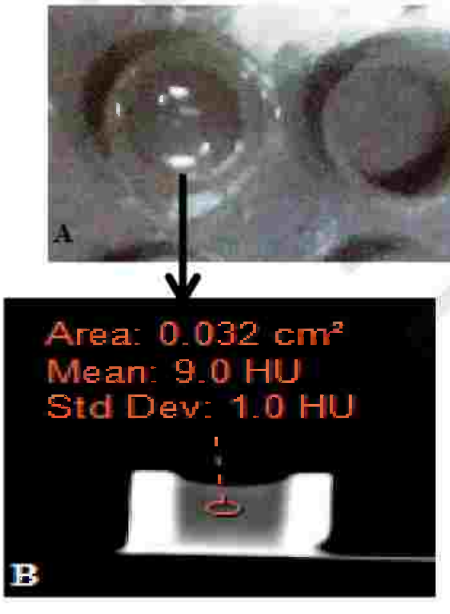

Figure (40): (A) demonstrates Phantom one: made up of Pyrex material filled with cobalt NPs, (B) shows the hounsienfield measurements in CT axial image of cobalt NPs with concentration 0.0125 mg/ml

Figure (41): (A) demonstrates Phantom one: made up of Pyrex material filled with cobalt NPs, (B) shows the hounsienfield measurements in CT axial image of cobalt NPs with concentration 0.00625 mg/ml

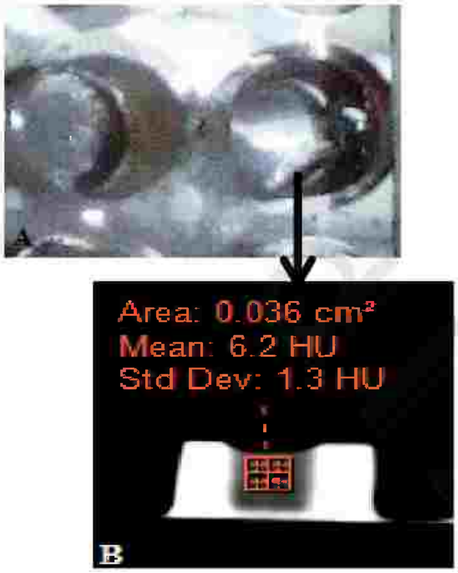

Figure (42): (A) demonstrates Phantom one: made up of Pyrex material filled with cobalt NPs, (B) shows the hounsienfield measurements in CT axial image of cobalt NPs with concentration 0.003125 mg/ml

Table (3) Hounsfield units (HU) measured for different concentrations of cobalt nanoparticles in CT images

Concentration (mg/ml)	HU measurement of Cobalt NPs
0.10000	13.6
0.05000	10.8
0.02500	9.4
0.01250	9
0.00625	8
0.00312	6.2

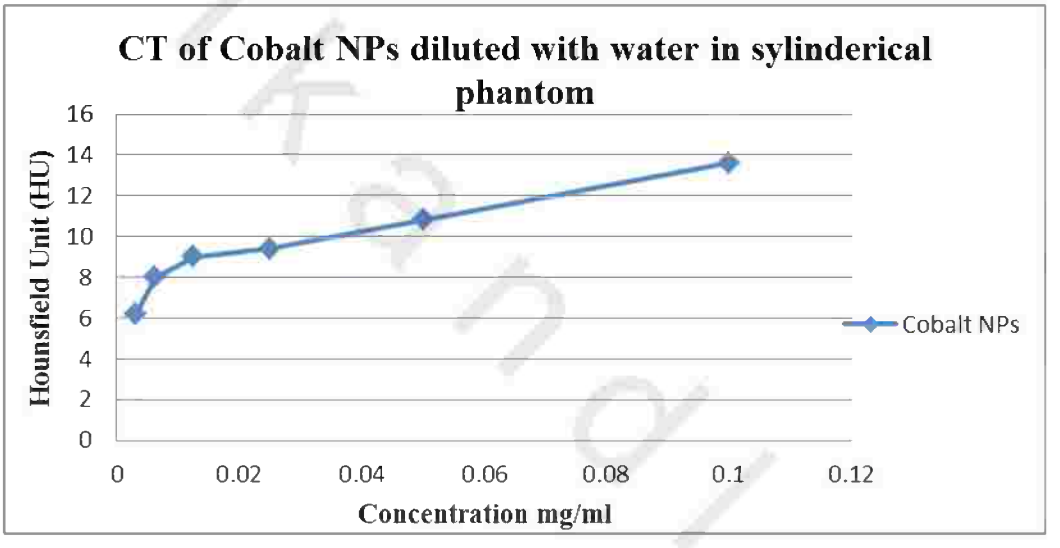

Figure (43): Variations in measured HU with different concentration of cobalt nanoparticles in CT images

2.2.3. Gold, Fe_3O_4 and cobalt nanoparticles

Table (4) HU measurements for Gold, Fe_3O_4 and cobalt nanoparticles

Concentration (mg/ml)	GNPs	Fe_3O_4NPs	Cobalt NPs
0.10000	21.2	14.9	13.6
0.05000	13.6	13.8	10.8
0.02500	10.5	12.5	9.4
0.01250	8.3	10.9	9
0.00625	7.8	8.5	8

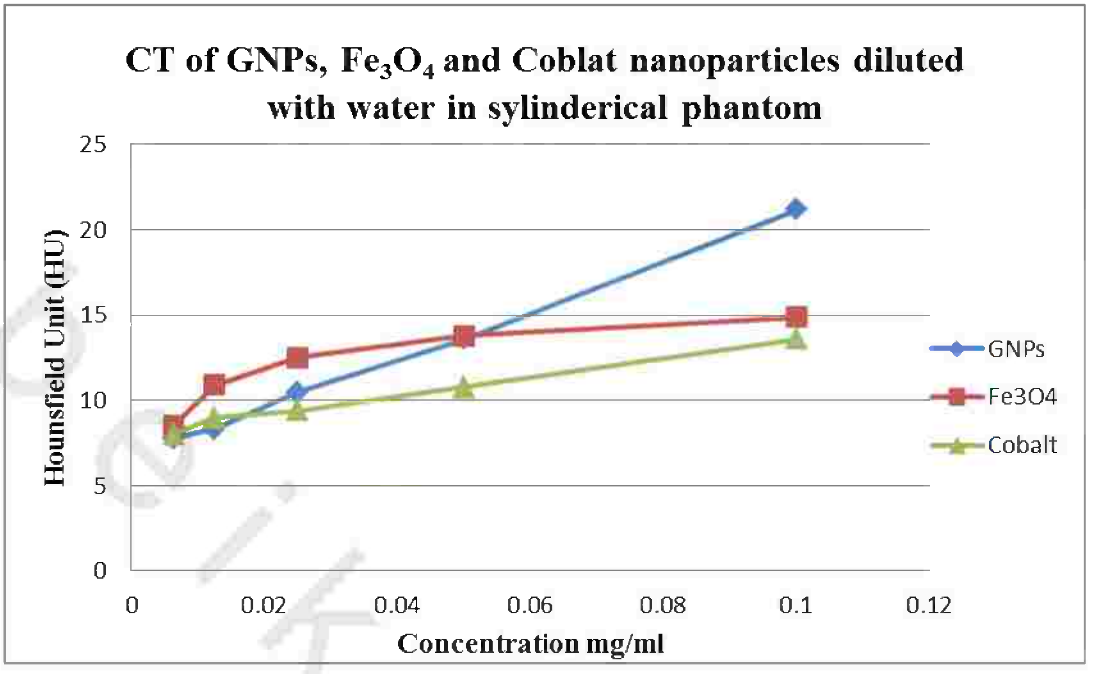

Figure (44): Variations in measured HU with different concentration of Gold, Fe_3O_4 and cobalt nanoparticles in CT images

2.3. X-ray Examination

An Anterior posterior (AP) view was performed for the phantom that contains nanoparticles diluted with water and the hounsfield unit (HU) was measured for each of them.

2.3.1. X-ray imaging of Gold nanoparticles diluted in water

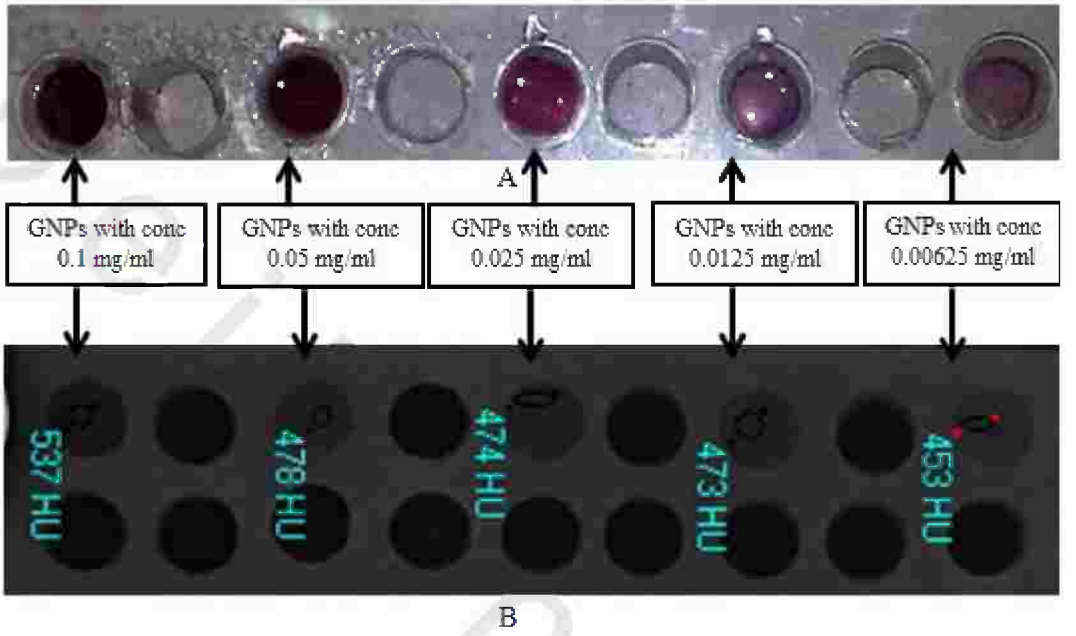

Figure (45): Measurement of HU of GNPs nanoparticles with different concentrations (0.1 mg/ml -0.05 mg/ml -0.025 mg/ml -0.0125 mg/ml -0.00625 mg/ml) using 46 KV and 5 mAs in x-ray image anterior posterior (AP) view

Table (5) Hounsfield units (HU) measured for different concentrations of gold nanoparticles in X-ray images

Concentration (mg/ml)	HU of GNPs
0.10000	537
0.05000	478
0.02500	474
0.01250	473
0.00625	453

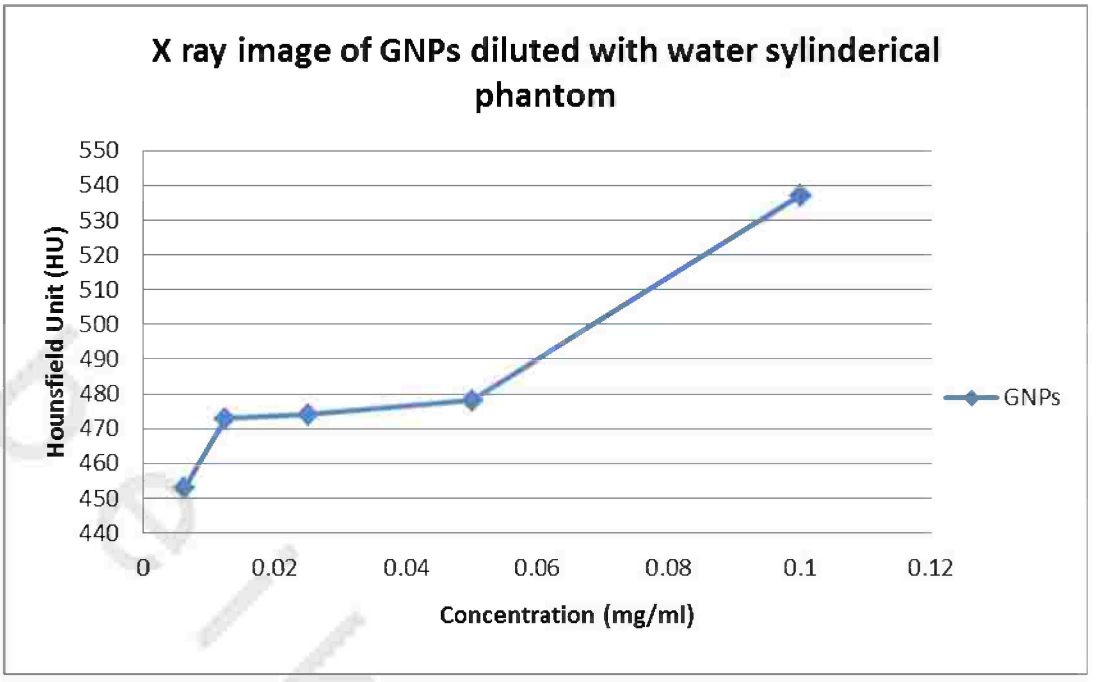

Figure (46): Measured HU with different concentration of GNPs in (AP) x-ray images using 46 Kv and 5 mAs.

2.3.2. X-ray imaging of iron oxide (Fe_3O_4) NPs diluted in water

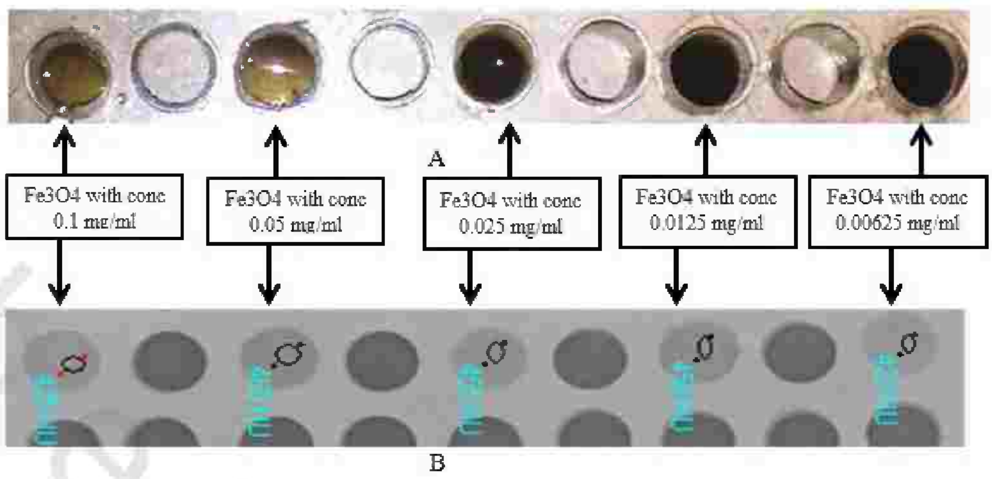

Figure (47): A. five Pyrex tubes of a 1 cm diameter and 1 cm height felled with Fe_3O_4 nanoparticles. b. Measurement of HU of Fe_3O_4 nanoparticles with different concentrations (0.1 mg/ml -0.05 mg/ml -0.025 mg/ml -0.0125 mg/ml -0.00625 mg/ml) using 46 KV and 5 mAs in x-ray image anterior posterior (AP) view

Table (6) HU measurements for different concentrations of Fe_3O_4 nanoparticles in X-ray images

Concentration (mg/ml)	HU of Fe_3O_4NPs
0.10000	435
0.05000	465
0.02500	455
0.01250	454
0.00625	428

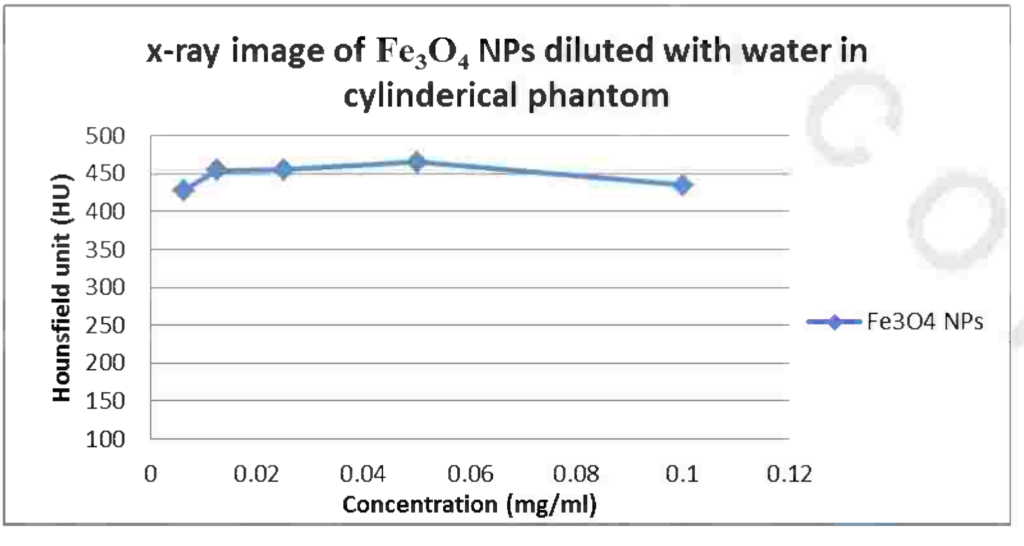

Figure (48): Measured HU with different concentration of Fe_3O_4 NPs in (AP) x-ray images using 46 Kv and 5 mAs.

2.3.3. X-ray imaging of cobalt NPs diluted in water

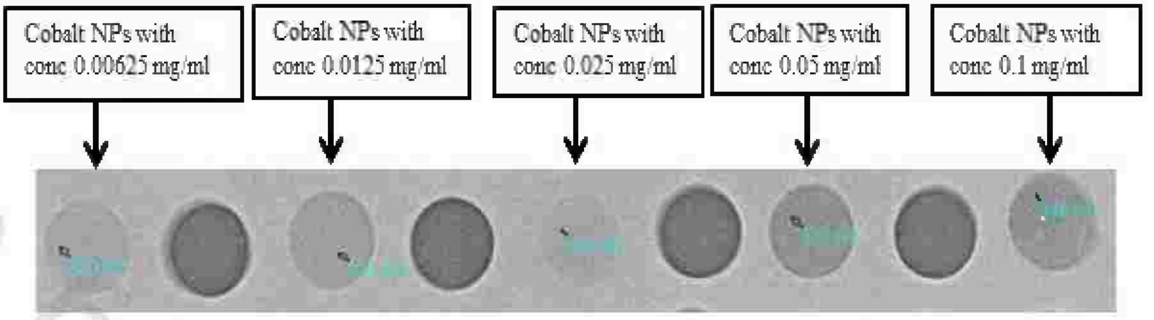

Figure (49): measurement of HU of cobalt NPs with different concentrations ((0.1 mg/ml - 0.05 mg/ml -0.025 mg/ml -0.0125 mg/ml -0.00625 mg/ml) using 46 KV and 5 mAs in x-ray image anterior posterior (AP) view

Table (7) HU measurements for different concentrations of cobalt NPs in X-ray images

Concentration (mg/ml)	HU of cobalt NPs
0.10000	448
0.05000	439
0.02500	378
0.01250	372
0.00625	360

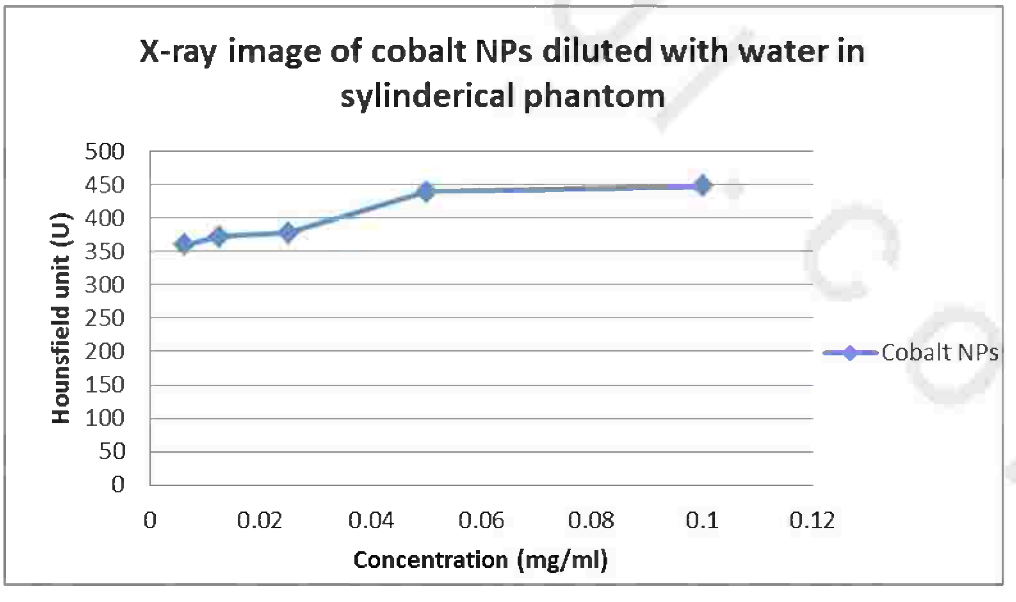

Figure (50): Measured HU with different concentration of cobalt NPs in (AP) x-ray images using 46 Kv and 5 mAs.

2.3.4. X-ray imaging of conventional contrast media (ultravest)

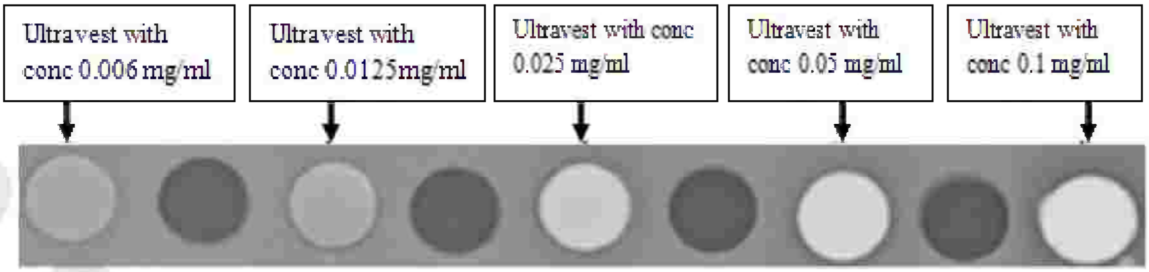

Figure (51): Measurement of HU of ultravest contrast media with different concentrations (0.1 mg/ml, 0.05 mg/ml, 0.025 mg/ml, 0.0125 mg/ml, 0.00625 mg/ml) using 46 KV and 5 mAs in x-ray image anterior posterior (AP) view.

Table (8) HU measurements for different concentrations of ultravest contrast media in X-ray images

Concentration (mg/ml)	HU of ultravest contrast media
0.10000	462
0.05000	400
0.02500	376
0.01250	264
0.00625	188

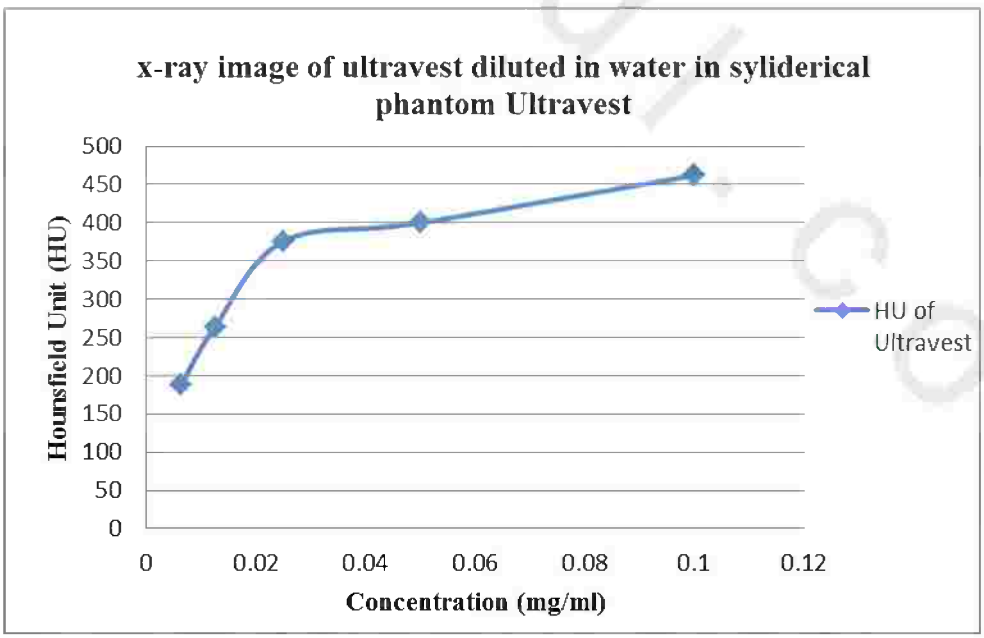

Figure (52): Measured HU with different concentration of ultravest contrast media in (AP) x-ray images using 46 Kv and 5 mAs.

2.3.5. Gold nanoparticles and Ultravest contrast media

Table (9) HU measurements for Gold nanoparticles and Ultravest contrast media in x-ray images

Concentration (mg/ml)	HU measurement for Ultravest contrast media	HU measurement GNPs
0.10000	462	537
0.05000	400	478
0.02500	376	474
0.01250	264	473
0.00625	188	453

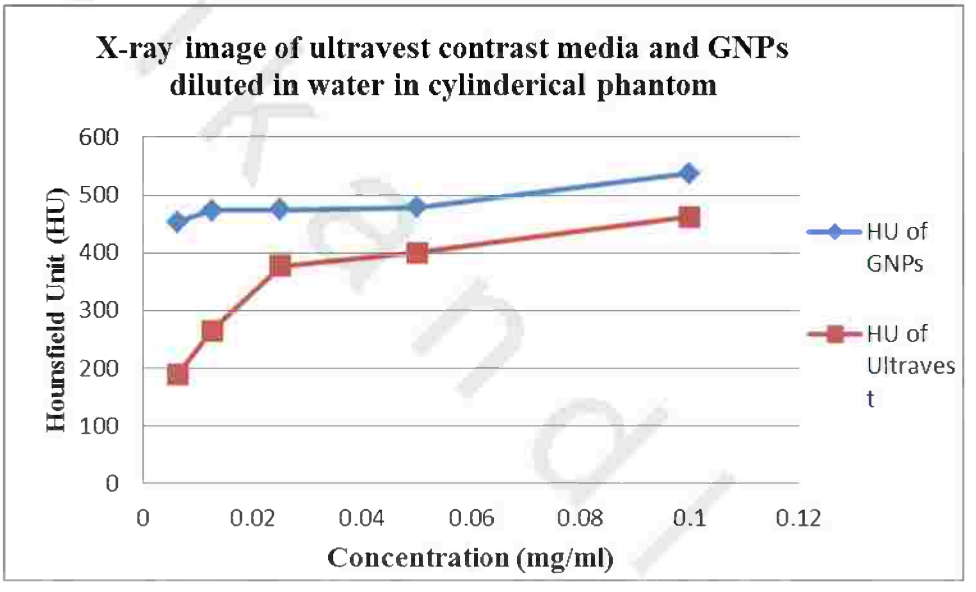

Figure (53): Variations in measured HU with different concentration of Gold NPs and Ultravest contrast media in x-ray images

2.3.6. Iron Oxide nanoparticles and Ultravest contrast media

Table (10) HU measurements for Iron Oxide nanoparticles and Ultravest contrast media in x-ray images

Concentration (mg/ml)	HU measurement Ultravest contrast media	HU measurement Fe_3O_4 NPs
0.10000	462	435
0.05000	400	465
0.02500	376	455
0.01250	264	454
0.00625	188	428

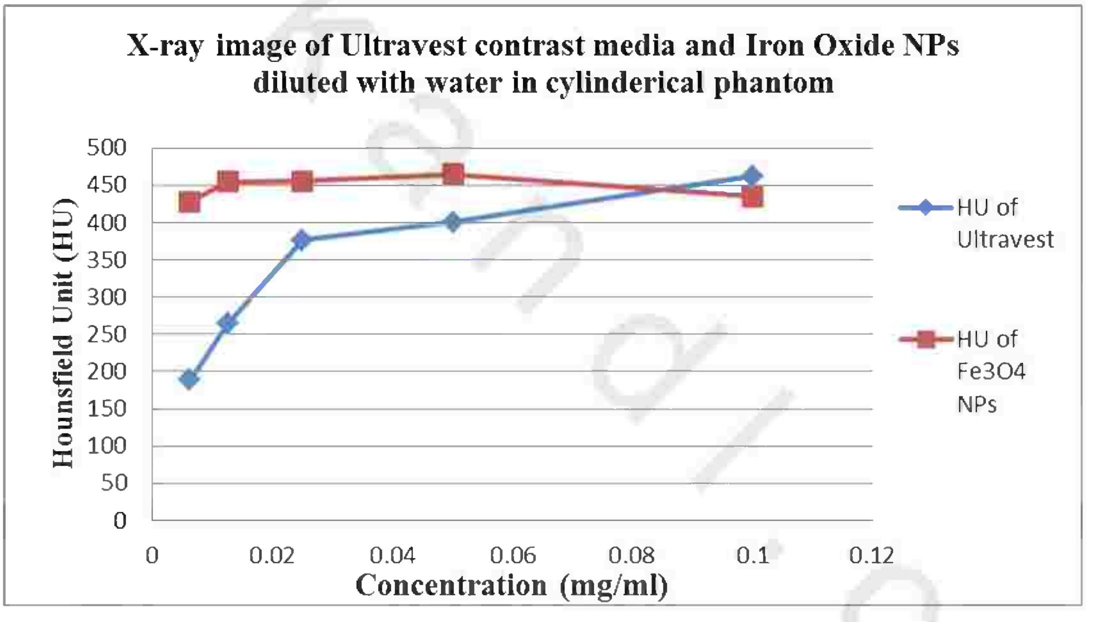

Figure (54): Variations in HU measurements of x-ray images between Ultravest contrast media and Iron Oxide nanoparticles

2.3.7. Cobalt nanoparticles and Ultravest contrast media

Table (11) HU measurements for Cobalt nanoparticles and Ultravest contrast media in x-ray images

Concentration (mg/ml)	HU measurements Ultravest contrast media	HU measurements Cobalt NPs
0.10000	462	13.6
0.05000	400	10.8
0.02500	376	9.4
0.01250	264	9
0.00625	188	8

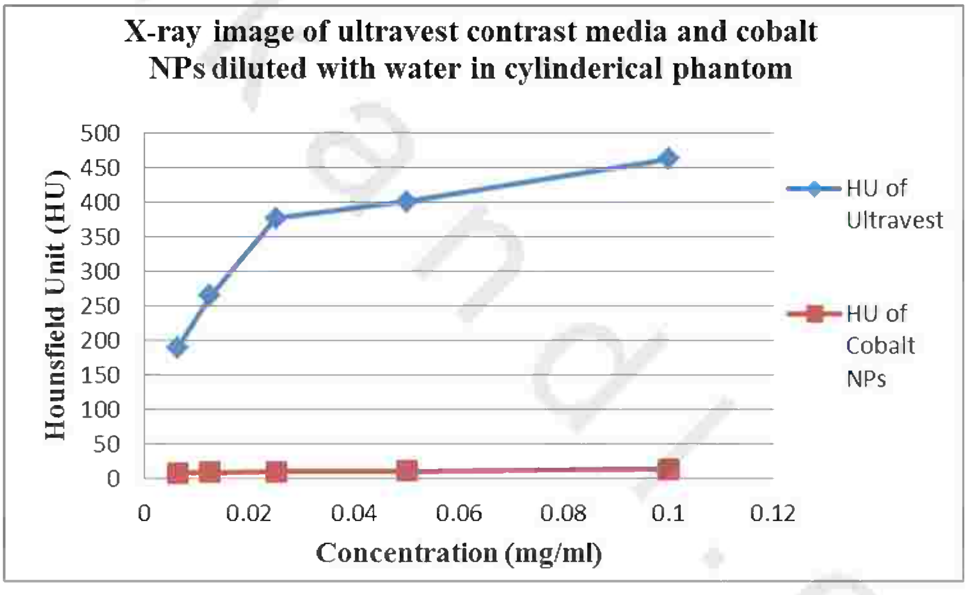

Figure (55): Variations in HU measurements of x-ray images between Ultravest contrast media and Cobalt nanoparticles

2.3.8. HU measurement of Gold, Fe_3O_4 and Cobalt nanoparticles images

Table (12) HU values for between GNPs, Iron oxide and Cobalt nanoparticles

Concentration (mg/ml)	HU of GNPs	HU of Fe_3O_4 NPs	HU of Cobalt NPs
0.10000	537	435	13.6
0.05000	478	465	10.8
0.025000	474	455	9.4
0.0125	473	454	9
0.00625	453	428	8

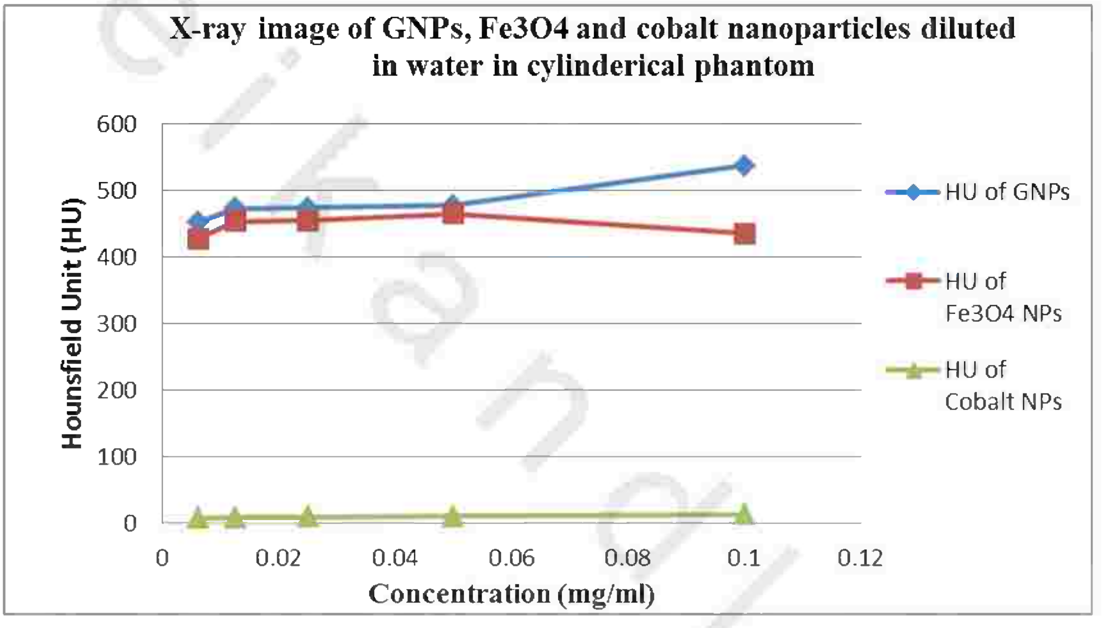

Figure (56): Variations in HU measurements of x-ray images between GNPs, Iron oxide and Cobalt nanoparticles

3. Experiment two

3.1. Phantom two

This phantom is made up of multiple tubes with 30 cm long and diameter 3 ml each tube is filled with blood and had been injected with different concentrations of gold and iron oxide nanoparticles (0.1 mg/ml -0.05 mg/ml -0.025 mg/ml -0.0125 mg/ml), then scanned in October 6 university, radiology department using (GE high speed model zx/i) Computed tomography (CT) machine with power 120 KV and 100 mAs and the hounsienfield unit (HU) had been measured.

Figure (57): Phantom two: made up multiple tubes with 30cm long and diameter 3ml each tube is filled with blood and had been injected with different concentrations of gold and iron oxide nanoparticles

3.2. CT Examination for GNPs & Fe_3O_4 nanoparticles

A CT axial cuts was performed for all tubes that contains nanoparticles that contains blood and injected with different concentrations on nanoparticles and the hounsfield unit (HU) was measured for each of them

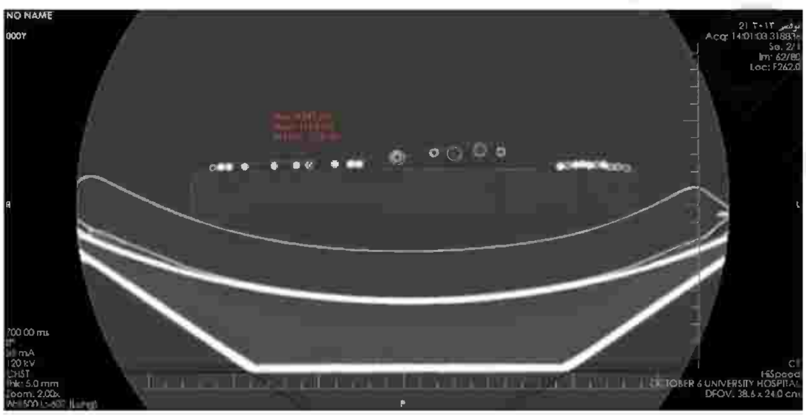

Figure (58): CT Image 1 with concentration (0.1 ml of GNPs)

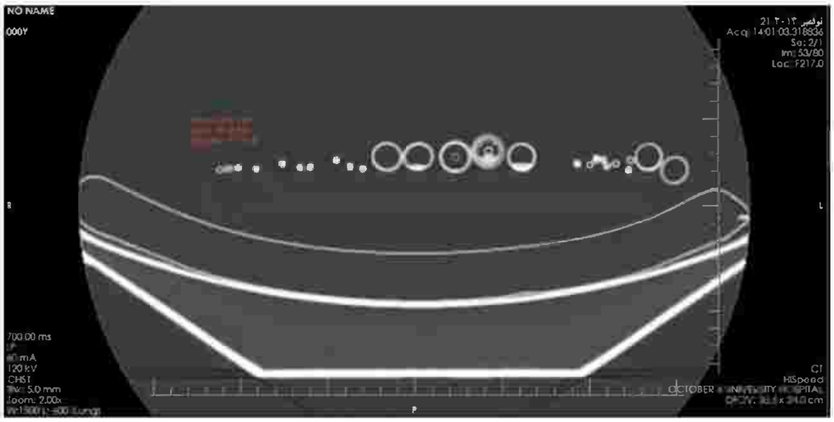

Figure (59): CT Image 1 with concentration (0.1 ml of Fe_3O_4 nanoparticles)

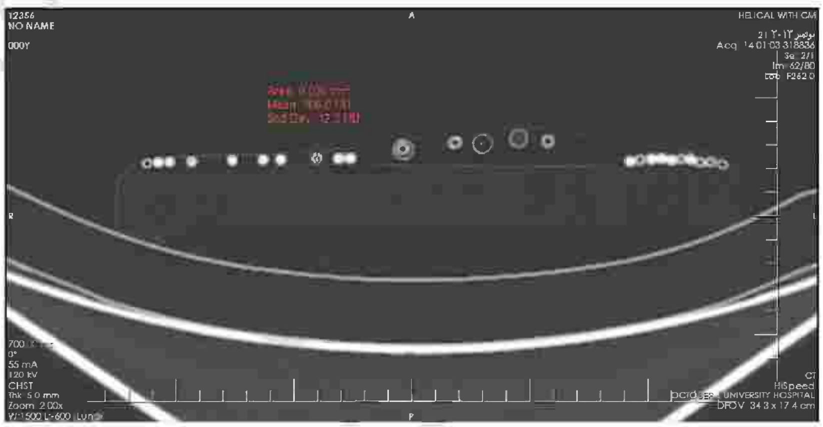

Figure (60): CT Image 2 with concentration (0.05ml of GNPs)

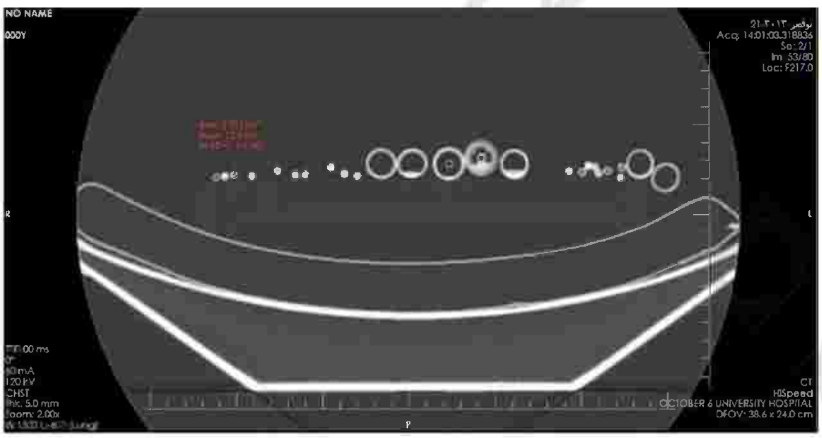

Figure (61): CT Image 2 with concentration (0.05 ml of Fe_3O_4 nanoparticles)

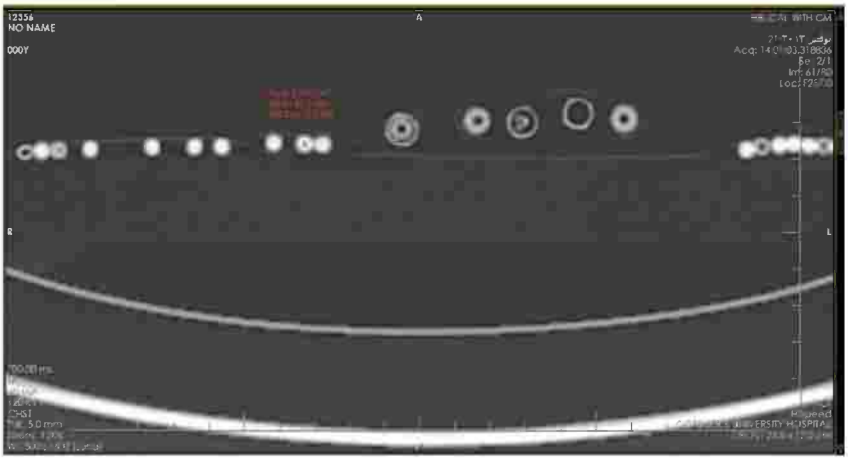

Figure (62): CT Image 3 with concentration (0.025 ml of GNPs)

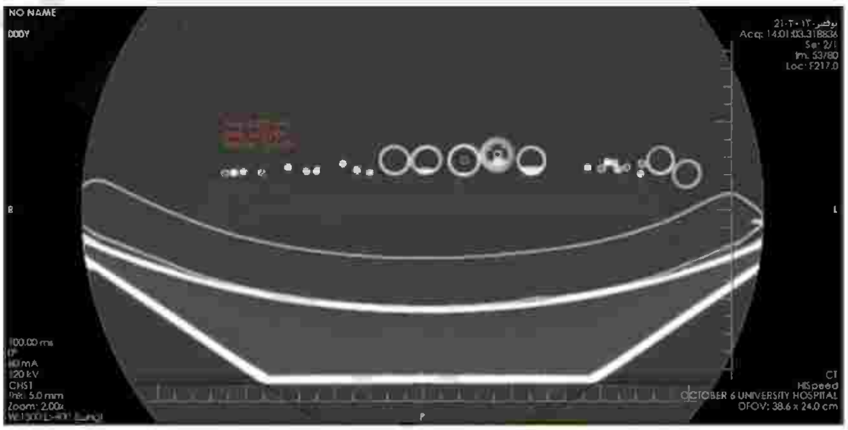

Figure (63): CT Image 3 with concentration (0.025 ml of Fe_3O_4 nanoparticles)

Figure (64): CT Image 4 with concentration (0.0125 ml of GNPs)

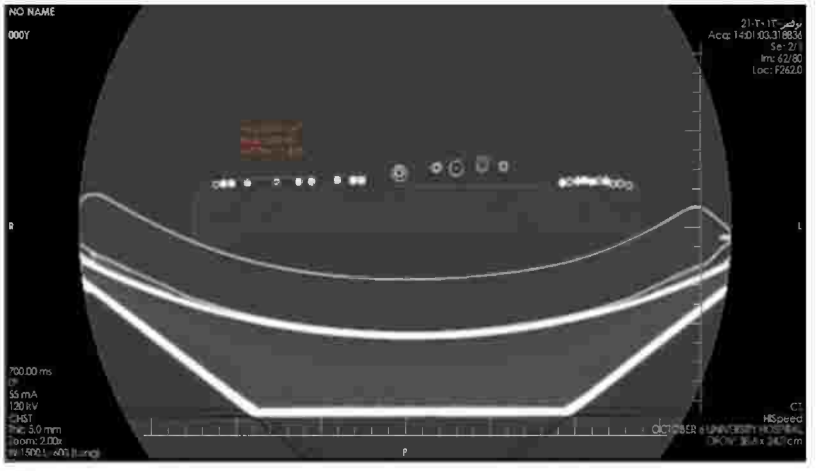

Figure (65): CT Image 4 with concentration (0.0125 ml of Fe_3O_4 nanoparticles)

Table (13) HU values for different concentrations of gold and iron oxide nanoparticles mixed with blood in CT images.

Concentration (mg/ml)	HU of GNPs	HU of Fe3O4
0.1000	114.3	85
0.0500	106	73.6
0.0250	93.5	67
0.0125	77.5	54.9

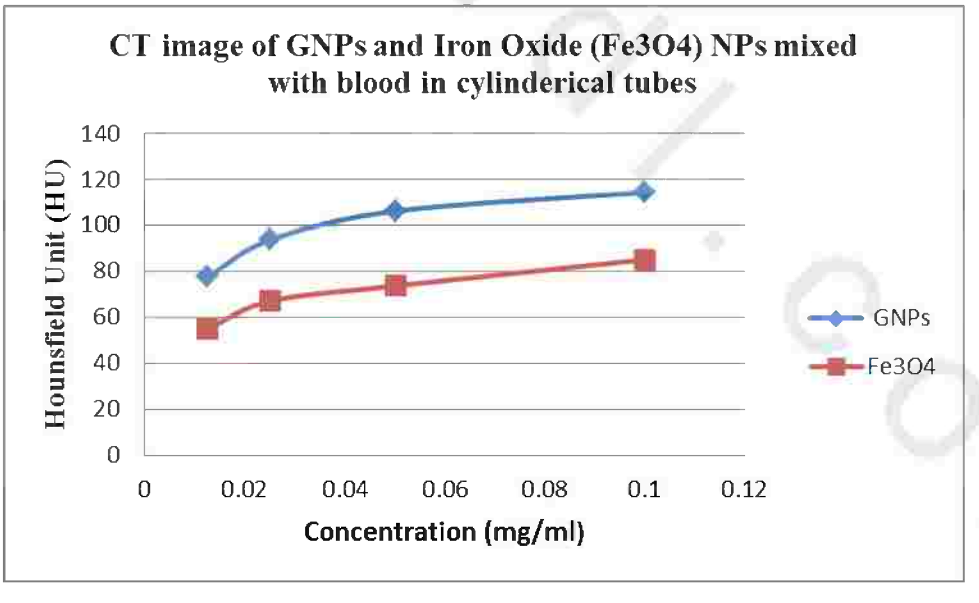

Figure (66): Variations in measured HU with different concentration of GNPs& Fe_3O_4 nanoparticles mixed with blood in CT images

3.3. X-ray images

An anterior posterior (AP) view was performed for all tubes that contains nanoparticles that contains blood and injected with different concentrations on nanoparticles and the hounsfield unit (HU) was measured for each of them.

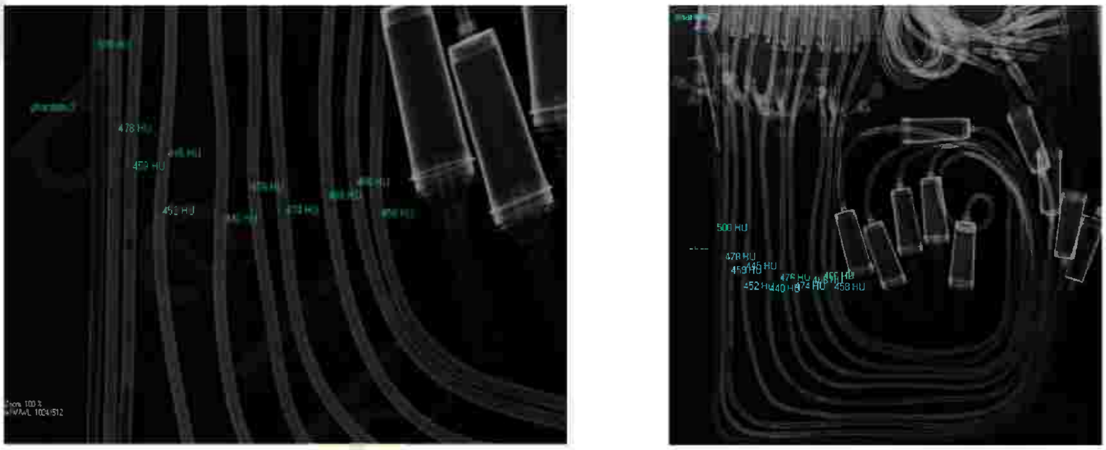

A B

Figure (67): A,B, shows the measurement of HU of GNPs and iron oxide nanoparticles with different concentrations (0.1 mg/ml -0.05 mg/ml -0.025 mg/ml -0.0125 mg/ml -0.00625 mg/ml) in x-ray image

Table (14) HU values for different concentrations of gold and iron oxide nanoparticles in X-ray images

Concentration (mg/ml)	HU of GNPs	HU of Fe3O4
0.10000	500	476
0.05000	478	474
0.02500	459	468
0.01250	445	465
0.00625	440	458

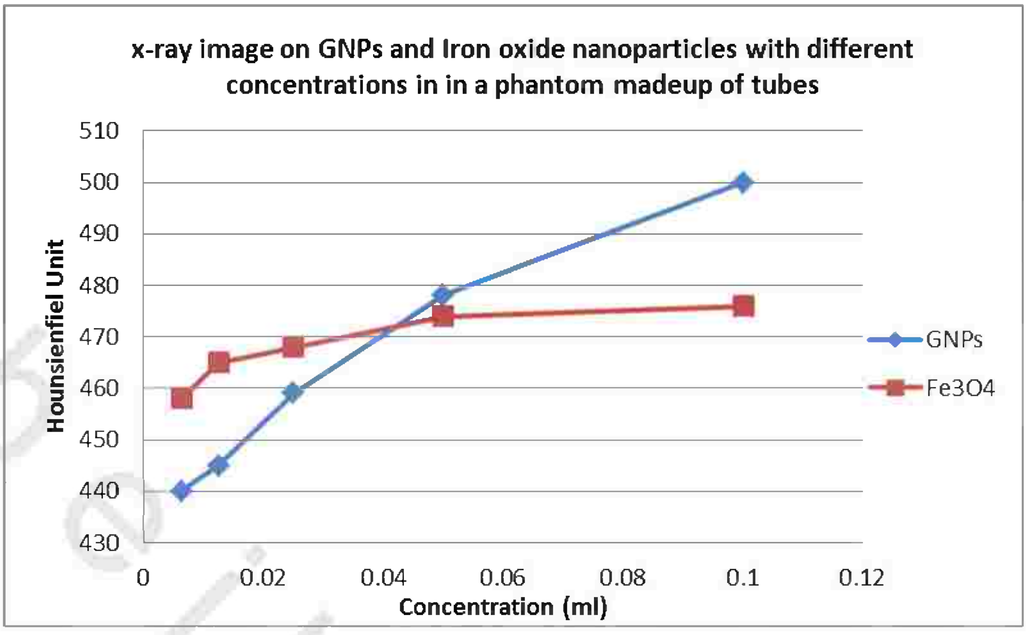

Figure (68): Variations in measured HU with different concentration of GNPs& Fe_3O_4 nanoparticles in x-ray images AP view.

4. Experiment Three

4.1. Phantom three

1 ml of the different nanoparticles (Gold, Fe_3O_4,Cobalt,Nickal and Titanium) with different concentrations (0.1, 0.051,0.0251, 0.01251 and 0.006251 mg/ml) was mixed with 1ml of human blood and injected in aplastic tube with 1cm diameter and 5cm height, then scanned with conventional x-ray, CT, MRI and Ultrasound.

A

B C

Figure (69): A, B, C, Demonstrates the different Nanoparticles mixed with blood

4.2. CT Examination of Nanoparticles

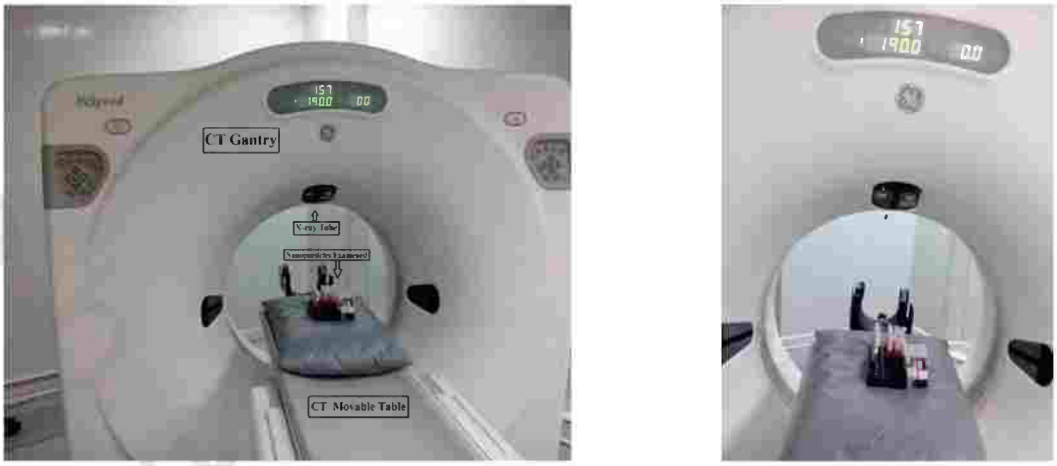

A B

Figure (70): A, B Nanoparticles during CT examination

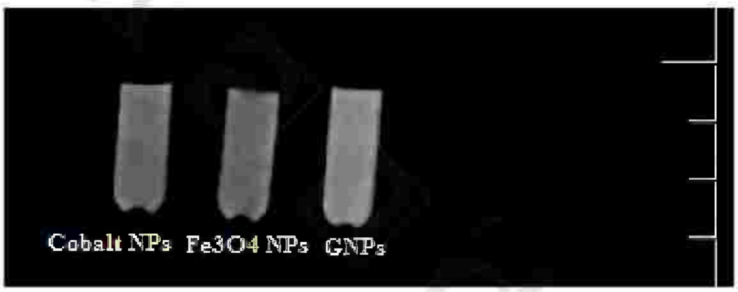

Figure (71): Axial CT image of (GNPS, Fe_3O_4 NPs and Cobalt NPs)

4.2.1. CT axial images for gold nanoparticles mixed with blood

A CT axial cuts was performed for each tube that contains GNPs mixed with blood and the hounsfield unit (HU) was measured for each of them

Figure (72): shows the tubes contains blood mixed with different concentration of GNPs

4.2.1.1. CT axial image for 0.1 mg/ml GNPs mixed with blood

A

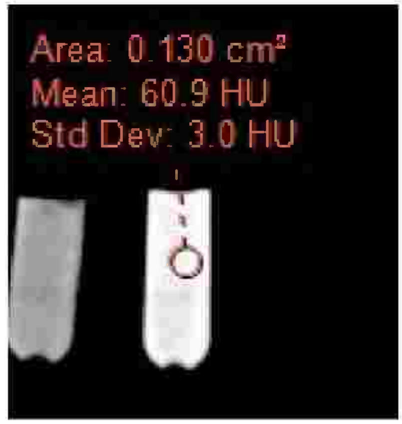

B

Figure (73): A, the test tube filled with blood that is mixed with 0.1 mg/ml GNPs. B, HU measurement for the axial CT image of the same tube

4.2.1.2. CT axial image for 0.05 mg/ml GNPs mixed with blood

A

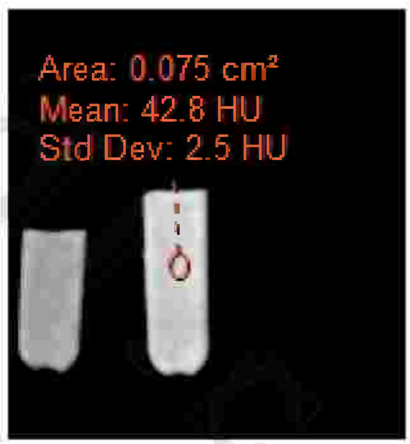

B

Figure (74): A, the test tube filled with blood that is mixed with 0.05 mg/ml GNPs. B, HU measurement for the axial CT image of the same tube

4.2.1.3. CT axial image for 0.025 mg/ml GNPs mixed with blood

A

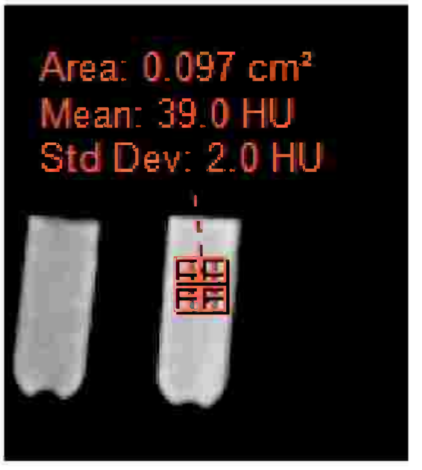

B

Figure (75): A, the test tube filled with blood that is mixed with 0.025 mg/ml GNPs. B, HU measurement for the axial CT image of the same tube

4.2.1.4. CT axial image for 0.0125 mg/ml GNPs mixed with blood

A

B

Figure (76): A, the test tube filled with blood that is mixed with 0.0125 mg/ml GNPs. B, HU measurement for the axial CT image of the same tube

4.2.1.5. CT axial image for 0.00625 mg/ml GNPs mixed with blood

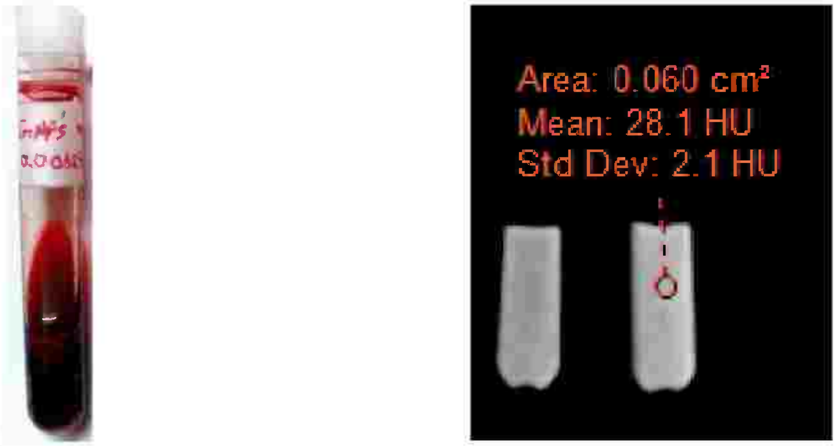

A B

Figure (77): A, the test tube filled with blood that is mixed with 0.00625 mg/ml GNPs. B, HU measurement for the axial CT image of the same tube

4.2.1.6. CT axial image for 0.003125 mg/ml GNPs mixed with blood

A B

Figure (78): A, the test tube filled with blood that is mixed with 0.003125 mg/ml GNPs. B, HU measurement for the axial CT image of the same tube

Table (15) HU values for different concentrations (0.1, 0.05, 0.025, 0.0125, 0.00625 and 0.00312 mg/ml) of gold nanoparticles mixed with blood in CT axial images

Concentration (mg/ml)	HU measurement of GNPs mixed with blood
0.10000	60.9
0.05000	42.8
0.02500	39
0.01250	32.7
0.00625	28.1
0.00312	13.5

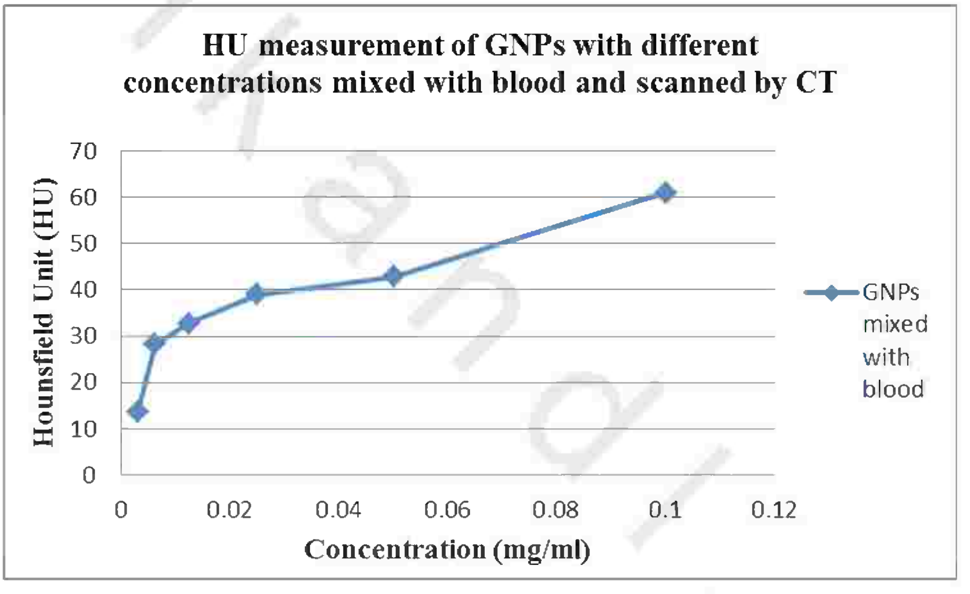

Figure (79): Variations in measured HU with different concentration of GNPs nanoparticles in CT axial images.

4.2.2. CT axial images for Iron Oxide (Fe_3O_4) nanoparticles mixed with blood

A CT axial cuts was performed for each tube that contains Fe_3O_4 NPs mixed with blood and the Hounsfield unit (HU) was measured for each of them

Figure (80): Shows the tubes contains blood mixed with different concentration of Fe_3O_4 NPs

4.2.2.1. CT axial image for 0.1 mg/ml Fe_3O_4 NPs mixed with blood

A B

Figure (81): A, the test tube filled with blood that is mixed with 0.1 mg/ml Fe_3O_4 NPs. B, HU measurement for the axial CT image of the same tube

4.2.2.2. CT axial image for 0.05 mg/ml Fe_3O_4 NPs mixed with blood

A B

Figure (82): A, the test tube filled with blood that is mixed with 0.05 mg/ml Fe_3O_4 NPs. B, HU measurement for the axial CT image of the same tube

4.2.2.3. CT axial image for 0.025 mg/ml Fe_3O_4 NPs mixed with blood

A B

Figure (83): A, the test tube filled with blood that is mixed with 0.025 mg/ml Fe_3O_4 NPs. B, HU measurement for the axial CT image of the same tube

4.2.2.4. CT axial image for 0.0125 mg/ml Fe_3O_4 NPs mixed with blood

A B

Figure (84): A, the test tube filled with blood that is mixed with 0.0125 mg/ml Fe_3O_4 NPs. B, HU measurement for the axial CT image of the same tube

4.2.2.5. CT axial image for 0.00625 mg/ml Fe_3O_4 NPs mixed with blood

A B

Figure (85): A, the test tube filled with blood that is mixed with 0.00625 mg/ml Fe_3O_4 NPs. B, HU measurement for the axial CT image of the same tube

4.2.2.6. CT axial image for 0.003125 mg/ml Fe_3O_4 NPs mixed with blood

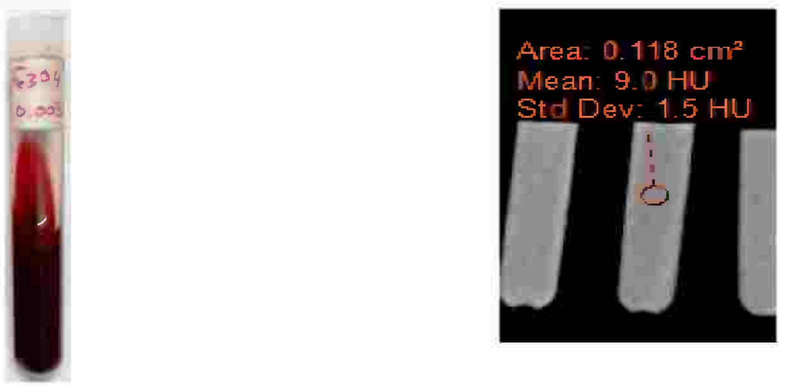

A B

Figure (86): A, the test tube filled with blood that is mixed with 0.003125 mg/ml Fe_3O_4 NPs. B, HU measurement for the axial CT image of the same tube

Table (16) HU values for different concentrations (0.1, 0.05, 0.025, 0.0125, 0.00625 and 0.00312 mg/ml) of Fe_3O_4 NPs mixed with blood in CT axial images

Concentration (mg/ml)	HU measurement of Fe_3O_4 NPs mixed with blood
0.10000	22.7
0.05000	21.4
0.02500	15.2
0.01250	14.5
0.00625	13.5
0.00312	9

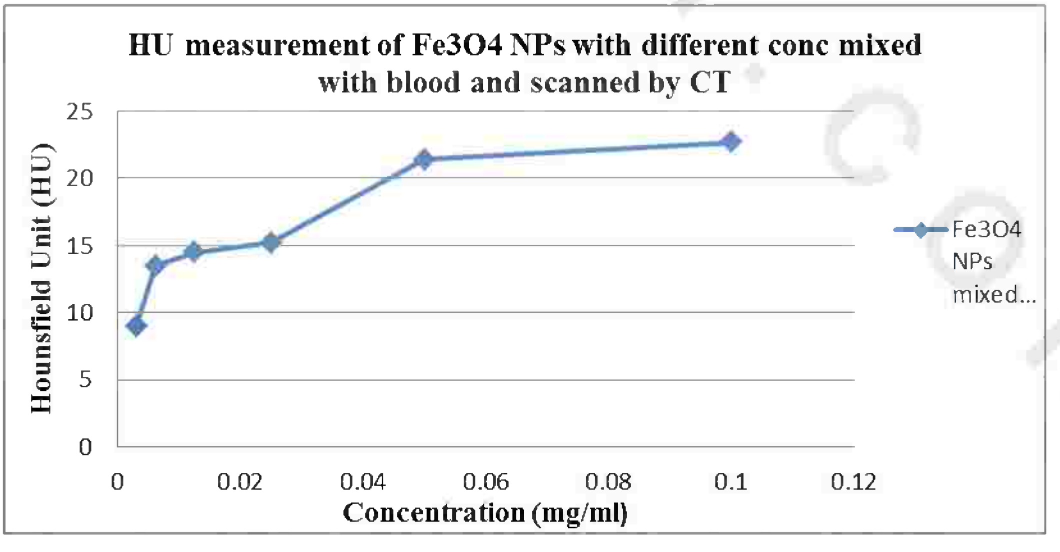

Figure (87): Variations in measured HU with different concentration of Fe_3O_4 NPs nanoparticles in CT axial images.

4.2.3. CT axial images for cobalt nanoparticles mixed with blood

A CT axial cuts was performed for each tube that contains Cobalt NPs mixed with blood and the Hounsfield unit (HU) was measured for each of them

Figure (88): Shows the tubes contains blood mixed with different concentration of cobalt NPs

4.2.3. 1. CT axial image for 0.1 mg/ml Cobalt NPs mixed with blood

A B

Figure (89): A, the test tube filled with blood that is mixed with 0.1 mg/ml Cobalt NPs. B, HU measurement for the axial CT image of the same tube

4.2.3. 2. CT axial image for 0.05 mg/ml Cobalt NPs mixed with blood

A B

Figure (90): A, the test tube filled with blood that is mixed with 0.05 mg/ml Cobalt NPs. B, HU measurement for the axial CT image of the same tube

4.2.3. 3. CT axial image for 0.025 mg/ml Cobalt NPs mixed with blood

A B

Figure (91): A, the test tube filled with blood that is mixed with 0.025 mg/ml Cobalt NPs. B, HU measurement for the axial CT image of the same tube

4.2.3. 4. CT axial image for 0.0125 mg/ml Cobalt NPs mixed with blood

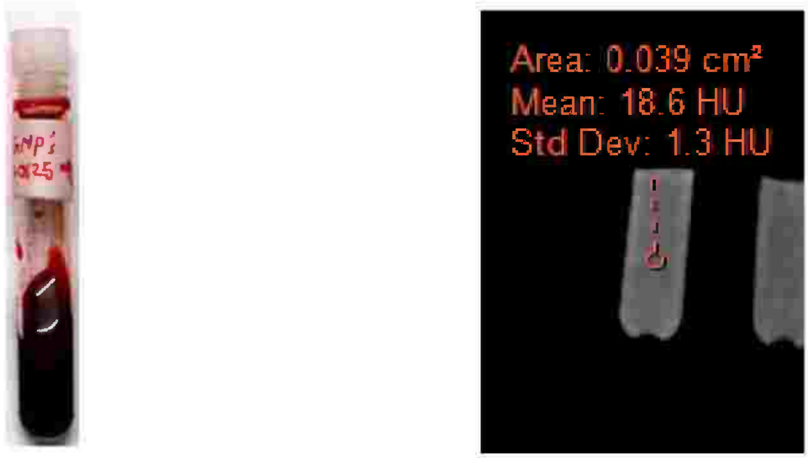

A B

Figure (92): A, the test tube filled with blood that is mixed with 0.0125 mg/ml Cobalt NPs. B, HU measurement for the axial CT image of the same tube

4.2.3. 5. CT axial image for 0.00625 mg/ml Cobalt NPs mixed with blood

A B

Figure (93): A, the test tube filled with blood that is mixed with 0.00625 mg/ml Cobalt NPs. B, HU measurement for the axial CT image of the same tube

4.2.3. 6. CT axial image for 0.003125 mg/ml Cobalt NPs mixed with blood

A B

Figure (94): A, the test tube filled with blood that is mixed with 0.003125 mg/ml Cobalt NPs. B, HU measurement for the axial CT image of the same tube

Table (17) HU values for different concentrations (0.1, 0.05, 0.025, 0.0125, 0.00625 and 0.00312 mg/ml) of Cobalt NPs mixed with blood in CT axial images

Concentration (mg/ml)	HU measurement of Cobalt NPs mixed with blood
0.10000	24.5
0.05000	20.9
0.02500	19.2
0.01250	18.6
0.00625	16.7
0.00312	7.3

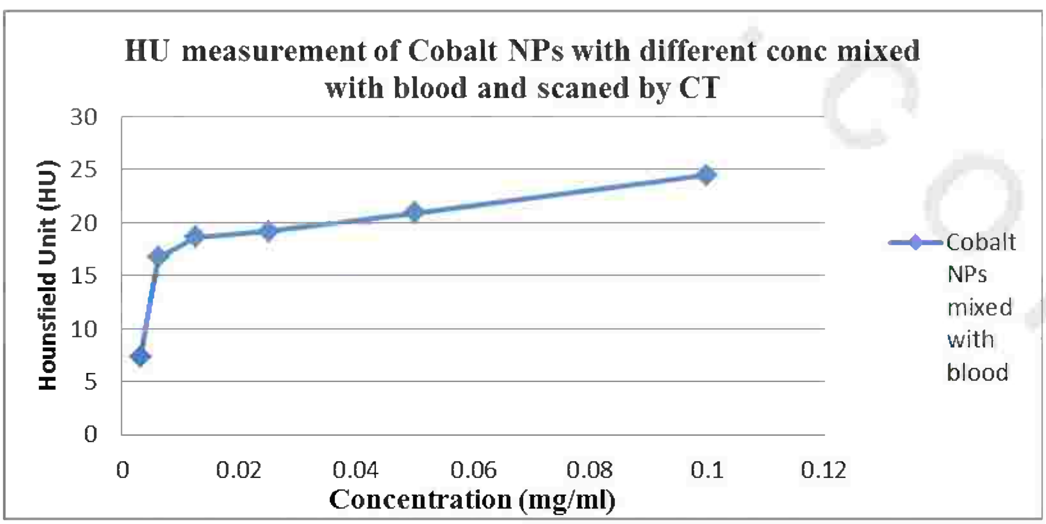

Figure (95): Variations in measured HU with different concentration of Cobalt NPs nanoparticles in CT axial images.

4.2.3. 7. HU measurement of GNPs & Fe_3O_4 NPs CT axial images

Table (18) HU values for GNPs & Fe_3O_4 NPs mixed with blood CT axial images

Concentration (mg/ml)	HU of GNPs mixed with blood	HU of Fe_3O_4 NPs mixed with blood
0.10000	60.9	22.7
0.05000	42.8	21.4
0.02500	39	15.2
0.01250	32.7	14.5
0.00625	28.1	13.5
0.00312	13.5	9

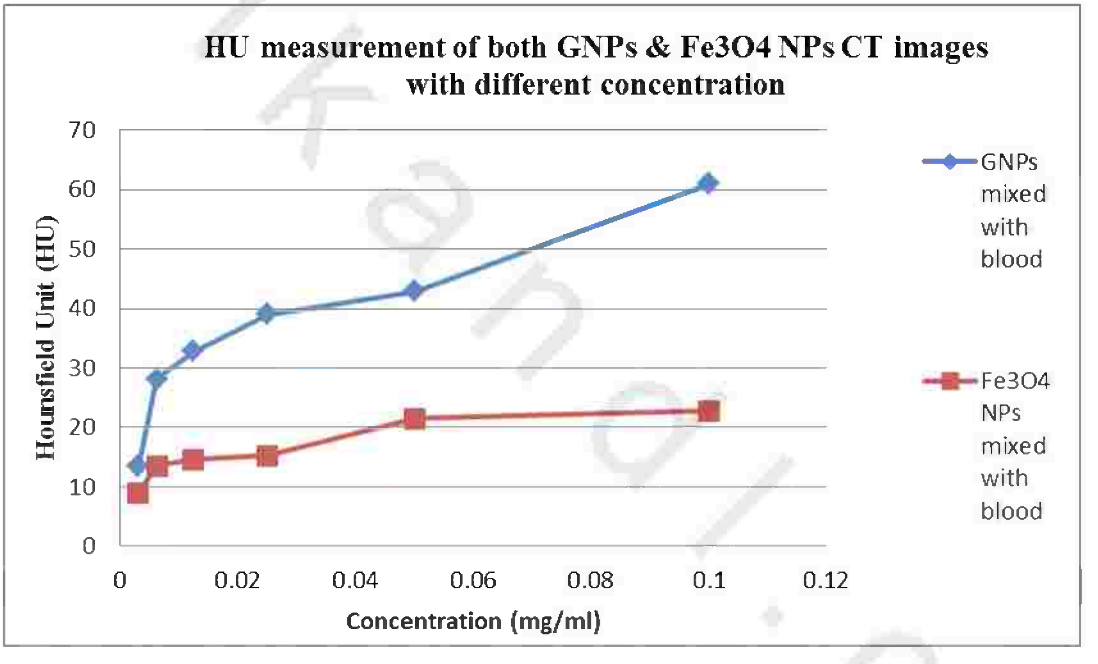

Figure (96): Variations in measured HU with different concentration of GNPs& **Fe_3O_4** nanoparticles in CT axial images

4.2.3. 8. HU measurement of GNPs & Cobalt NPs CT axial images

Table (19) Hounsfield units measured for GNPs & Cobalt NPs mixed with blood CT axial images

Concentration (mg/ml)	GNPs mixed with blood	Cobalt NPs mixed with blood
0.10000	60.9	24.5
0.05000	42.8	20.9
0.02500	39	19.2
0.01250	32.7	18.6
0.00625	28.1	16.7
0.00312	13.5	7.3

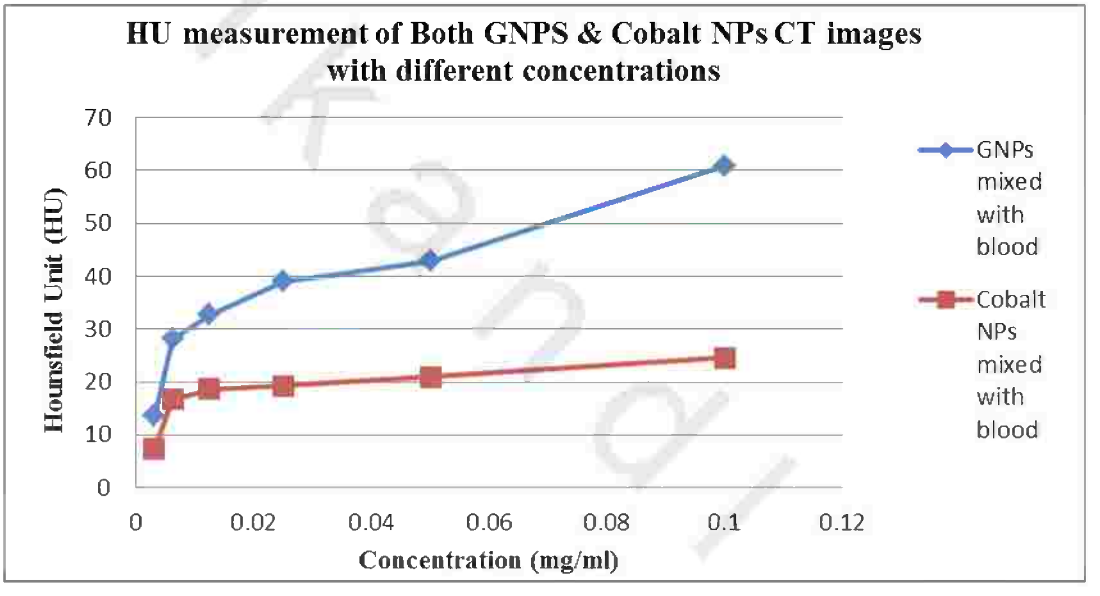

Figure (97): Variations in measured HU with different concentration of GNPs&Cobalt nanoparticles in CT axial images

4.2.4. CT axial images for nickel & titanium nanoparticles mixed with blood

4.2.4. 1. CT axial images for nickel nanoparticles mixed with blood

A CT axial cuts was performed for each tube that contains Cobalt NPs mixed with blood and the Hounsfield unit (HU) was measured for each of them

Figure (98): Shows the tubes contains blood mixed with different concentration of nickel NPs

4.2.4. 2. CT axial image for 0.1 mg/ml nickel NPs mixed with blood

B

A

Figure (99): A, the test tube filled with blood that is mixed with 0.1 mg/ml nickel NPs. B, HU measurement for the axial CT image of the same tube

4.2.4. 3. CT axial image for 0.05 mg/ml nickel NPs mixed with blood

B

A

Figure (100): A, the test tube filled with blood that is mixed with 0.05 mg/ml nickel NPs. B, HU measurement for the axial CT image of the same tube

4.2.4. 4. CT axial image for 0.025 mg/ml nickel NPs mixed with blood

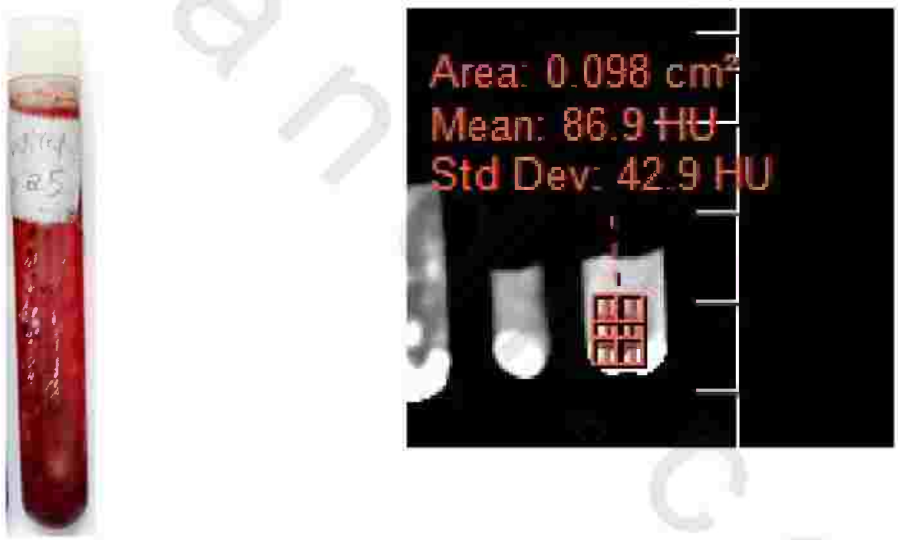

B

A

Figure (101): A, the test tube filled with blood that is mixed with 0.025 mg/ml nickel NPs. B, HU measurement for the axial CT image of the same tube

4.2.4. 5. CT axial image for 0.0125 mg/ml nickel NPs mixed with blood

A

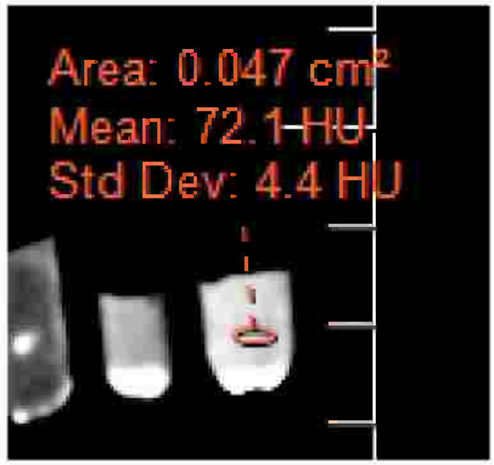

B

Figure (102): A, the test tube filled with blood that is mixed with 0.0125 mg/ml nickel NPs. B, HU measurement for the axial CT image of the same tube

4.2.4.6. CT axial image for 0.00625 mg/ml nickel NPs mixed with blood

A

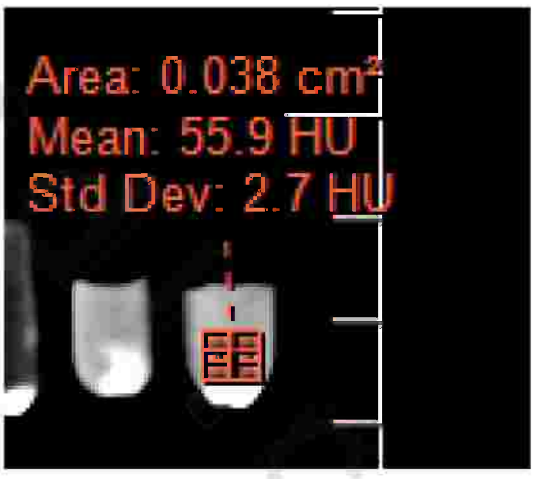

B

Figure (103): A, the test tube filled with blood that is mixed with 0.00625 mg/ml nickel NPs. B, HU measurement for the axial CT image of the same tube

Table (20) Hounsfield units measured for different concentrations (0.1, 0.05, 0.025, 0.0125, 0.00625 and 0.00312 mg/ml) of nickel NPs in CT axial images.

Concentration (mg/ml)	HU measurement of nickel NPs mixed with blood
0.10000	104
0.05000	88
0.02500	86
0.01250	72
0.00625	55.9

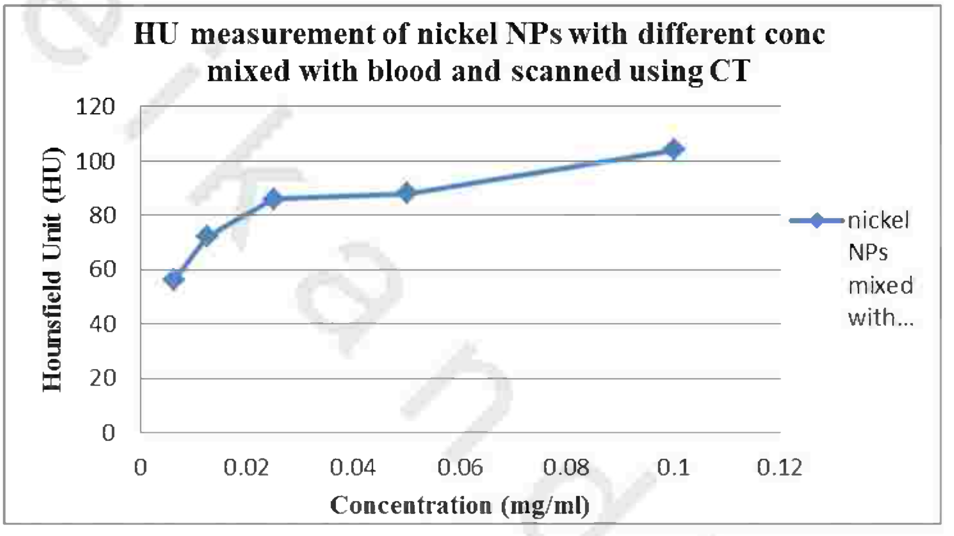

Figure (104): Variations in measured HU with different concentration of nickel NPs nanoparticles in CT axial images.

4.2.5. CT axial images for titanium nanoparticles mixed with blood

A CT axial cuts was performed for each tube that contains titanium NPs mixed with blood and the hounsfield unit (HU) was measured for each of them

Figure (105): Shows the tubes contains blood mixed with different concentration of titanium NPs

4.2.5.1. CT axial image for 0.1 mg/ml titanium NPs mixed with blood

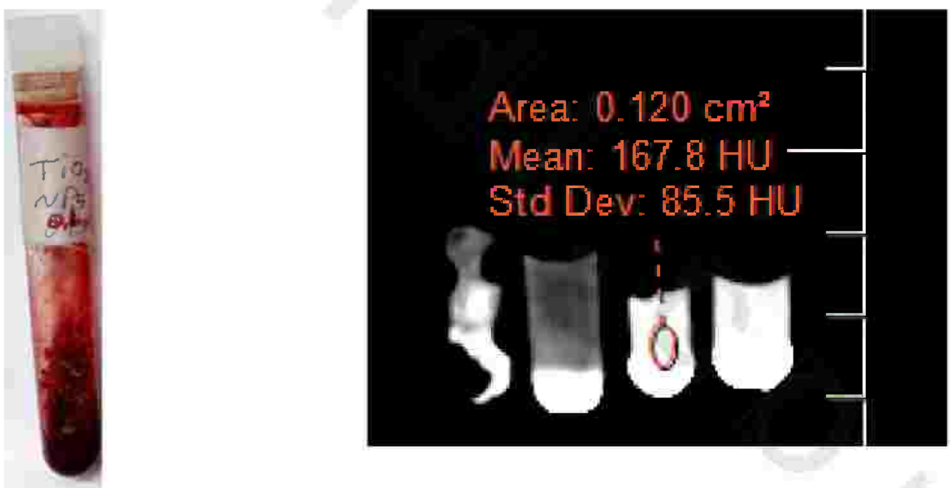

A

B

Figure (106): A, the test tube filled with blood that is mixed with 0.1 mg/ml titanium NPs. B, HU measurement for the axial CT image of the same tube

4.2.5.2. CT axial image for 0.05 mg/ml titanium NPs mixed with blood

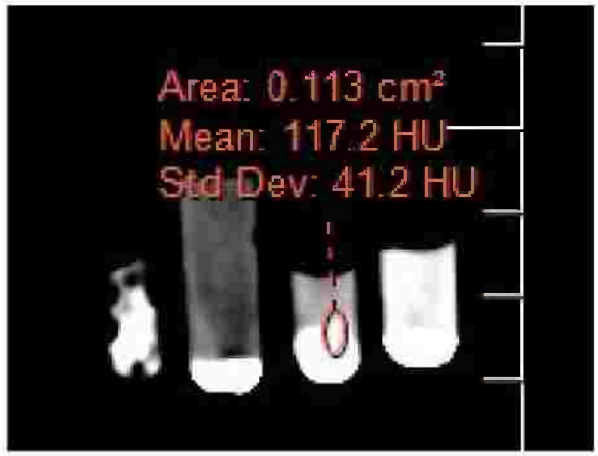

A B

Figure (107): A, the test tube filled with blood that is mixed with 0.05 mg/ml titanium NPs. B, HU measurement for the axial CT image of the same tube

4.2.5.3. CT axial image for 0.025 mg/ml titanium NPs mixed with blood

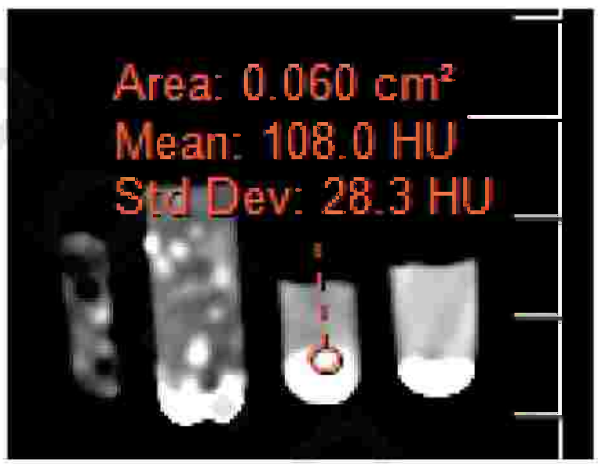

A B

Figure (108): A, the test tube filled with blood that is mixed with 0.025 mg/ml titanium NPs. B, HU measurement for the axial CT image of the same tube

4.2.5.4. CT axial image for 0.0125 mg/ml titanium NPs mixed with blood

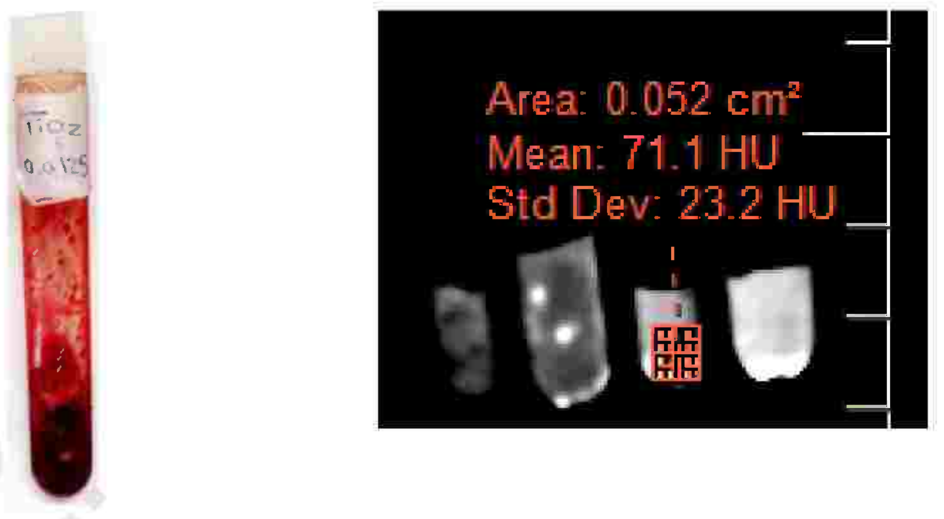

A B

Figure (109): A, the test tube filled with blood that is mixed with 0.0125 mg/ml titanium NPs. B, HU measurement for the axial CT image of the same tube

4.2.5.5. CT axial image for 0.00625 mg/ml titanium NPs mixed with blood

A B

Figure (110): A, the test tube filled with blood that is mixed with 0.00625 mg/ml titanium NPs. B, HU measurement for the axial CT image of the same tube

Table (21) The different hounsienfield units measured for different concentrations (0.1, 0.05, 0.025, 0.0125, 0.00625 and 0.00312 mg/ml) of titanium NPs mixed with blood in CT axial images.

Concentration (mg/ml)	HU measurement of titanium NPs mixed with blood
0.10000	167.8
0.05000	117.2
0.02500	108
0.01250	71.1
0.00625	67.8

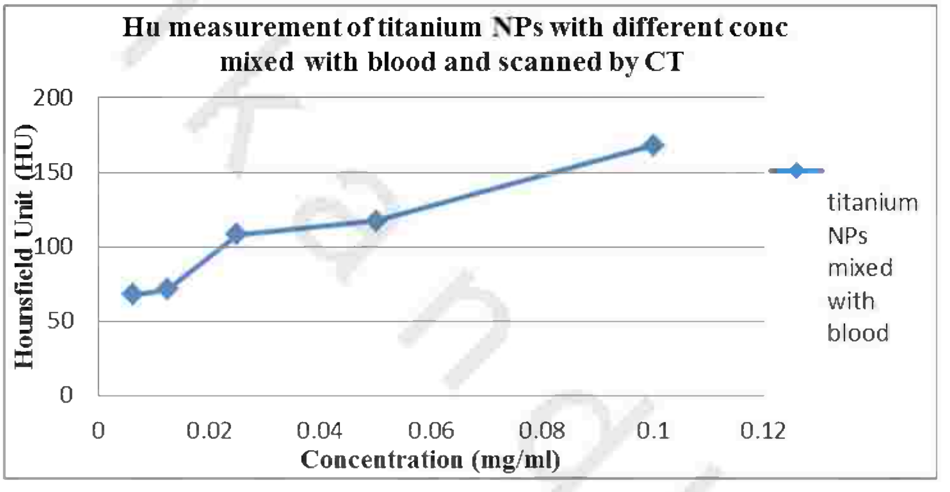

Figure (111): Variations in measured HU with different concentration of titanium NPs nanoparticles in CT axial images

4.2.5.6. CT of both Nickel & Titanium Nanoparticles

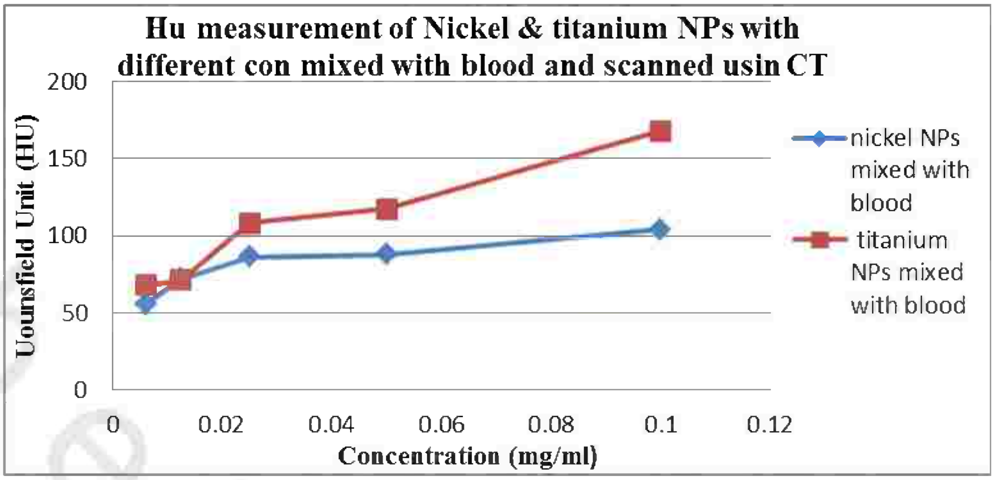

Figure (112): Variations in HU measurements of CT axial images between Nickel & Titanium nanoparticles

2.4. Magnetic Resonance Imaging of Nanoparticles

A B

Figure (113): A, the Neusoft MRI machine unit & the main components of the equipment, B, Nanoparticles placed in the knee coil during the examination

2.4. 1. Planning Procedure

Phantom tree was scanned with 0.35 tesla MRI machine using knee Coil in different planes (sagittal, axial and coronal).

2.4.1.1. Planning Block

Planning block was done to specify the part being examined

A B

Figure (114): A, B, the different blocks for Sagittal, coronal and axial planes

2.4.1.2. Planning

Figure (115): MRI Planning, Each of these lines represents an MRI image

2.4.1.3. Scanning planes

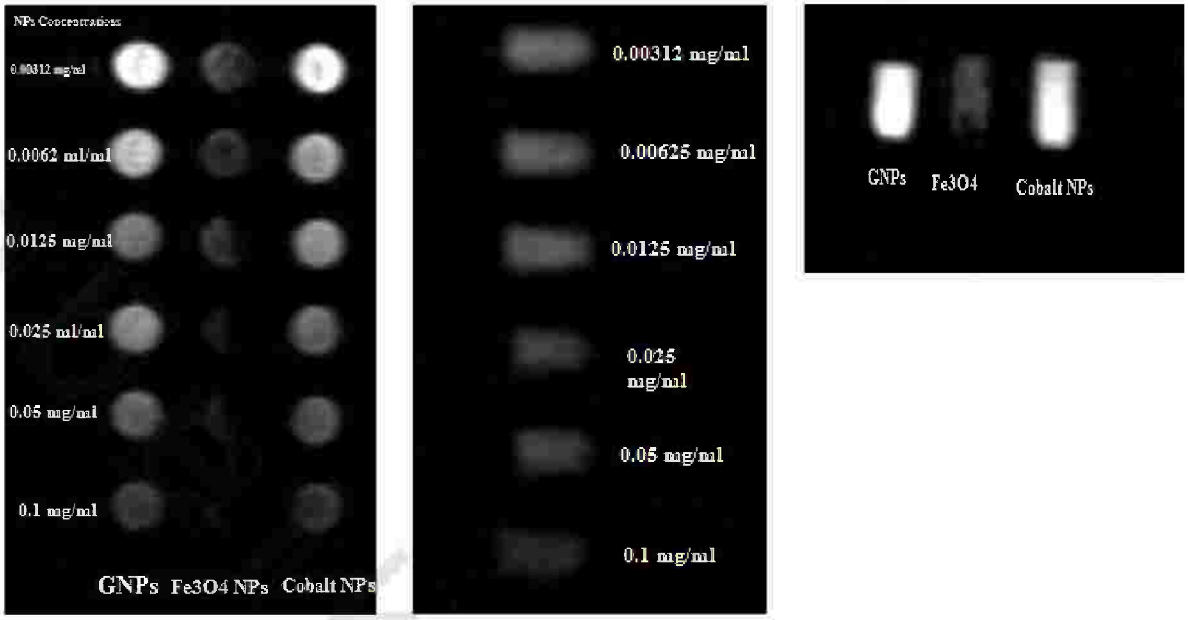

A B C

Figure (116): A, MRI coronal plane, B, MRI sagittal plane, C, MRI axial plane of GNPs, Fe_3O_4 and Cobalt nanoparticles

2.4.2. GNPs Nanoparticles diluted in water in a test tube with 1cm diameter and 1cm height.

2.4.2.1. Coronal Images (T1 sequence)

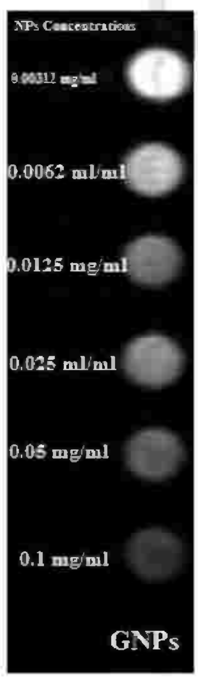

Figure (117): A, MRI coronal plane of GNPs

2.4.2.1.1. MRI coronal images for GNPs diluted in distal water

A MRI coronal cuts was performed for each tube that contains GNPs diluted in distal water and the Hounsfield unit (HU) was measured for each of them

2.4.2.1.1.1. MRI coronal image for 0.1 mg/ml GNPs diluted in water

Figure (118): MRI signal intensity measurement for coronal MRI image of 0.1 mg/ml of GNPs diluted in water

2.4.2.1.1. 2. MRI coronal image for 0.05 mg/ml GNPs diluted in water

Figure (119): MRI signal intensity measurement for coronal MRI image of 0.05 mg/ml of GNPs diluted in water

2.4.2.1.1. 3. MRI coronal image for 0.025 mg/ml GNPs diluted in water

Figure (120): MRI signal intensity measurement for coronal MRI image of 0.025 mg/ml of GNPs diluted in water

2.4.2.1.1. 4. MRI coronal image for 0.0125 mg/ml GNPs diluted in water

Figure (121): MRI signal intensity measurement for coronal MRI image of 0.0125 mg/ml of GNPs diluted in water

2.4.2.1.1. 5. MRI coronal image for 0.00625 mg/ml GNPs diluted in water

Figure (122): MRI signal intensity measurement for coronal MRI image of 0.00625 mg/ml of GNPs diluted in water

2.4.2.1.1.6. MRI coronal image for 0.003125 mg/ml GNPs diluted in water

Figure (123): MRI signal intensity measurement for coronal MRI image of 0.003125 mg/ml of GNPs diluted in water

Table (22) The different MRI signal intensity measurement measured for different concentrations (0.1, 0.05, 0.025, 0.0125, 0.00625 and 0.00312 mg/ml) of GNPs in MRI coronal images

Concentration (mg/ml)	MRI signal intensity measurement of GNPs diluted in water
0.10000	41.8
0.05000	72.3
0.02500	94.1
0.01250	112.5
0.00625	151.1
0.00312	192.3

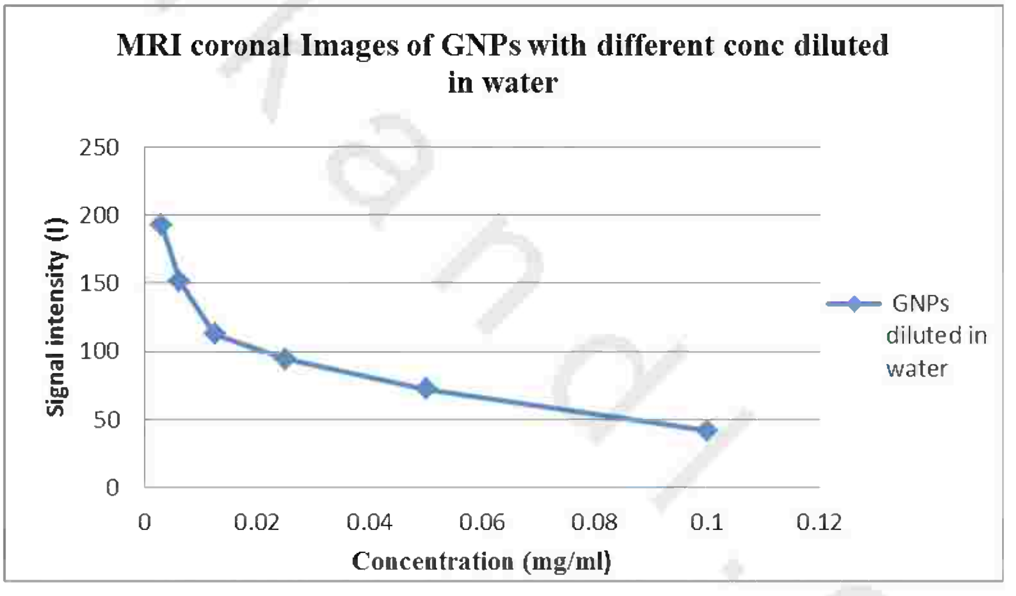

Figure (124): Variations in measured signal intensity with different concentration of GNPs nanoparticles in MRI coronal images

2.4.2.1.2. MRI coronal images for Fe_3O_4 NPs diluted in distal water

A MRI coronal cuts was performed for each tube that contains Fe_3O_4 NPs diluted in distal water and the signal intensity was measured for each of them

2.4.2.1.2.1. MRI coronal image for 0.1 mg/ml Fe_3O_4 NPs diluted in water

Figure (125): MRI signal intensity measurement for coronal MRI image of 0.1 mg/ml of Fe_3O_4 NPs diluted in water

2.4.2.1.2. 2.MRI coronal image for 0.05 mg/ml Fe_3O_4 NPs diluted in water

Figure (126): MRI signal intensity measurement for coronal MRI image of 0.05 mg/ml of Fe_3O_4 NPs diluted in water

2.4.2.1.2. 3.MRI coronal image for 0.025 mg/ml Fe_3O_4 NPs diluted in water

Figure (127): MRI signal intensity measurement for coronal MRI image of 0.025 mg/ml of Fe_3O_4 NPs diluted in water

2.4.2.1.2. 4.MRI coronal image for 0.0125 mg/ml Fe_3O_4 **NPs diluted in water**

Figure (128) MRI signal intensity measurement for coronal MRI image of 0.0125 mg/ml of Fe_3O_4 NPs diluted in water

2.4.2.1.2. 5.MRI coronal image for 0.00625 mg/ml Fe_3O_4 NPs diluted in water

Figure (129): MRI signal intensity measurement for coronal MRI image of 0.00625 mg/ml of Fe_3O_4 NPs diluted in water

2.4.2.1.2. 6.MRI coronal image for 0.003125 mg/ml Fe_3O_4 NPs diluted in water

Figure (130): MRI signal intensity measurement for coronal MRI image of 0.003125 mg/ml of GNPs diluted in water

Table (23) The different MRI signal intensity measured for different concentrations (0.1, 0.05, 0.025, 0.0125, 0.00625 and 0.00312 mg/ml) of Fe_3O_4 NPs in MRI coronal images.

Concentration (mg/ml)	MRI signal intensity measurement of Fe_3O_4 NPs diluted in water
0.10000	15
0.05000	24.3
0.02500	27
0.01250	31.6
0.00625	36.3
0.00312	54.3

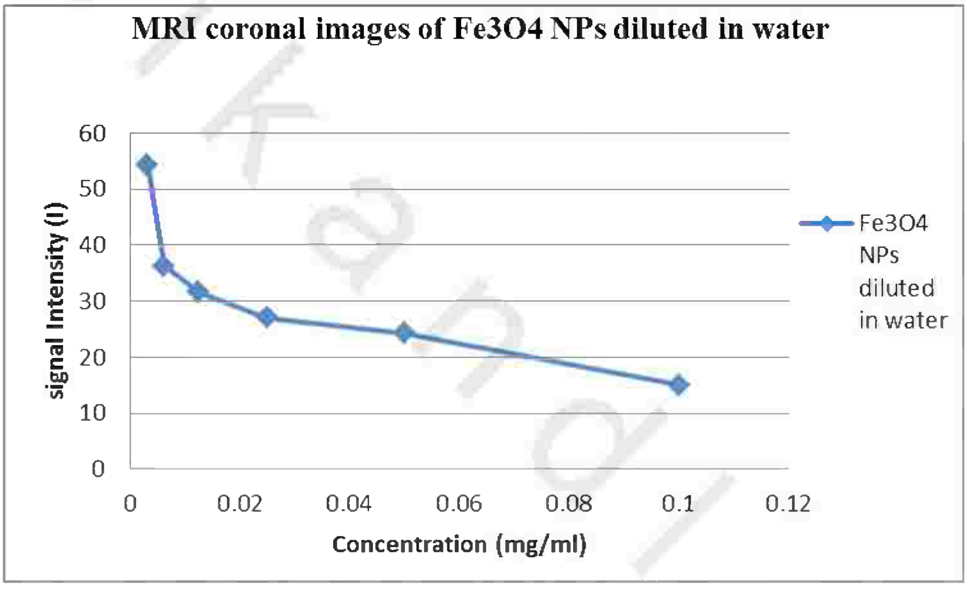

Figure (131): Variations in measured HU with different concentration of Fe_3O_4 NPs nanoparticles in MRI coronal images

2.4. 2.1.3. MRI coronal images for cobalt NPs diluted in distal water

A MRI coronal cuts was performed for each tube that contains cobalt NPs diluted in distal water and the signal intensity was measured for each of them

2.4. 2.1.3. 1. MRI coronal image for 0.1 mg/ml cobalt NPs diluted in water

Figure (132): MRI signal intensity measurement for coronal MRI image of 0.1 mg/ml of cobalt NPs diluted in water

2.4. 2.1.3. 2. MRI coronal image for 0.05 mg/ml cobalt NPs diluted in water

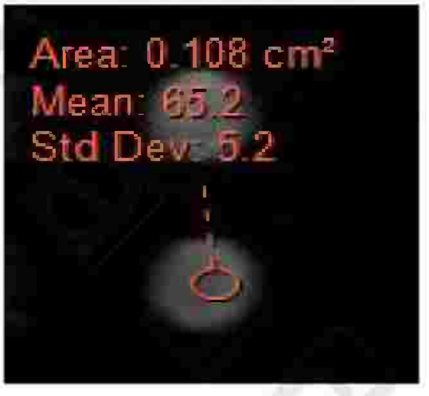

Figure (133): MRI signal intensity measurement for coronal MRI image of 0.05 mg/ml of cobalt NPs diluted in water

2.4. 2.1.3. 3. MRI coronal image for 0.025 mg/ml cobalt NPs diluted in water

Figure (134): MRI signal intensity measurement for coronal MRI image of 0.025 mg/ml of cobalt NPs diluted in water

2.4. 2.1.3. 4. MRI coronal image for 0.0125 mg/ml cobalt NPs diluted in water

Figure (135): MRI signal intensity measurement for coronal MRI image of 0.0125 mg/ml of cobalt NPs diluted in water

2.4. 2.1.3. 5. MRI coronal image for 0.00625 mg/ml cobalt NPs diluted in water

Figure (136): MRI signal intensity measurement for coronal MRI image of 0.00625 mg/ml of cobalt NPs diluted in water

2.4. 2.1.3. 6. MRI coronal image for 0.003125 mg/ml cobalt NPs diluted in water

Figure (137): MRI signal intensity measurement for coronal MRI image of 0.003125 mg/ml of cobalt NPs diluted in water

Table (24) The different MRI signal intensity measurement measured for different concentrations (0.1, 0.05, 0.025, 0.0125, 0.00625 and 0.00312 mg/ml) of cobalt NPs in MRI coronal images.

Concentration (mg/ml)	MRI signal intensity measurement of cobalt NPs diluted in water
0.10000	31.5
0.05000	65.2
0.02500	78.8
0.01250	111.4
0.00625	123
0.00312	183

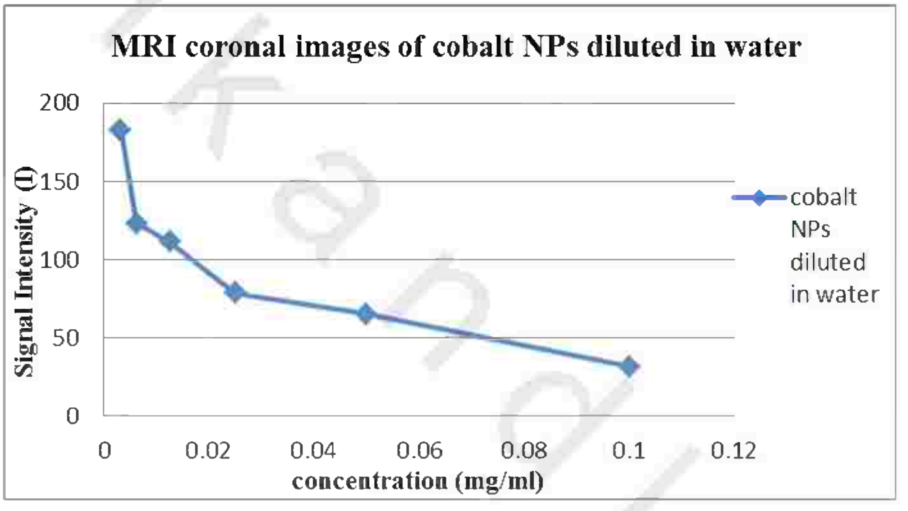

Figure (138): Variations in measured signal intensity with different concentration of cobalt NPs in MRI coronal images

2.4. 2.1.3. 7. HU measurement of MRI coronal images for GNPs Fe_3O_4 and Cobalt NPs

Table (25) Signal intensity measurements of MRI coronal images for GNPs Fe_3O_4 and Cobalt NPs diluted in water

Concentration (mg/ml)	Signal intensity measurement cobalt NPs diluted in water	Signal intensity measurement Fe_3O_4 NPs diluted in water	Signal intensity measurement GNPs diluted in water
0.10000	31.5	15	41.8
0.05000	65.2	24.3	72.3
0.02500	78.8	27	94.1
0.01250	111.4	31.6	112.5
0.00625	123	36.3	151.1
0.00312	183	54.3	192.3

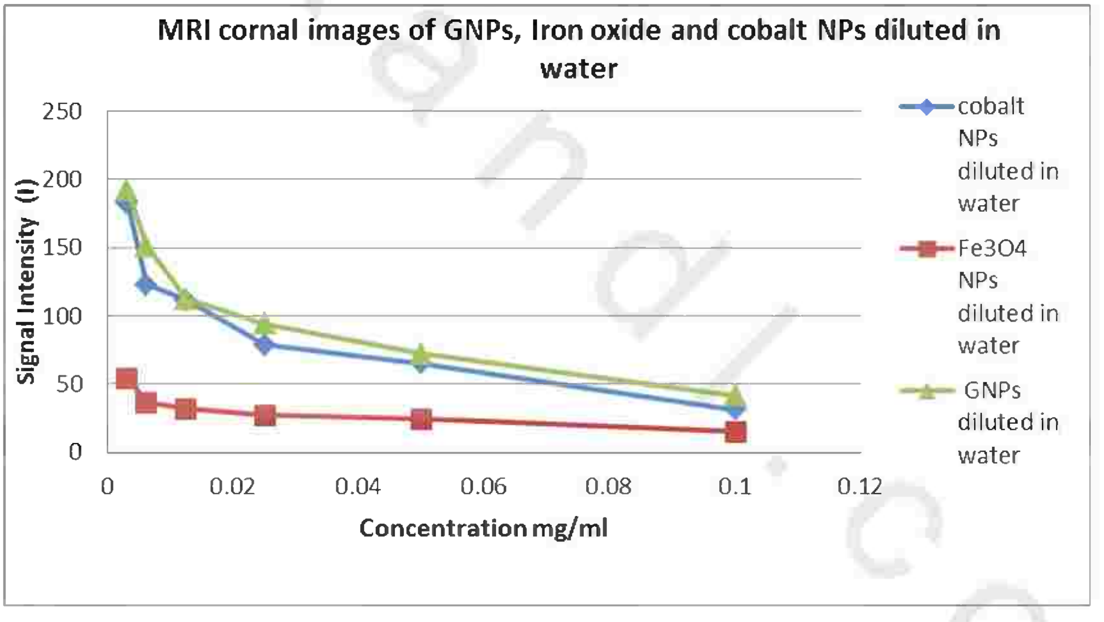

Figure (139): Variations in signal intensity measurements of MRI coronal images between GNPs, Fe_3O_4 and Cobalt NPs

2.4. 2.2. Axial Images (T1 sequence)

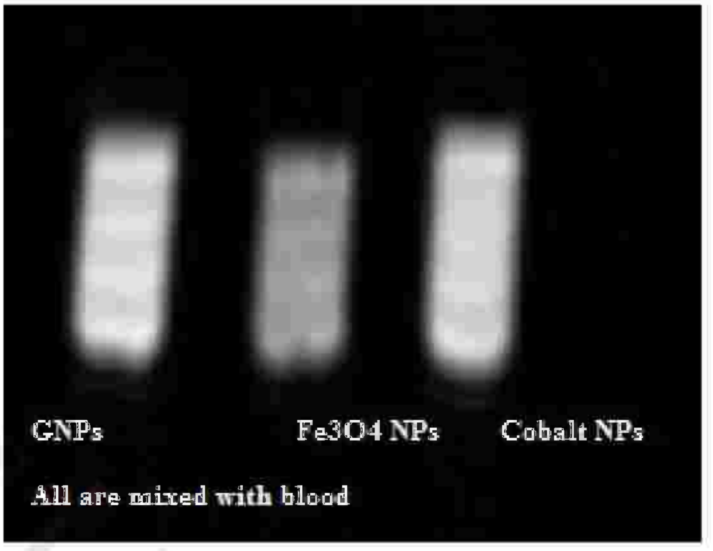

Figure (140): MRI axial plane of GNPs, Fe34 and Cobalt nanoparticles

2.4. 2.2. 1. MRI axial images for GNPs mixed with blood

A MRI coronal cuts was performed for each tube that contains GNPs mixed with blood and the signal intensity was measured for each of them

2.4. 2.2.2.1. MRI axial image for 0.1 mg/ml GNPs mixed with blood

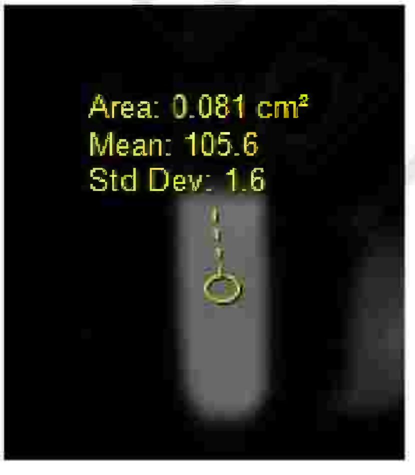

Figure (141): MRI signal intensity measurement for axial MRI image of 0.1 mg/ml of GNPs mixed with blood

2.4. 2.2.2.2. MRI axial image for 0.05 mg/ml GNPs mixed with blood

Figure (142): MRI signal intensity measurement for axial MRI image of 0.05 mg/ml of GNPs mixed with blood

2.4. 2.2.2.3. MRI axial image for 0.025 mg/ml GNPs mixed with blood

Figure (143): MRI signal intensity measurement for axial MRI image of 0.025 mg/ml of GNPs mixed with blood

2.4. 2.2.2.4. MRI axial image for 0.0125 mg/ml GNPs mixed with blood

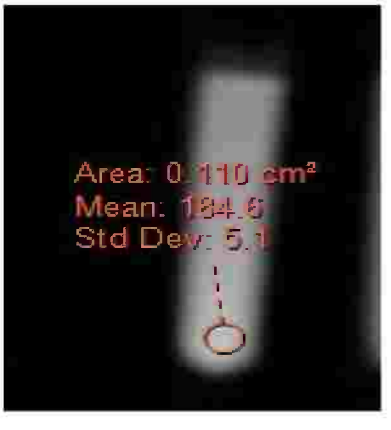

Figure (144): MRI signal intensity measurement for axial MRI image of 0.0125 mg/ml of GNPs mixed with blood

2.4. 2.2.2.5. MRI axial image for 0.00625 mg/ml GNPs mixed with blood

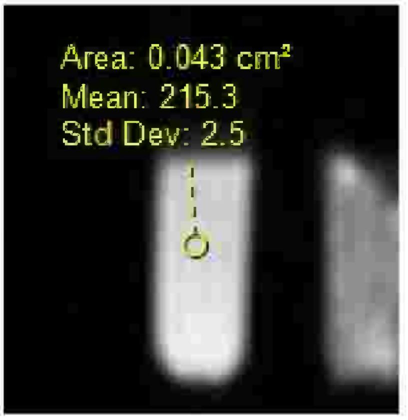

Figure (145): MRI signal intensity measurement for axial MRI image of 0.00625 mg/ml of GNPs mixed with blood

2.4. 2.2.2.6. MRI axial image for 0.003125 mg/ml GNPs mixed with blood

Figure (146): MRI signal intensity measurement for axial MRI image of 0.003125 mg/ml of GNPs mixed with blood

Table (26) MRI signal intensity measurements for different concentrations (0.1, 0.05, 0.025, 0.0125, 0.00625 and 0.00312 mg/ml) of GNPs in MRI axial images

Concentration (mg/ml)	MRI signal intensity measurement of GNPs mixed with blood
0.10000	105.6
0.05000	133.4
0.02500	182
0.01250	184.6
0.00625	215.3
0.00312	217.7

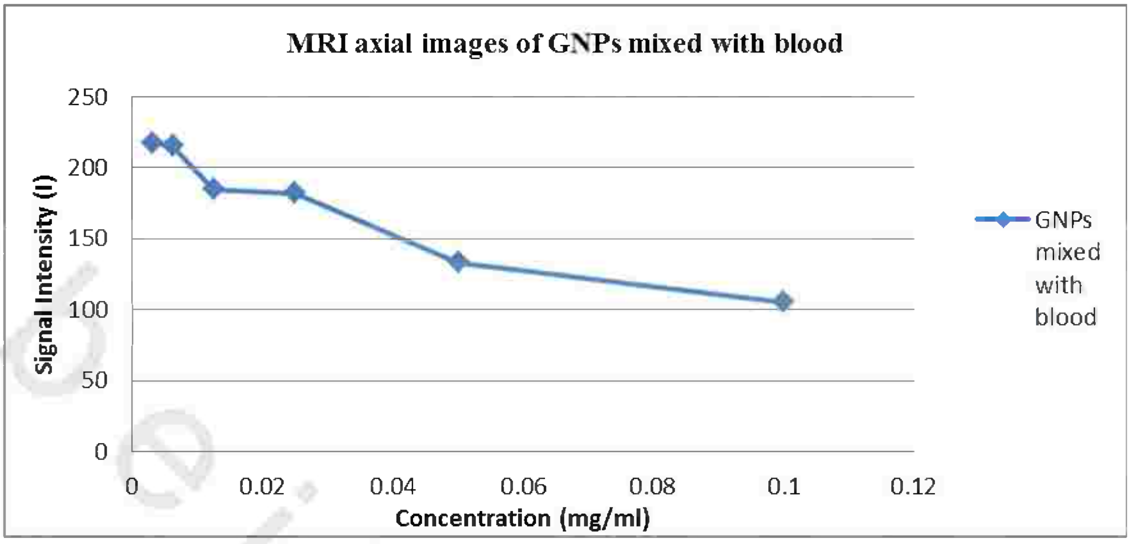

Figure (147): Variations in signal intensity measured with different concentration of GNPs nanoparticles in MRI axial images

2.4. 2.2.2.MRI axial images for Fe_3O_4 NPs mixed with blood

A MRI axial cuts was performed for each tube that contains Fe_3O_4 NPs mixed with blood and the signal intensity was measured for each of them

2.4. 2.2.2.1. MRI axial image for 0.1 mg/ml Fe_3O_4 NPs mixed with blood

Figure (148): MRI signal intensity measurement for axial MRI image of 0.1 mg/ml of Fe_3O_4 NPs mixed with blood

2.4. 2.2.2.2. MRI axial image for 0.05 mg/ml Fe_3O_4 NPs mixed with blood

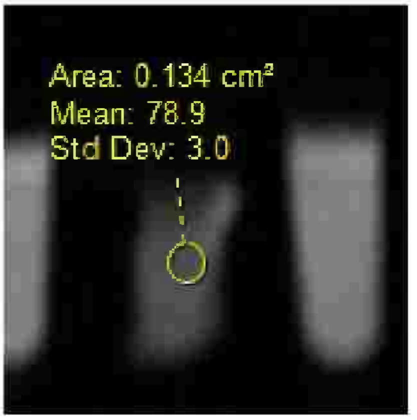

Figure (149): MRI signal intensity measurement for axial MRI image of 0.05 mg/ml of Fe_3O_4 NPs mixed with blood

2.4. 2.2.2.3. MRI axial image for 0.025 mg/ml Fe_3O_4 NPs mixed with blood

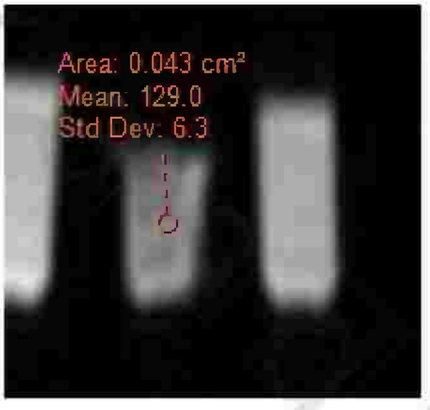

Figure (150): MRI signal intensity measurement for axial MRI image of 0.025 mg/ml of Fe_3O_4 NPs mixed with blood

2.4. 2.2.2.4. MRI axial image for 0.0125 mg/ml Fe_3O_4 NPs mixed with blood

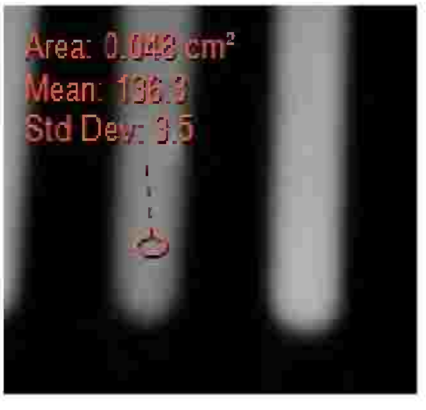

Figure (151): MRI signal intensity measurement for axial MRI image of 0.0125 mg/ml of Fe_3O_4 NPs mixed with blood

2.4. 2.2.2.5. MRI axial image for 0.00625 mg/ml Fe_3O_4 NPs mixed with blood

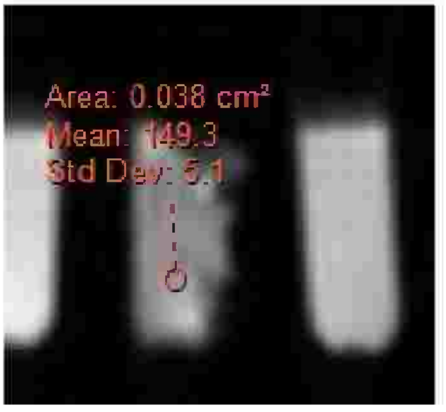

Figure (152): MRI signal intensity measurement for axial MRI image of 0.00625 mg/ml of Fe_3O_4 NPs mixed with blood

2.4. 2.2.2.6. MRI axial image for 0.003125 mg/ml Fe_3O_4 NPs mixed with blood

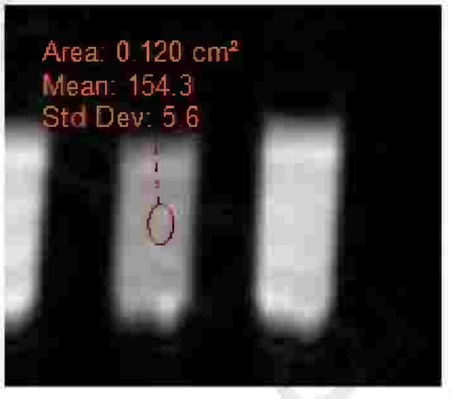

Figure (153): MRI signal intensity measurement for axial MRI image of 0.003125 mg/ml of GNPs mixed with blood

Table (27) MRI signal intensity measurements for different concentrations (0.1, 0.05, 0.025, 0.0125, 0.00625 and 0.00312 mg/ml) of Fe_3O_4 NPs in MRI axial images

Concentration (mg/ml)	MRI signal intensity measurement of Fe_3O_4 NPs mixed with blood
0.10000	60.8
0.05000	78.9
0.02500	129
0.01250	136.3
0.00625	149.3
0.00312	154.3

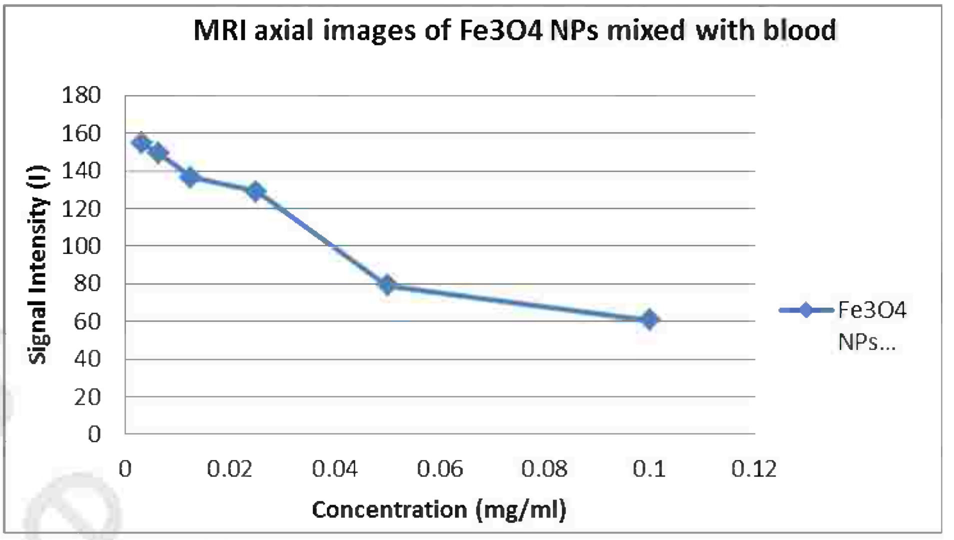

Figure (154): Variations in measured signal intensity with different concentration of Fe_3O_4 NPs nanoparticles in MRI axial images

2.4. 2.2.2.7. MRI axial images for cobalt NPs mixed with blood

A MRI axial cuts was performed for each tube that contains cobalt NPs mixed with blood and the signal intensity was measured for each of them

2.4. 2.2.3.MRI axial image for 0.1 mg/ml cobalt NPs mixed with blood

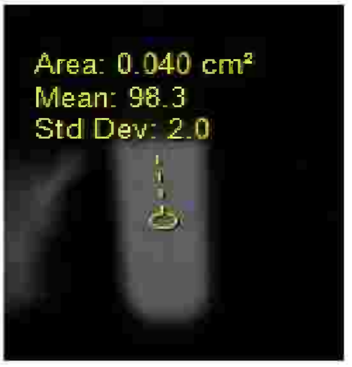

Figure (155): MRI signal intensity measurement for axial MRI image of 0.1 mg/ml of cobalt NPs mixed with blood

2.4. 2.2.3.1. MRI axial image for 0.05 mg/ml cobalt NPs mixed with blood

Figure (156): MRI signal intensity measurement for axial MRI image of 0.05 mg/ml of cobalt NPs mixed with blood

2.4. 2.2.3.2. MRI axial image for 0.025 mg/ml cobalt NPs mixed with blood

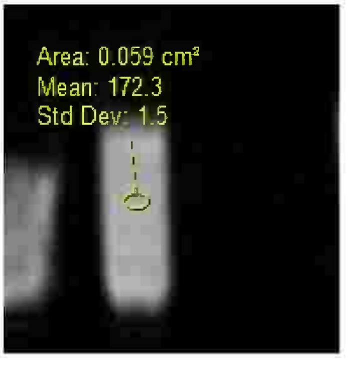

Figure (157): MRI signal intensity measurement for axial MRI image of 0.025 mg/ml of cobalt NPs mixed with blood

2.4. 2.2.3.3. MRI axial image for 0.0125 mg/ml cobalt NPs mixed with blood

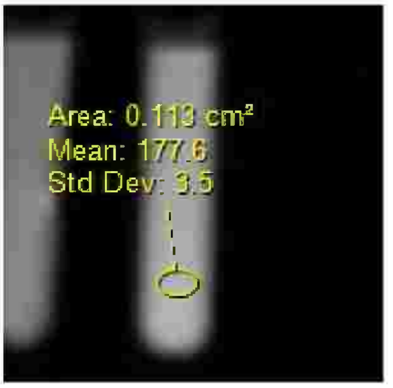

Figure (158): MRI signal intensity measurement for axial MRI image of 0.0125 mg/ml of cobalt NPs mixed with blood

2.4. 2.2.3.4. MRI axial image for 0.00625 mg/ml cobalt NPs mixed with blood

Figure (159): MRI signal intensity measurement for axial MRI image of 0.00625 mg/ml of cobalt NPs mixed with blood

2.4. 2.2.3.5. MRI axial image for 0.003125 mg/ml cobalt NPs mixed with blood

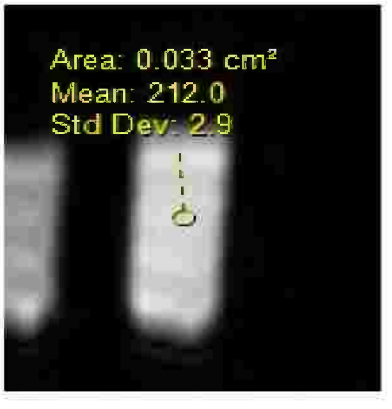

Figure (160): MRI signal intensity measurement for axial MRI image of 0.003125 mg/ml of cobalt NPs mixed with blood

Table (28) MRI signal intensity measurements for different concentrations (0.1, 0.05, 0.025, 0.0125, 0.00625 and 0.00312 mg/ml) of cobalt NPs in MRI axial images.

Concentration (mg/ml)	MRI signal intensity measurement of cobalt NPs mixed with blood
0.10000	98.3
0.05000	124.2
0.02500	172.3
0.01250	177.6
0.00625	188
0.00312	212

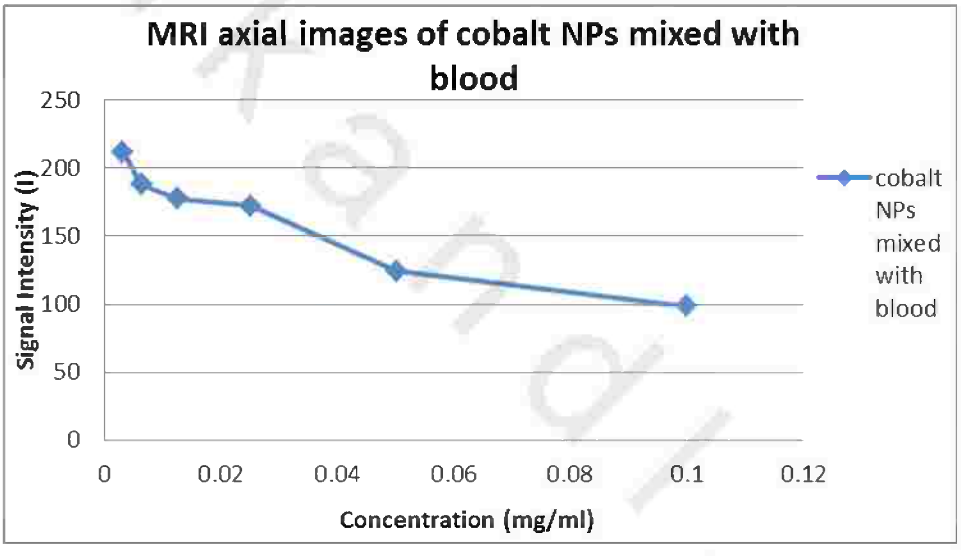

Figure (161): Variations in measured signal intensity with different concentration of axial NPs in MRI axial images

2.4. 2.2.3.6. MRI axial images measurements for GNPs Fe_3O_4 and Cobalt NPs

Table (29) signal intensity measurement values for GNPs Fe_3O_4 and Cobalt NPs

Concentration (mg/ml)	signal intensity measurement of GNPs mixed with blood	signal intensity measurement of Fe_3O_4 NPs mixed with blood	signal intensity measurement of cobalt NPs mixed with blood
0.10000	105.6	60.8	98.3
0.05000	133.4	78.9	124.2
0.02500	182	129	172.3
0.01250	184.6	136.3	177.6
0.00625	215.3	149.3	188
0.00312	217.7	154.3	212

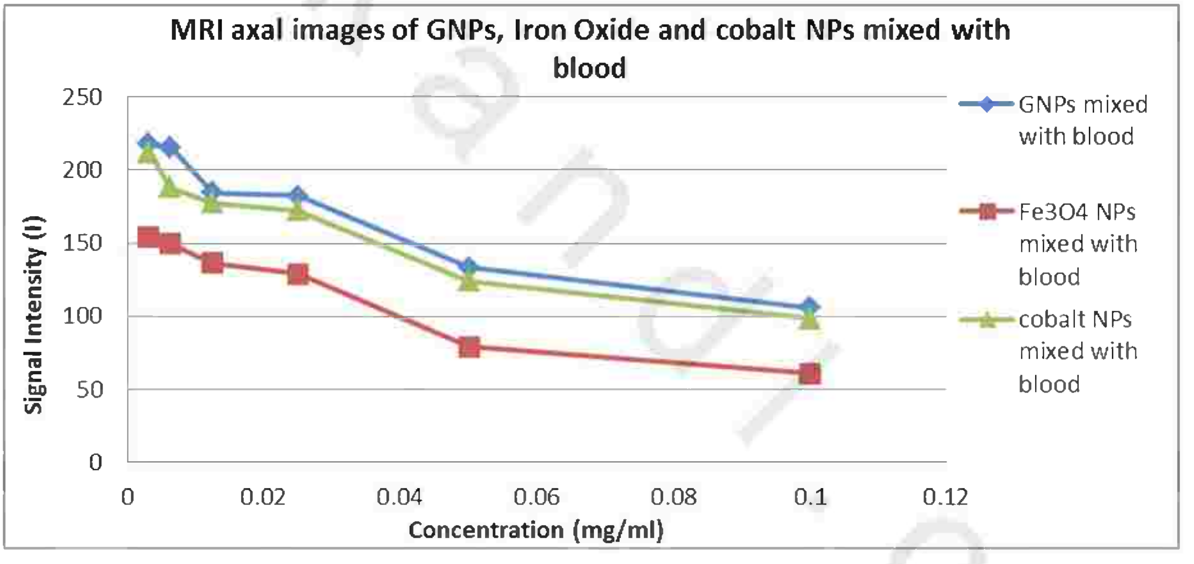

Figure (162): Variations in signal intensity measurements of MRI axial images between GNPs Fe_3O_4 and Cobalt NPs

5. Experiment Four

5.1. Phantom Four

1 ml of nickel and titanium nanoparticles with different concentrations was mixed with 1ml gel material in a plastic tube with 1cm diameter and 5cm height then scanned with different radiological equipments.

A

B

Figure (163): A, titanium nanoparticles with different concentrations mixed with 1ml gel material, B, nickel nanoparticles with different concentrations mixed with 1ml gel material in plastic tube

5.2. CT axial images for Titanium nanoparticles mixed with gel material

A CT axial cuts was performed for each tube that contains Titanium nanoparticles mixed with gel material and the hounsfield unit (HU) was measured for each of them

5.2.1. CT axial image for 0.1 mg/ml Titanium NPs mixed with gel material

A

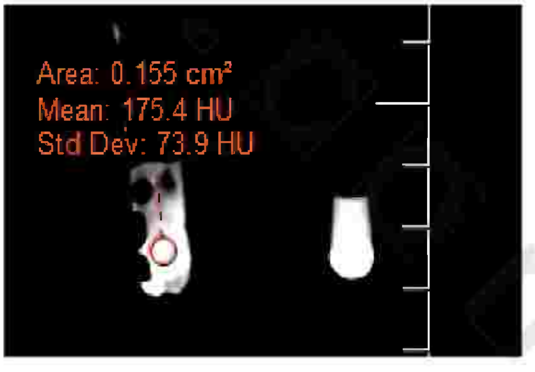

B

Figure (164): A, the test tube filled with gel that is mixed with 0.1 mg/ml Titanium NPs. B, HU measurement for the axial CT image of the same tube

5.2.2. CT axial image for 0.05 mg/ml Titanium NPs mixed with gel material

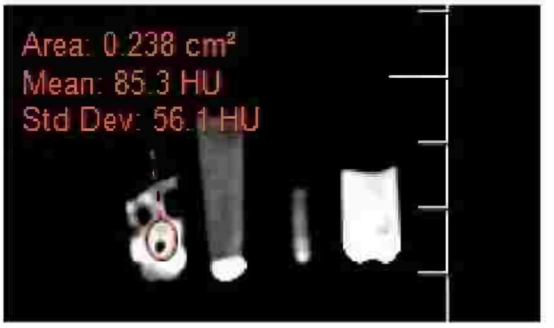

A B

Figure (165): A, the test tube filled with gel that is mixed with 0.05 mg/ml Titanium NPs. B, HU measurement for the axial CT image of the same tube

5.2.3. CT axial image for 0.025 mg/ml Titanium NPs mixed with gel material

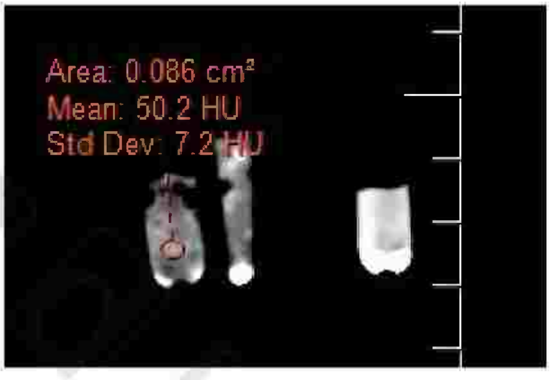

A B

Figure (166): A, the test tube filled with gel that is mixed with 0.025 mg/ml Titanium NPs. B, HU measurement for the axial CT image of the same tube

5.2.4. CT axial image for 0.0125 mg/ml Titanium NPs mixed with gel material

A

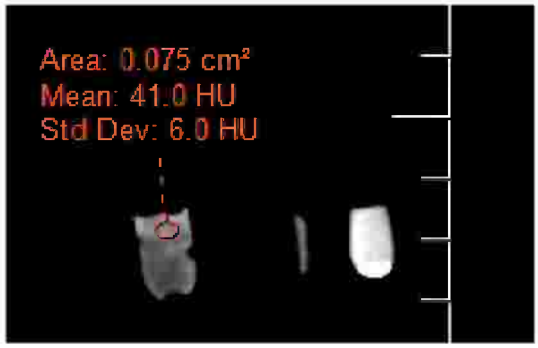

B

Figure (167): A, the test tube filled with gel that is mixed with 0.0125 mg/ml Titanium NPs. B, HU measurement for the axial CT image of the same tube

4.2.5. CT axial image for 0.00625 mg/ml Titanium NPs mixed with gel material

A

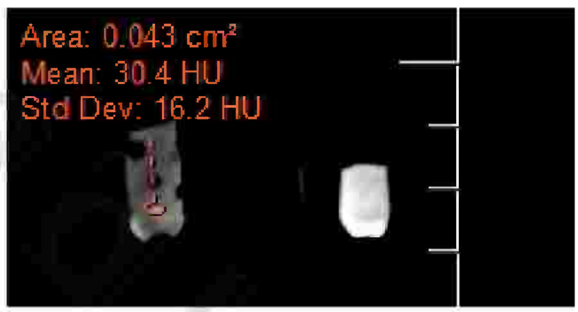

B

Figure (168): A, the test tube filled with gel that is mixed with 0.00625 mg/ml Titanium NPs. B, HU measurement for the axial CT image of the same tube

Table (30) Hounsfield units measurements for different concentrations (0.1, 0.05, 0.025, 0.0125 and 0.00625 mg/ml) of Titanium NPs in CT axial images

Concentration (mg/ml)	HU measurement of Titanium NPs mixed with gel
0.10000	175.4
0.05000	85.3
0.02500	50.2
0.01250	41
0.00625	30.4

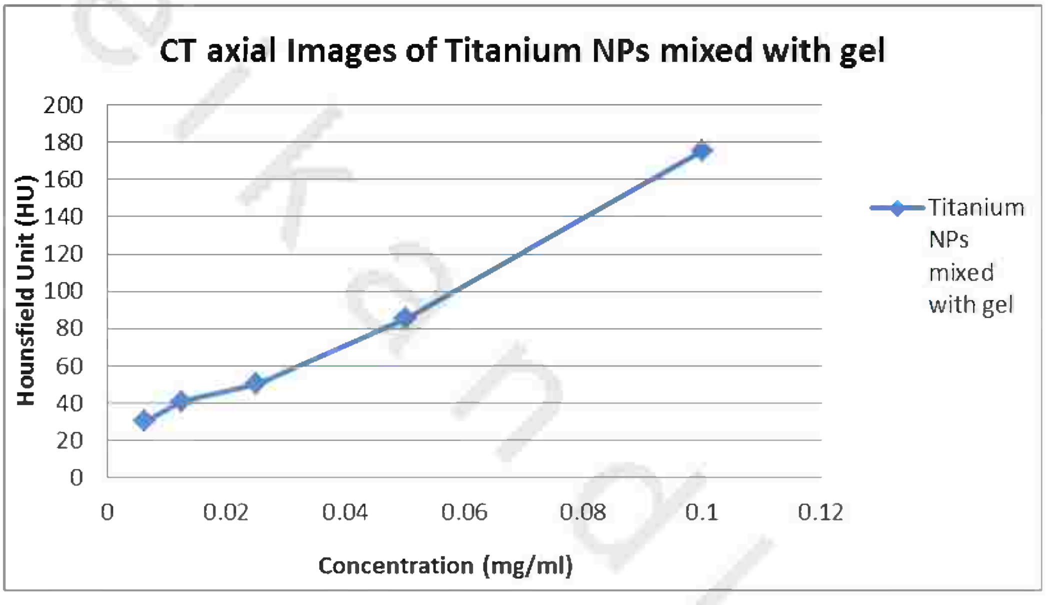

Figure (169): Variations in measured HU with different concentration of Titanium NPs in CT axial images.

5.3. CT axial images for nickel nanoparticles mixed with gel material

A CT axial cuts was performed for each tube that contains nickel nanoparticles mixed with gel material and the Hounsfield unit (HU) was measured for each of them

5.3.1. CT axial image for 0.1 mg/ml nickel NPs mixed with gel material


A

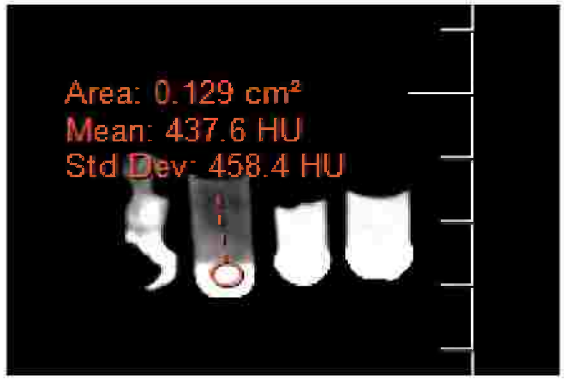

B

Figure (170): A, the test tube filled with gel that is mixed with 0.1 mg/ml nickel NPs. B, HU measurement for the axial CT image of the same tube

5.3.2. CT axial image for 0.05 mg/ml Titanium nickel NPs mixed with gel material


A

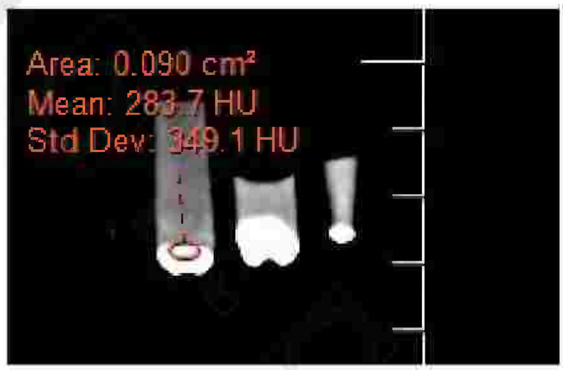

B

Figure (171): A, the test tube filled with gel that is mixed with 0.05 mg/ml nickel NPs. B,HU measurement for the axial CT image of the same tube

5.3.3. CT axial image for 0.025 mg/ml nickel NPs mixed with gel material

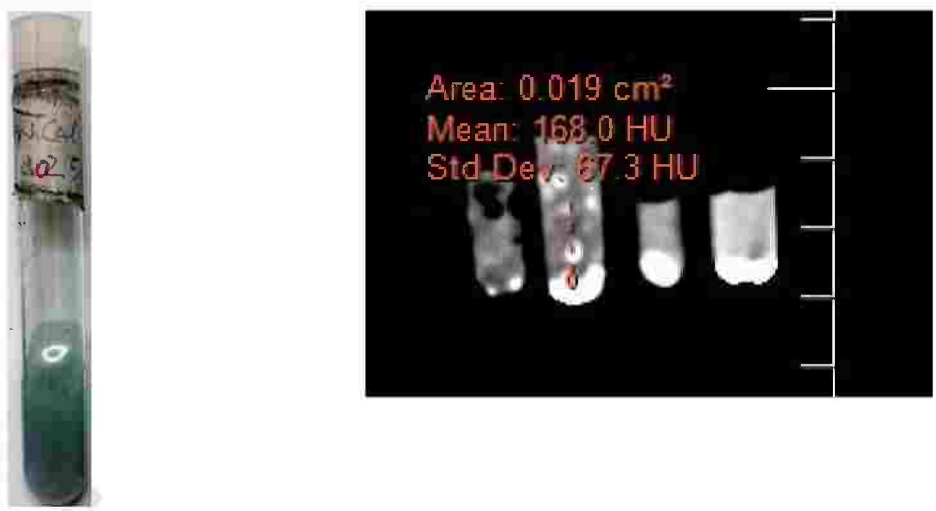

A B

Figure (172): A, the test tube filled with gel that is mixed with 0.025 mg/ml nickel NPs. B, HU measurement for the axial CT image of the same tube

5.3.4. CT axial image for 0.0125 mg/ml nickel NPs mixed with gel material

A B

Figure (173): A, the test tube filled with gel that is mixed with 0.0125 mg/ml nickel NPs. B, HU measurement for the axial CT image of the same tube

5.3.5. CT axial image for 0.00625 mg/ml nickel NPs mixed with gel material

A

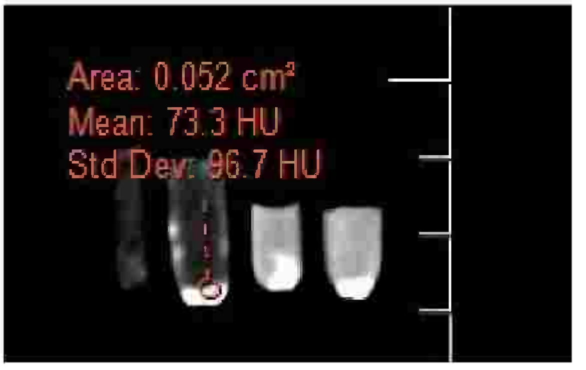

B

Figure (174): A, the test tube filled with gel that is mixed with 0.00625 mg/ml nickel NPs. B, HU measurement for the axial CT image of the same tube

Table (31) Hounsfield units measurements for different concentrations (0.1, 0.05, 0.025, 0.0125 and 0.00625 mg/ml) of nickel NPs in CT axial images

Concentration (mg/ml)	HU measurement of nickel NPs mixed with gel
0.10000	437.6
0.05000	283.7
0.02500	168
0.01250	110
0.00625	73.3

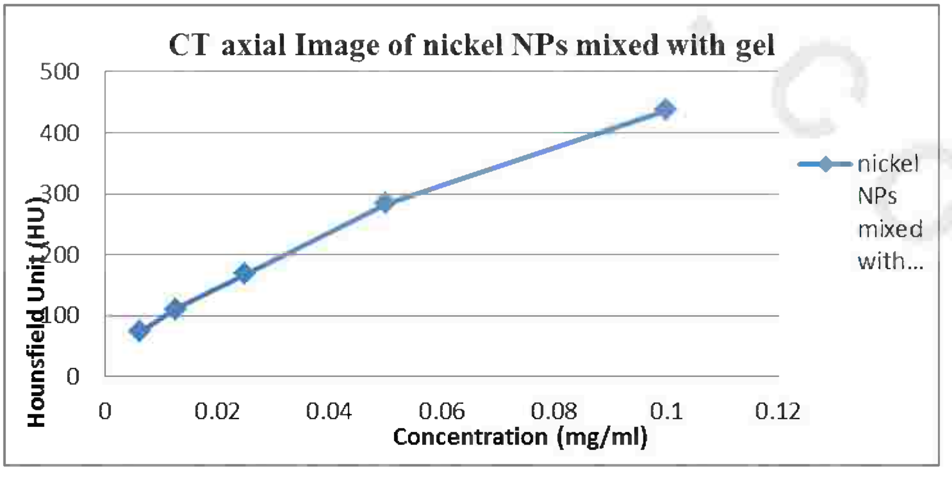

Figure (175): Variations in measured HU with different concentration of nickel NPs in CT axial images

5.3.6. HU measurements of CT axial images for TiO & Cobalt NPs

Table (32) HU measurement values for Titanium & Nickel NPs

Concentration (mg/ml)	HU measurement for Titanium NPs mixed with gel	HU measurement for nickel NPs mixed with gel
0.10000	175.4	437.6
0.05000	85.3	283.7
0.02500	50.2	168
0.01250	41	110
0.00625	30.4	73.3

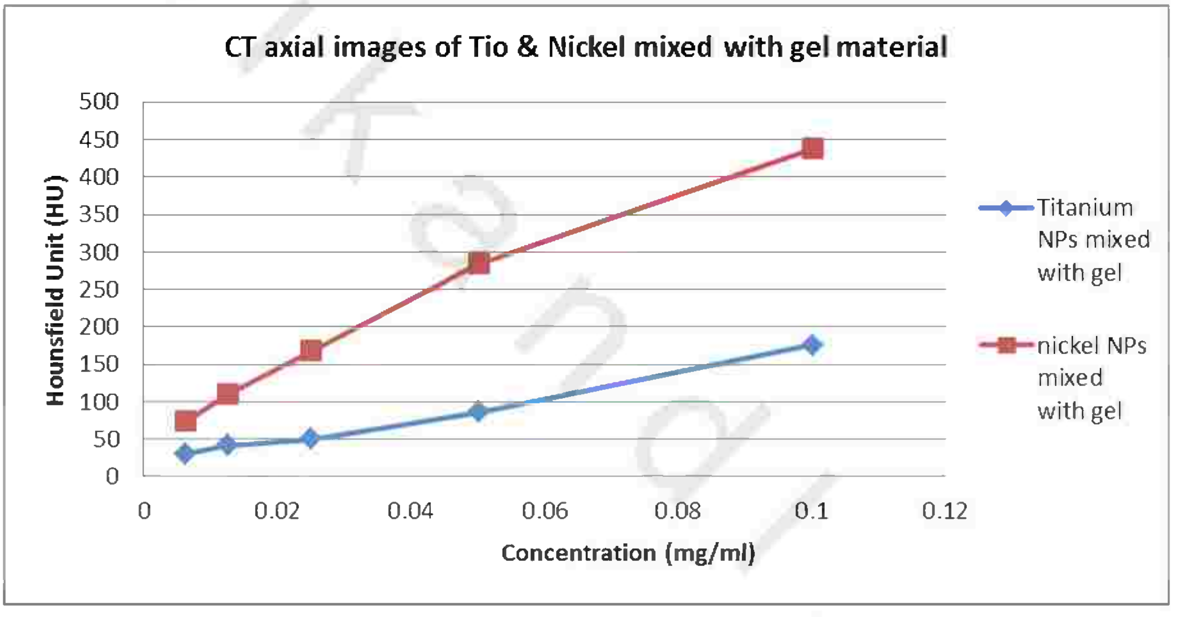

Figure (176): Variations in HU measurements of MRI axial images between Titanium & Nickel NPs

6. Experiment Five

6.1. Ultrasound examination for nanoparticles mixed with blood

A Longitudinal and transverse views s performed for each tube that contains NPs mixed with blood at different concentrations observing the different in echogenicity for each concentration.

Figure (177): Ultrasound imaging of phantom 5 containing the GNPs in Transverse position

6.2. Ultrasound Images

6.2.1. GNPs

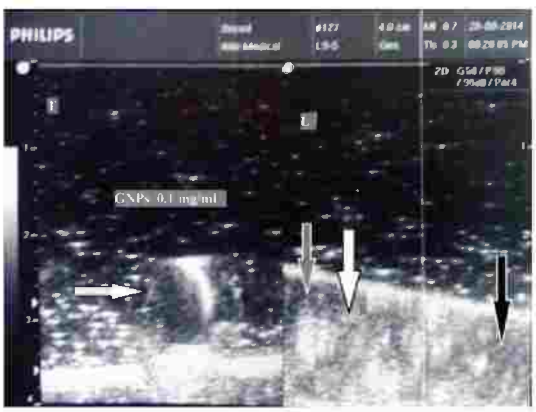

Figure (178): US image of tube that contains GNPs mixed with blood with concentration 0.1 mg/ml in two different views longitudinal & Transverse (Arrows)

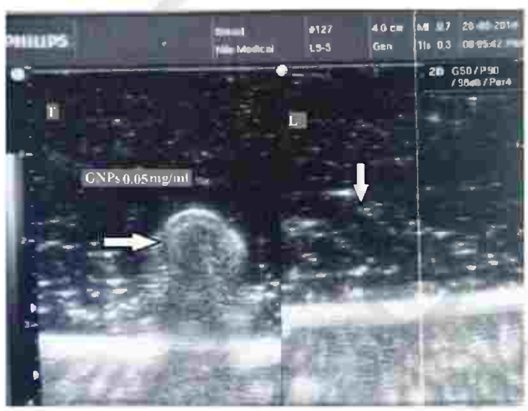

Figure (179): US image of tube that contains GNPs mixed with blood with concentration 0.05 mg/ml in two different views longitudinal & Transverse (Arrows)

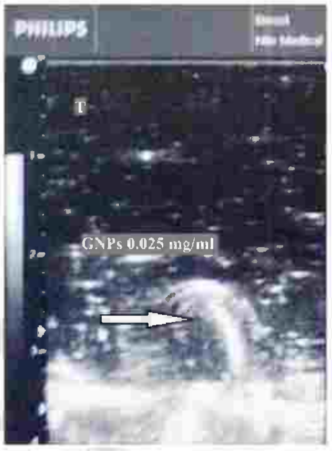

Figure (180): US image of tube that contains GNPs mixed with blood with concentration 0.025 mg/ml in Transverse view (Arrow)

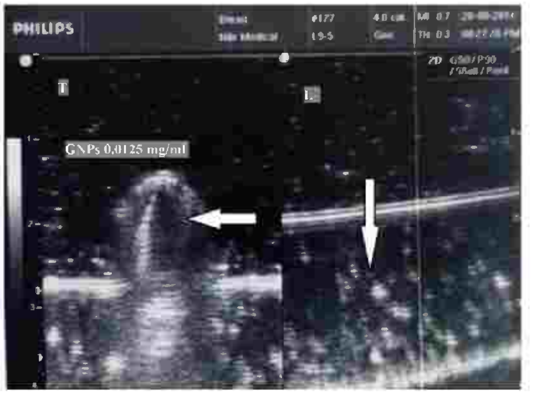

Figure (181): US image of tube that contains GNPs mixed with blood with concentration 0.0125 mg/ml in two different views longitudinal & Transverse (Arrows)

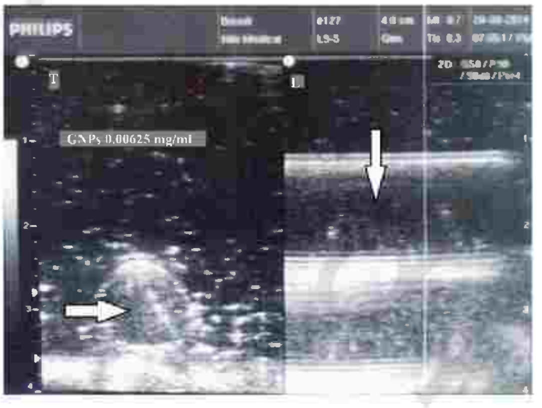

Figure (182): US image of tube that contains GNPs mixed with blood with concentration 0.00625 mg/ml in two different views longitudinal & Transverse (Arrows)

In the previous US images after neglecting the US shadow that results from the test tube containing the GNPs we had found that there is a different in echogenicity between different concentrations of the nanoparticles but it was not significant seen by the true eye in the transverse images (which appears as a hyper echoic circular object) but significant in the longitudinal images (which appears as a longitudinal tube with different echogenicity)and shows that the degree of echogenicity decreases with decreasing concentration of the nanoparticles.

6.2.2. Iron Oxide NPs

Figure (183): US image of tube that contains Fe_3O_4 NPs mixed with blood with concentration 0.1 mg/ml in two different views longitudinal & Transverse (Arrows)

Figure (184): US image of tube that contains Fe_3O_4 NPs mixed with blood with concentration 0.05 mg/ml in two different views longitudinal & Transverse (Arrows)

Figure (185): US image of tube that contains Fe_3O_4 NPs mixed with blood with concentration 0.025 mg/ml in two different views longitudinal & Transverse (Arrows)

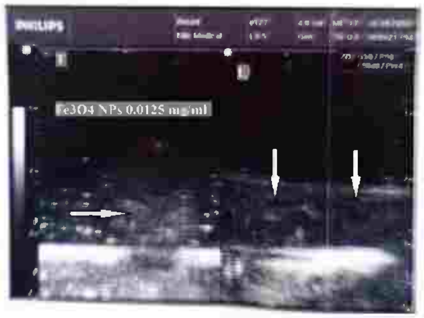

Figure (186): US image of tube that contains Fe_3O_4 NPs mixed with blood with concentration 0.0125 mg/ml in two different views longitudinal & Transverse (Arrows)

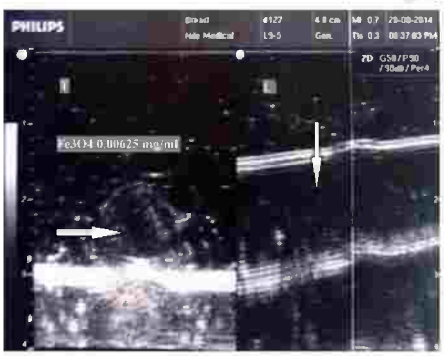

Figure (187): US image of tube that contains Fe_3O_4 NPs mixed with blood with concentration 0.00625 mg/ml in two different views longitudinal & Transverse (Arrows)

In the previous US images after neglecting the US shadow that results from the test tube containing the Fe_3O_4 nanoparticles we had found that there is a significant difference seen by the true eye in the transverse and longitudinal images and shows that the degree of echogenicity decreases with decreasing concentration of the nanoparticles.

7. Computational Simulations

7.1. Computational study of the EF intensity distribution around nanoparticles in phantom I

Determination of Gap Distance between GNPs Because of nanoparticles tiny size, atoms and molecules cannot be counted by direct observation. But much as we do when "counting" beans in a jar, we can estimate the number of particles in a sample of an element or compound if we have some idea of the volume occupied by each particle and the volume of the container. By knowing the following:

1- The concentration of the sample,

2- The volume of single GNPs.

We can determine the gap distance between two neighboring GNPs, since the radios of a single GNPs which is (2.5 nm), so the volume of it can be determined, by multiply volume of a single GNPs by the density of each sample we get the mass of a single GNPs, by dividing the total mass by the mass of a single GNPs we get the total number of GNPs in each concentration in cm3

We can do the following to calculate the gap distance between GNPs for different concentration:

1- After calculating the total number of GNPs in each concentration in cm3 ,

2- Taking the cubic root we get the number of GNPs in a one cm3,

3- Taking the inverse of the number of GNPs in a one cm we get the space between GNPs in cm units,

4- Multiplying this space by 107, we get the space between GNPs in nm units.

By applying the previous four steps for the GNPs of the five concentrations (0.1ml, 0.05ml, 0.025ml, 0.0125ml and 0.00625ml) a gap distance (S) between GNPs (Figure.188) calculated as shown in (Table 32), and fig 189.a.

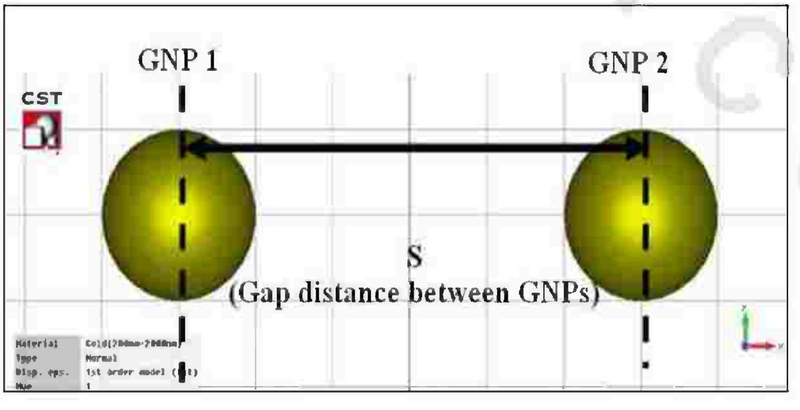

Figure (188): Gap distance (S) between GNPs.

Table (33) Gap distance (S) between GNPs for different concentration

Concentration (mg/ml)	Gap distance (S) between GNPs (nm)
0.10000	23
0.05000	30
0.02500	37
0.01250	47
0.00625	59

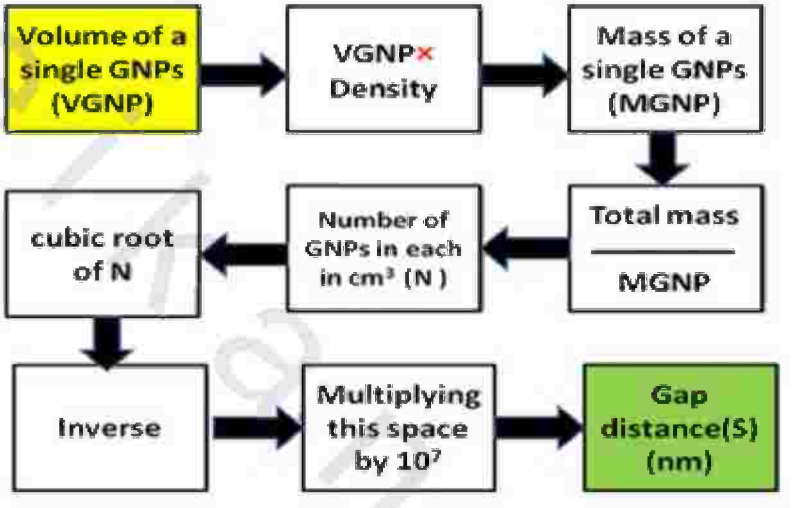

Figure (189): Calculation diagram for gap distance calculation

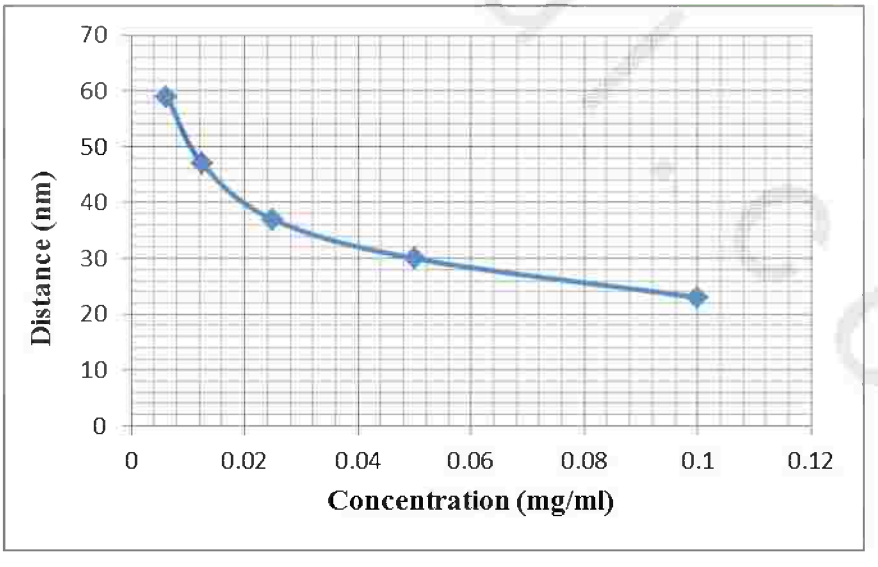

Figure (190): Shows the gap distance (S) change for different concentration, it note that by decreasing the concentration the gap distance increases, i.e we have indirect proportion between GNPs concentration (mg/ml) and gap distance (S).

7.1.1. The Model

The modeling and simulation was performed in CST STUDIO SUITE electromagnetic simulation software. Preliminary simulation and proof of concept were conducted in CST STUDIO Designer, while the complete simulation was conducted in CST STUDIO frequency domain solve.

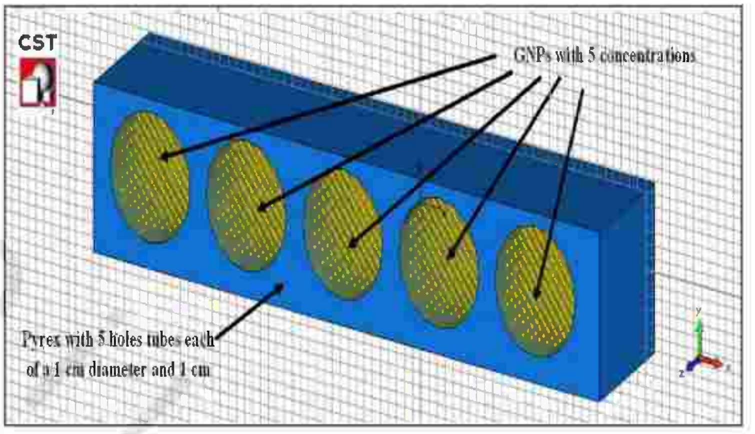

Figure (191): The Phantom model simulated in CST STUDIO.

Figure (191) shows the phantom model represented in CST STUDIO, which consists of five Pyrex tubes of a 1 cm diameter and 1 cm height felled with GNPs wilt 5 concentrations.

Simplify the Calculation By making a simple mathematical calculation for the tube volume which is a cylinder , and a single GNPs with Spherical shape , we get the total count of GNPs in concentration(1) which is equal approximately 12×106 GNPs.

In order to keep the problem under simple limits of complexity, the simulation will be performed on a two neighbor GNPs.

7.1.1.1. Electric Field Simulation for the Five Concentrations Simulation performed in six steps:

1- Step from 1 to 5, is the simulation of electric field (EF) intensity at both the gap distance (S) between GNPs and at the edges of GNPs for the five concentrations according to the change of gap distances (s) (23, 30, 37, 47 and 59 nm).

2- Merge the results obtained from step 1 to 5 to study the relation between gap distance change due concentration change and the EF intensity values which effect on the X-ray diagnoses.

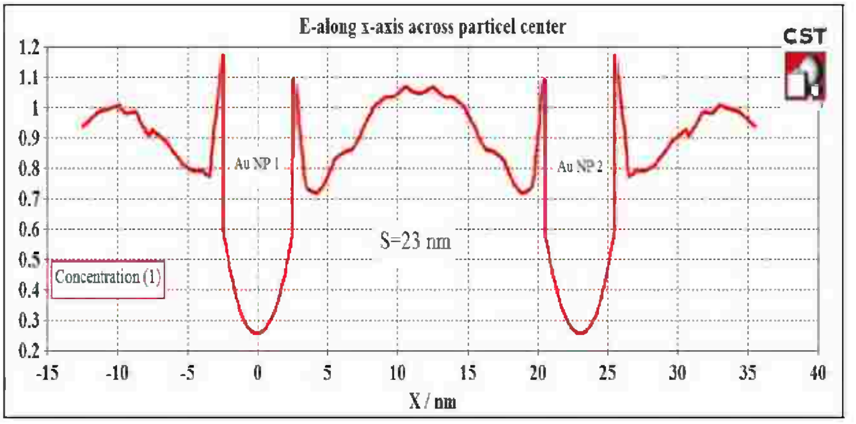

(a)

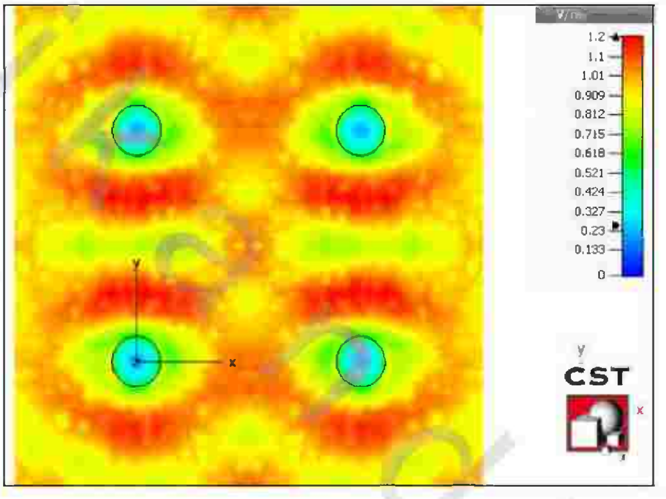

(b)

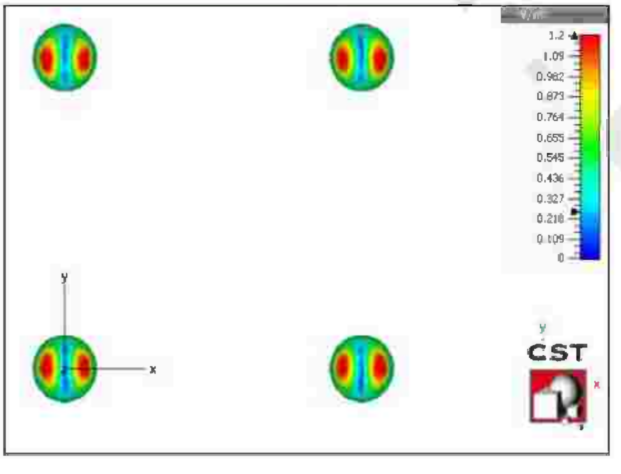

(c)

Figure (192): (a) The Electric field (EF) intensity distribution for GNPs for concentration (1), 2D of EF intensity, (b) EF intensity distribution, (c) 3D EF intensity

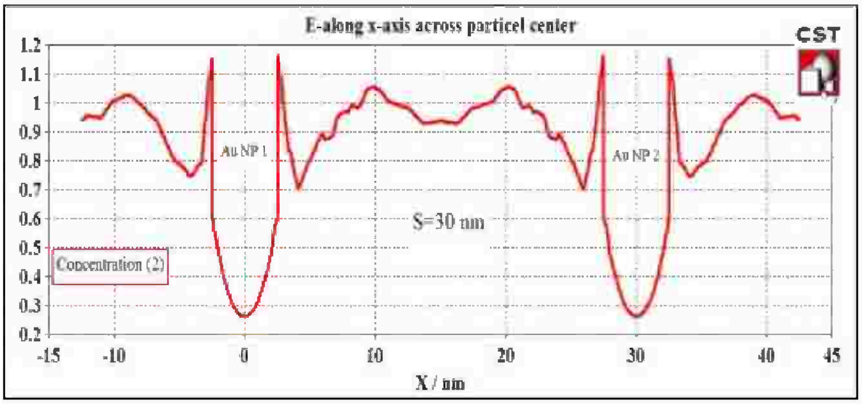
E-along x-axis across particel center
CST
Au NP 1
Au NP 2
S=30 nm
Concentration (2)
X / nm

(a)

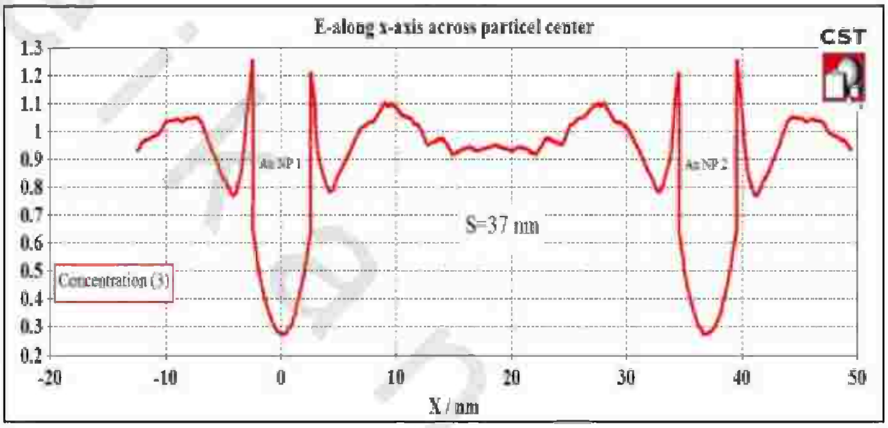
E-along x-axis across particel center
CST
Au NP 1
Au NP 2
S=37 nm
Concentration (3)
X / nm

(b)

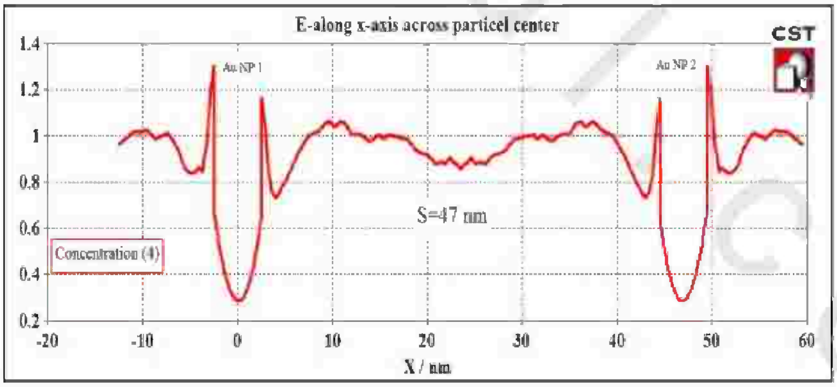
E-along x-axis across particel center
CST
Au NP 1
Au NP 2
S=47 nm
Concentration (4)
X / nm

(c)

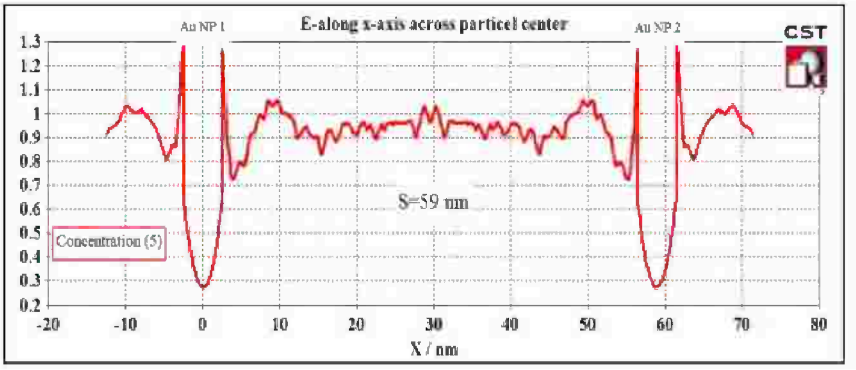

(d)

Figure (193): The 2D Electric field (EF) intensity, (a) concentration (2), (b) concentration (3), (c) concentration (4) , (d) concentration (5)

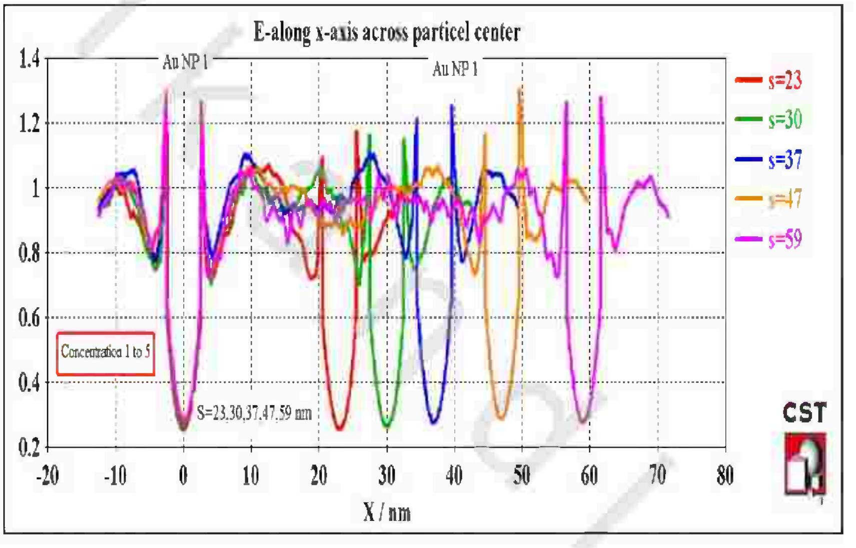

Figure (194): The 2D electric field (EF) intensity after merging the results of the five concentrations

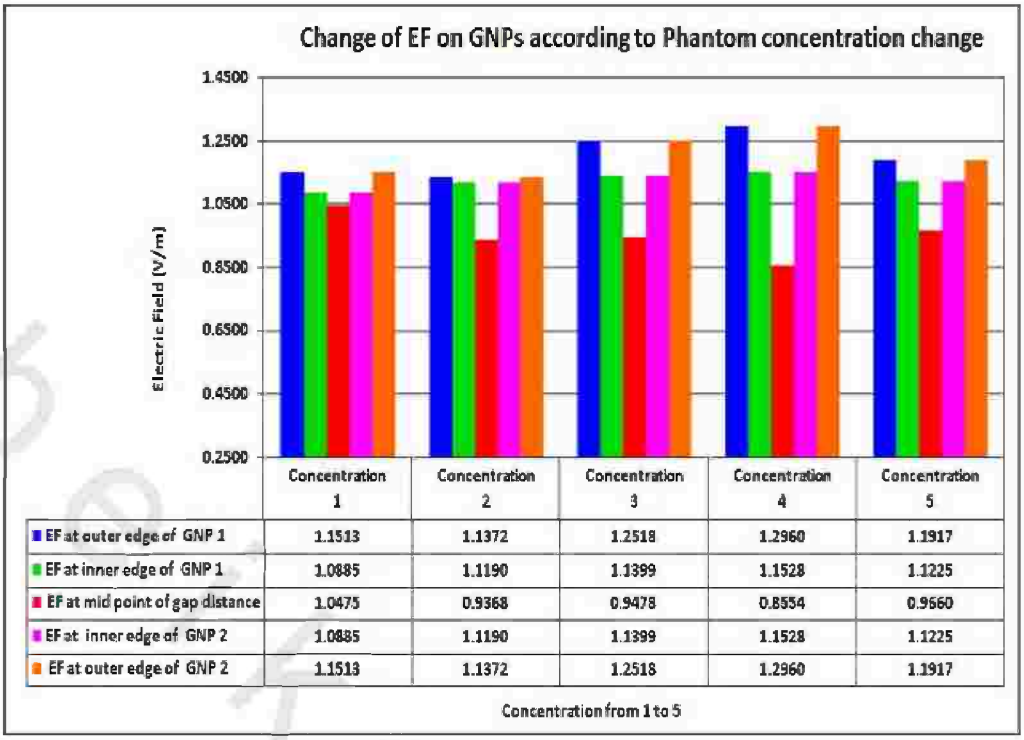

	Concentration 1	Concentration 2	Concentration 3	Concentration 4	Concentration 5
EF at outer edge of GNP 1	1.1513	1.1372	1.2518	1.2960	1.1917
EF at inner edge of GNP 1	1.0885	1.1190	1.1399	1.1528	1.1225
EF at mid point of gap distance	1.0475	0.9368	0.9478	0.8554	0.9660
EF at inner edge of GNP 2	1.0885	1.1190	1.1399	1.1528	1.1225
EF at outer edge of GNP 2	1.1513	1.1372	1.2518	1.2960	1.1917

Figure (195): The 2D electric field (EF) intensity at midpoint of gap distance (red), outer edges of gold nanoparticles 1 (blue), inner edges of gold nanoparticles 1 (green), outer edges of gold nanoparticles 2 (orange), inner edges of gold nanoparticles 2 (pink).

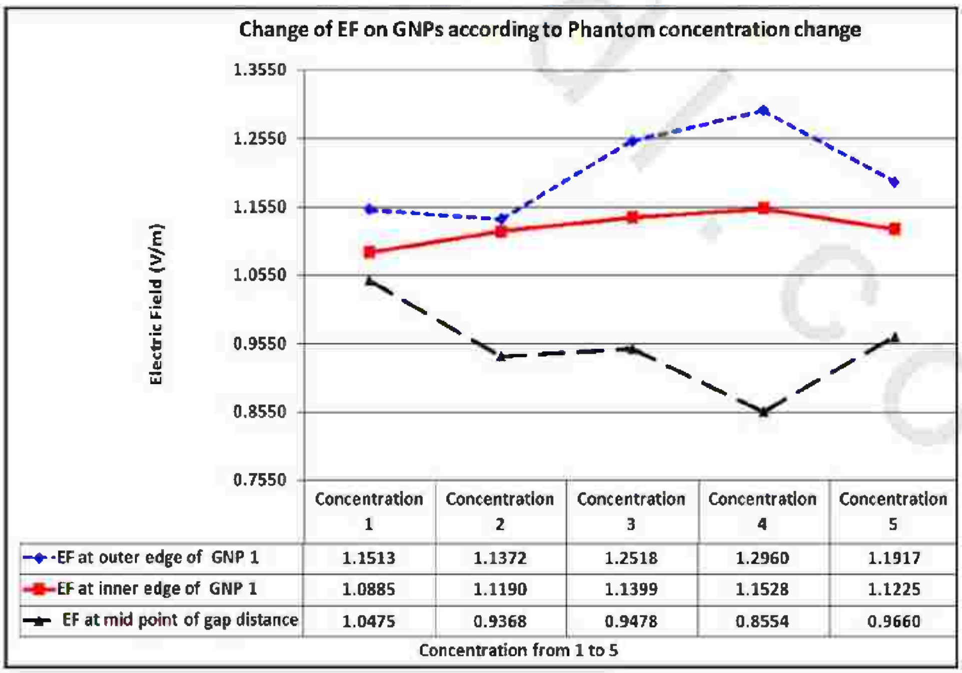

	Concentration 1	Concentration 2	Concentration 3	Concentration 4	Concentration 5
EF at outer edge of GNP 1	1.1513	1.1372	1.2518	1.2960	1.1917
EF at inner edge of GNP 1	1.0885	1.1190	1.1399	1.1528	1.1225
EF at mid point of gap distance	1.0475	0.9368	0.9478	0.8554	0.9660

Figure (196): The 2D Electric field (EF) intensity on midpoint of gap distance and outer, inner edges of GNP

From figures (180 to 184) and table.4 which represent the EF intensity distribution on the gap distance between GNPs and on the inner and outer edges of them for the five concentrations of GNPs, the following results noted:

1. By decreasing the concentrations the gap distances (S) increases gradually from (23 nm) at concentration (1) , until it reach (59 nm) at concentration (5),
2. The multipacks electric field at the gap distance decreases gradually from (1.0475V/m) at concentration (1), until it reach (0.9660 V/m) at concentration (5).
3. The EF at the inner edges of GNPs fluctuated during the five concentrations between (1.0885 V/m) and (1.1528V/m).
4. The EF at the inner edges of GNPs fluctuated during the five concentrations between (1.2960 V/m) and (1.1372V/m).
5. The average of EF intensity of all EF value (midpoint , outer edges of GNPs 1, inner edges of GNPs 1, outer edges of GNPs 2,and inner edges of GNPs 2) have value ≈ 1 V/m.

Table (34) The value of EF intensity (V/m) at midpoint of gap distance, outer edges of GNPs 1, inner edges of GNPs 1 , outer edges of GNPs 2 , and inner edges of GNPs 2

ration Concent	Electric Field (V/m) at				
	outer edge of GNP 1	**inner edge of GNP 1**	**midpoint of gap distance**	**inner edge of GNP 2**	**outer edge of GNP 2**
1	1.1513	1.0885	1.0475	1.0885	1.1513
2	1.1372	1.1190	0.9368	1.1190	1.1372
3	1.2518	1.1399	0.9478	1.1399	1.2518
4	1.2960	1.1528	0.8554	1.1528	1.2960
5	1.1917	1.1225	0.9660	1.1225	1.1917

7.2. Computational Study of EF distribution around nanoparticles in phantomII:

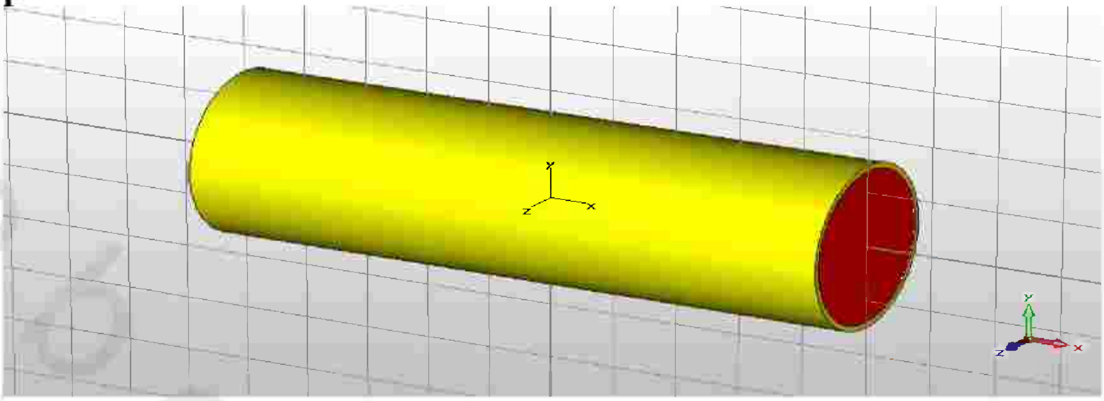

(a)

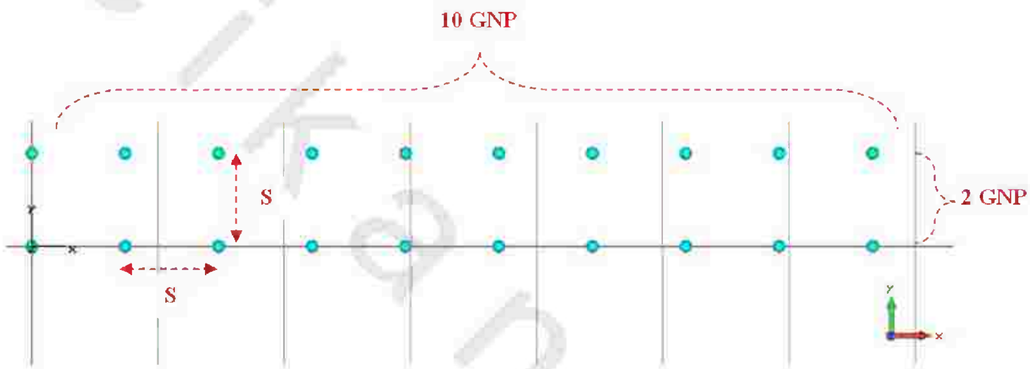

(b)

Figure (197): (a) 3D view of the phantom ,(b) An Array of 20 GNP (2×10), where S is the space between nanoparticles which change by change the concentration.

This phantom is made up of multiple tubes with 30cm long and diameter 3ml each tube is filled with blood and had been injected with different concentrations of gold and iron oxide nanoparticles (0.1ml-0.05ml-0.025ml-0.0125ml)

The volume of each tube in nm scale is 2.12×10^{21} nm^3 , at concentration (1) (0.1 ml) the distance between gold nanoparticles (S = 23 nm), by knowing the volume of a single GNP which is 65.45 nm^3 , we will have about 1.4×10^{18} gold nanoparticles , and it's impossible to simulate this huge amount of GNP , so in order to simplify the computation and simulation , an array slab of (20 GNP) (2×10) is taken as a sample for simulation as shown in fig (197).

The space (S) is changed by changing the concentration to be 23,30,37,47,and 59 for the five concentrations.

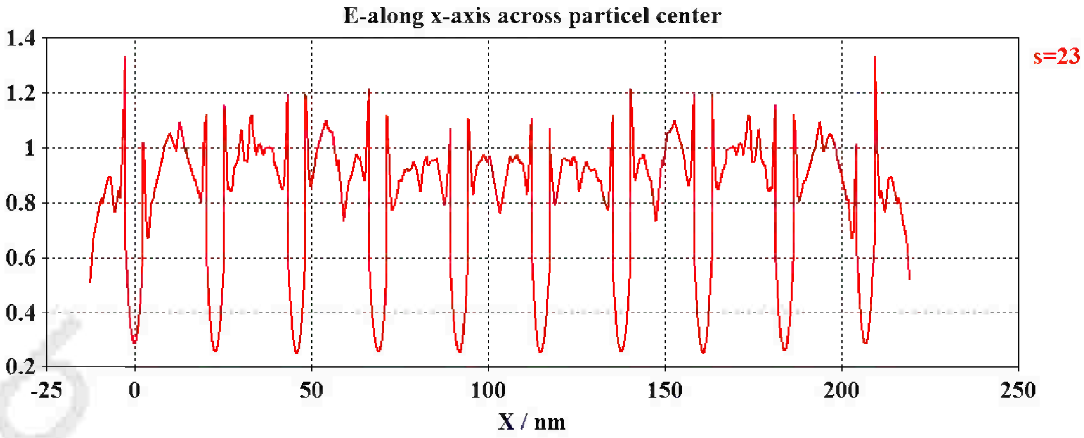

Figure (198): A 2D of the Electric field (EF) intensity distribution for GNPs for concentration (1)

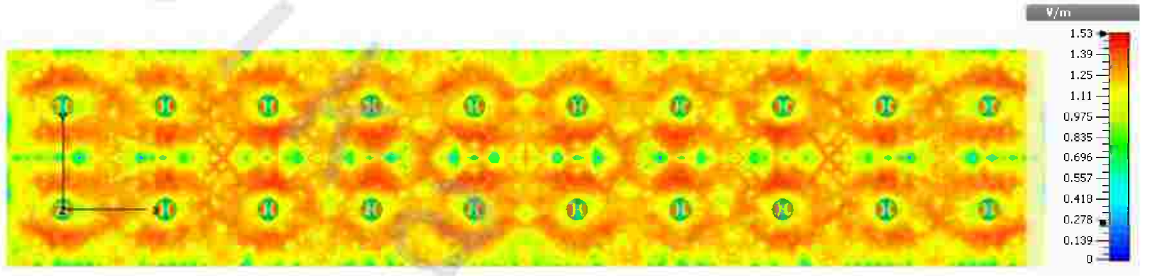

Figure (199): The Electric field (EF) intensity distribution for GNPs for concentration (1) front view

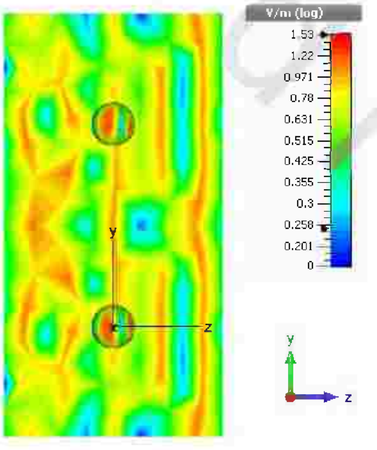

Figure (200): The Electric field (EF) intensity distribution for GNPs for concentration (1) side vie

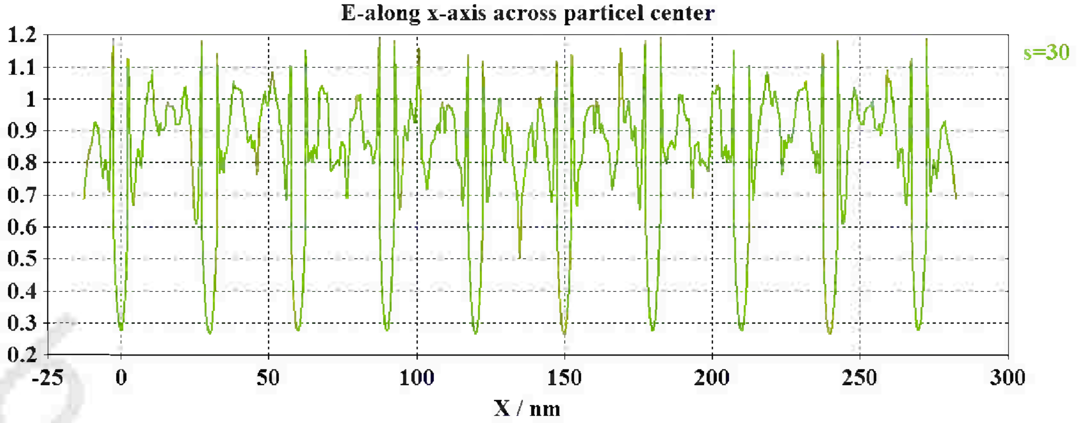

Figure (201): A 2D of the Electric field (EF) intensity distribution for GNPs for concentration (2)

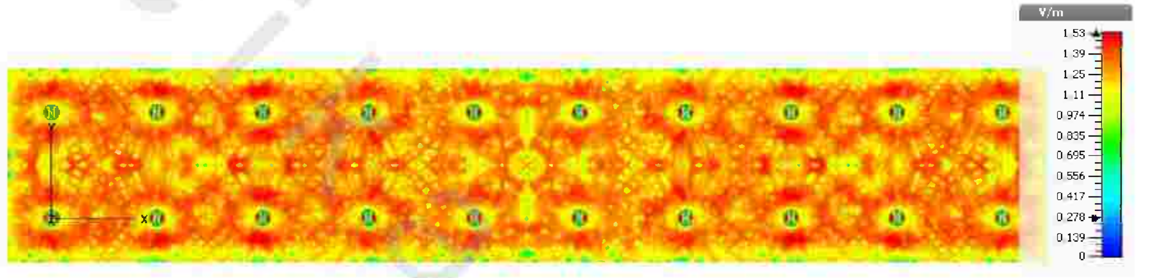

Figure (202): The Electric field (EF) intensity distribution for GNPs for concentration (2) front view

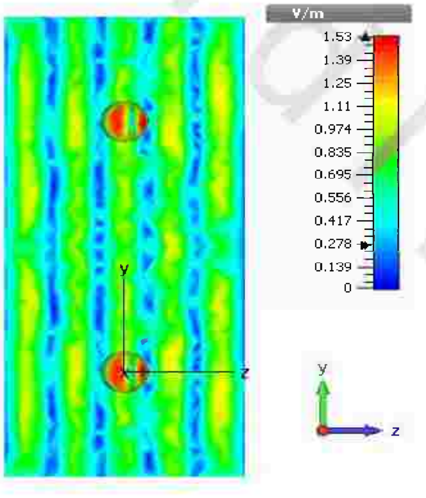

Figure (203): The Electric field (EF) intensity distribution for GNPs for concentration (2) side view

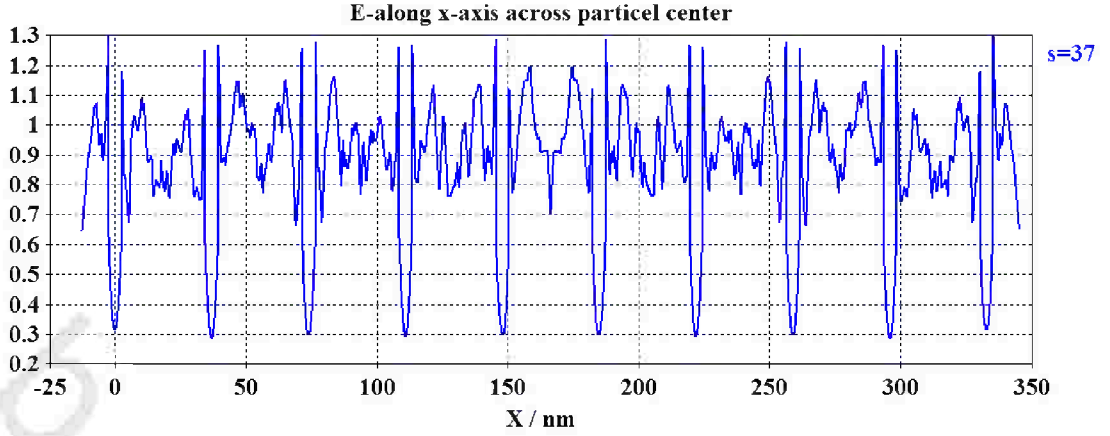

Figure (204): A 2D of the Electric field (EF) intensity distribution for GNPs for concentration (3)

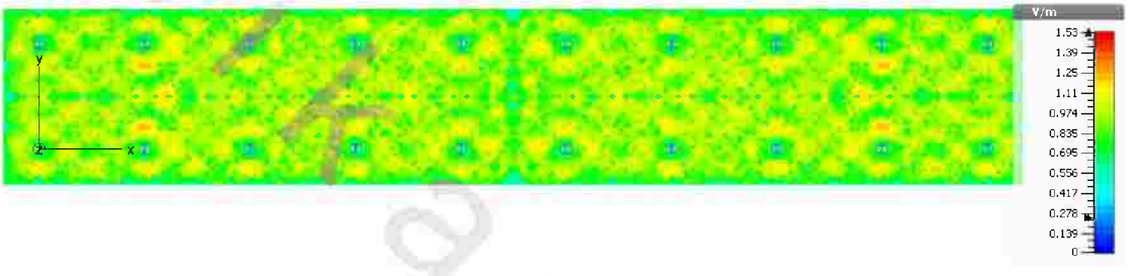

Figure (205): The Electric field (EF) intensity distribution for GNPs for concentration (3) front view

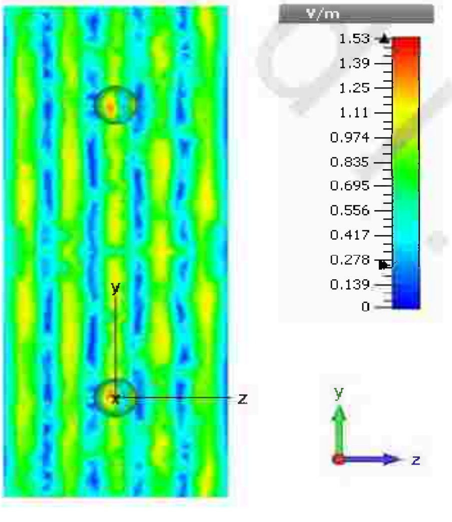

Figure (206): The Electric field (EF) intensity distribution for GNPs for concentration (3) side view

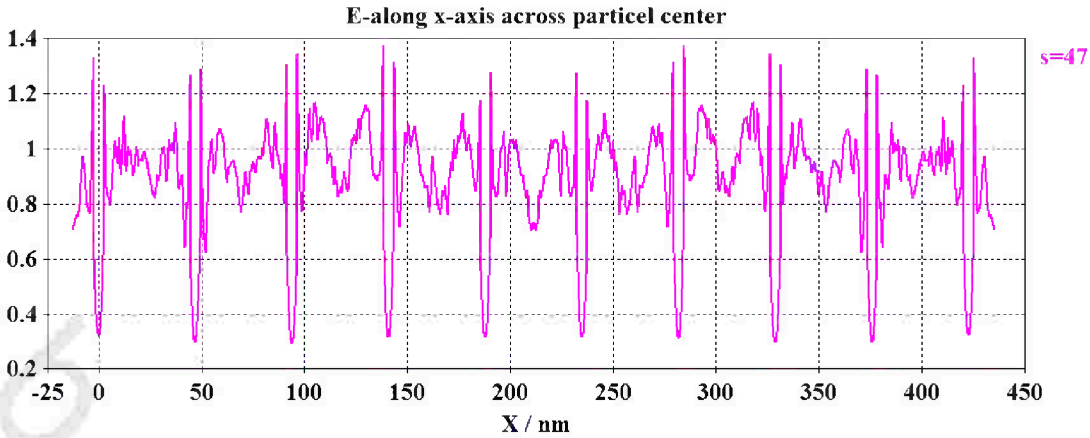

Figure (207): A 2D of the Electric field (EF) intensity distribution for GNPs for concentration (4)

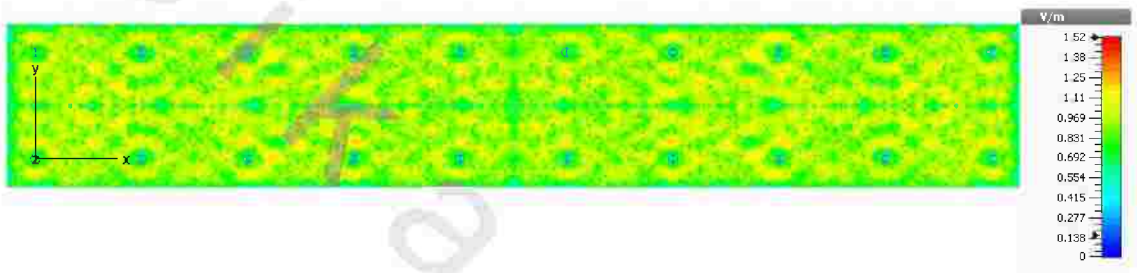

Figure (208): The Electric field (EF) intensity distribution for GNPs for concentration (4) front view

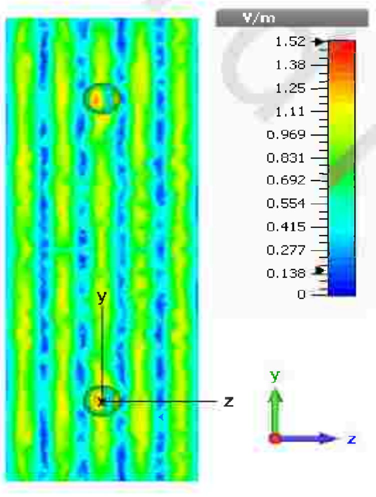

Figure (209): The Electric field (EF) intensity distribution for GNPs for concentration (4) side view

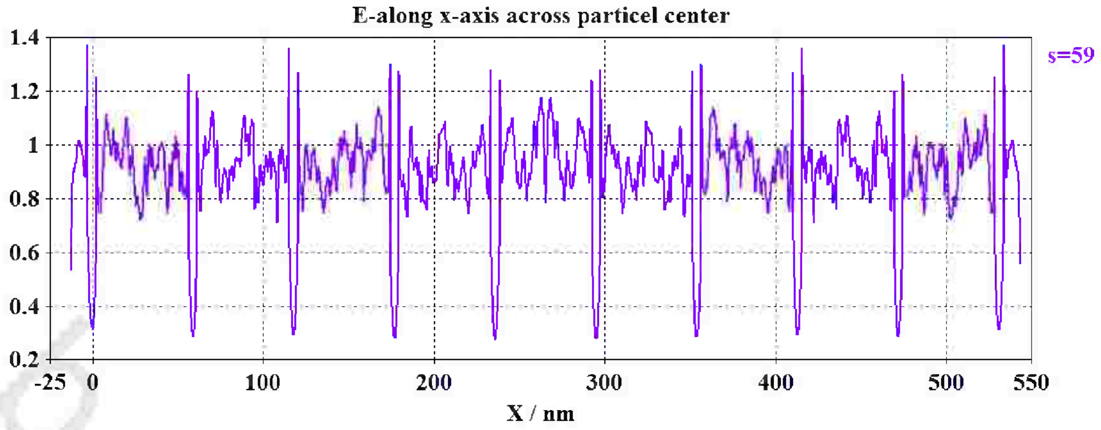

Figure (210): A 2D of the Electric field (EF) intensity distribution for GNPs for concentration (5)

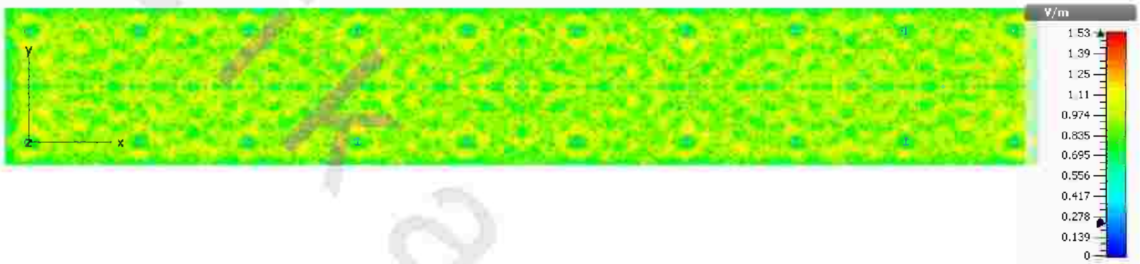

Figure (211): The Electric field (EF) intensity distribution for GNPs for concentration (5) front view

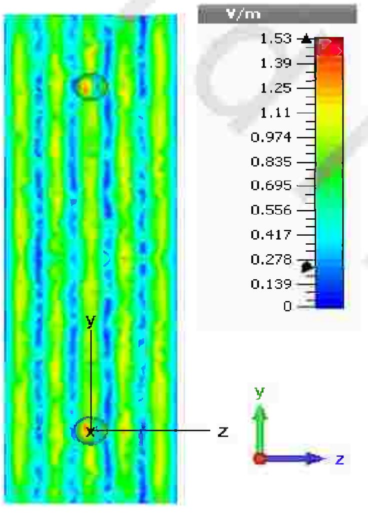

Figure (212): The Electric field (EF) intensity distribution for GNPs for concentration (5) side view

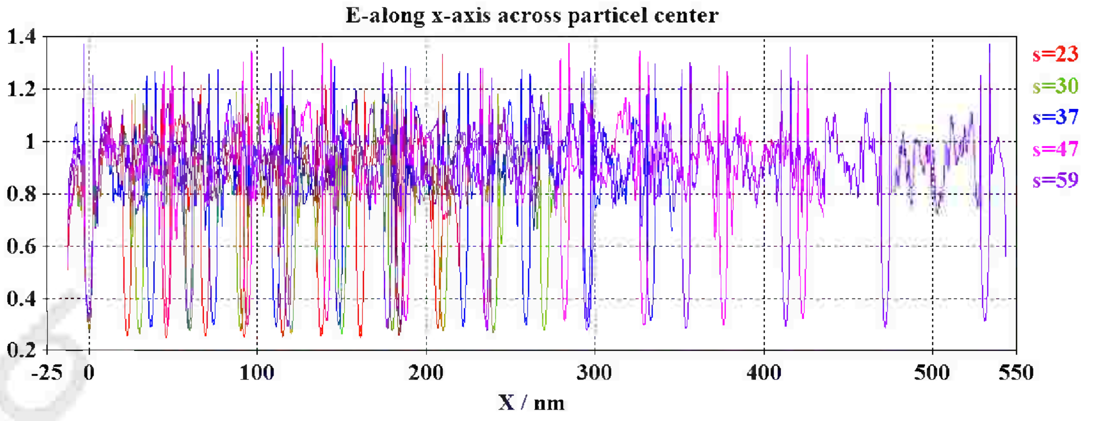

Figure (213): A 2D of the Electric field (EF) intensity distribution for GNPs for concentration (1,2,3,4 and 5)

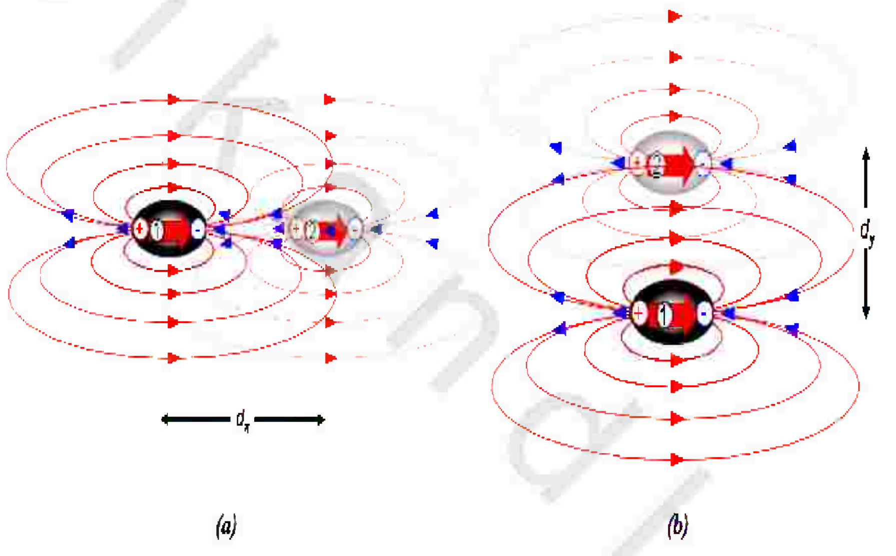

Figure (214): A sketch of the field distribution of two neighboring nanoparticles. The excitation field is polarized along the x-direction for both sketches

The distance between the particles in the x and y directions are d_x and d_y respectively. In this setup, the light incident on the particle array is polarized along the x-direction. Let us first consider the effect of particles aligned along the x-direction. The charge oscillations induced in an isolated particle (particle 1) create a field distribution which is sketched in Fig 214. (a). Particle 2, which is drawn in a lighter color, also has a similar field distribution. The dipole field of particle 1 at the center of particle 2 is in the same direction as the field of particle 2.

The restoring force on the displaced electron cloud of a particle depends directly on the field inside the particle. Since the field of particle 1 enhances the field inside particle 2, the restoring force is increased, resulting in a blue-shift of the resonance frequency of the Froehlich mode.

Now consider the interactions between neighboring particles in the y-direction. The fields of two particles are shown in Fig 214. (b). Here, the field of particle 1 at the center of particle 2 opposes the internal field of particle 2. Thus, as the field strength is reduced inside the particle, the resonance frequency is also decreased.

Clearly, as the distance dx or dy increases, the influence of a particle on its neighboring particle reduces. Correspondingly, the deviation of the particle's resonance frequency from its individual resonance frequency decreases. This dependence of particle resonance on inter-particle spacing was demonstrated by Maier et al [(128)] and Sweatlock et al. [(129)]

The above description is applicable for the near-field region, in which the quasi-static approximation is valid. However, when the inter-particle distance is increased to the order of the wavelength, diffractive contributions start playing an important role. Zou et al. [(230)] studied a one-dimensional array of nanoparticles, of various sizes with various spacings. They found that the scattered light showed the features of the individual dipoles, as well as diffractive features of the entire array.

7.3. Computational study of the attachment of NPs on cancer cell:

The free electrons in the metal are free to travel through the material. The mean free path in gold is 50 nm; therefore in particles smaller than this, no scattering is expected from the bulk. Thus, all interactions are expected to be with the surface.

When the wavelength of light is much larger than the nanoparticle size it can set up standing resonance conditions.

Light in resonance with the surface Plasmon oscillation causes the free-electrons in the metal to oscillate. As the wave front of the light passes, the electron density in the particle is polarized to one surface and oscillates in resonance with the light's frequency causing a standing oscillation. The resonance condition is determined from absorption and scattering spectroscopy and is found to depend on the shape, size, and dielectric constants of both the metal and the surrounding material. This is referred to as the surface Plasmon resonance, since it is located at the surface, as the shape or size of the nanoparticle changes, the surface geometry changes causing a shift in the electric field density on the surface. This causes a change in the oscillation frequency of the electrons, generating different cross-sections for the optical properties including absorption and scattering[(131-132)]

The electrons in metal are not bound to individual atoms; instead, they form a cloud around the atomic core Fig.215. The mobile electron cloud enables metals to transfer their charges easily. Due to this feature, the conductivity of metals is high. This also explains why metals shine; light hitting the electron cloud surrounding metal surfaces reflects back to our eyes. Since atomic cores are blocked by the electron cloud, they do not absorb photons. Consequently, the brightness of metals is associated with the photons reflecting back to our eyes. [(133)]

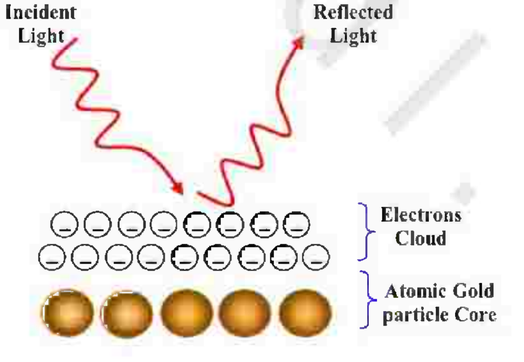

Figure (215): The electron cloud surrounding metals prevents incident light from being absorbed by the nucleus

As we further know from quantum mechanics, electrons can behave as waves or particles. If we consider the electrons inside an electron cloud as waves within a certain energy value, we can envision a situation where it is possible for light of the same wavelength to be absorbed by the electron cloud and move through the electron cloud by producing resonance.

When a metal absorbs light at the length of the resonance wavelength, this causes the electrons to vibrate and scatter energy. This process generally occurs on the surface of metals.

It continues through the electron cloud and is therefore called surface plasmon resonance. The name 'plasmon' originates from the oscillations of the electron cloud. (134) Gold nanostructures with surface plasmon resonance have become prominent in optical imaging applications owing to their strong light absorption and scattering in the visual and near infrared portion of the spectrum. (135-136) these optical skills, which depend on the size, shape, and dielectric constant of nanoparticles, enable applications where particles are used as imaging and sensing probes.

The GNPs are injected through the blood circulatory system which delivered them to the site of the targeting cancer, and since GNP is 100 smaller than the red blood cell its own the unique ability of passing through tissue molecules and would only seek out cancer cells, leaving healthy cells and tissue untouched, then it will attach to the surface membrane of the cancer cell.

Cancer cells are generally larger than normal cells and its dimension in the range of micrometer (μm), for demonstration, simulate the imaging of a sphere cancer cell of a diameter (T_D=1 μm) surrounded by an array of GNPs consisting of 36 GNP each of a diameter (P_D=100 nm) as shown in fig. (215)

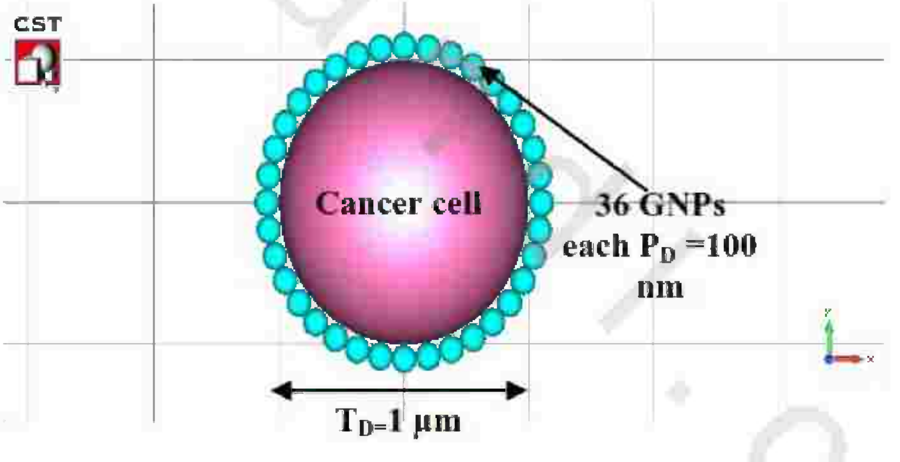

Figure (216): A Cancer cell surrounding by 36 NGPs

Figure (216) shows the EF intensity distribution of a single cancer cell with a diameter 1 μm Surrounded by 36 gold nanoparticle (GNP) with a diameter 100 nm, it note that the 36 attached GNP

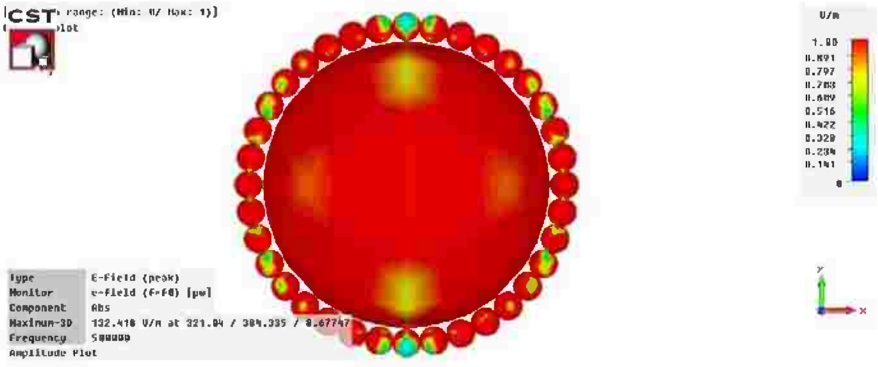

(a)

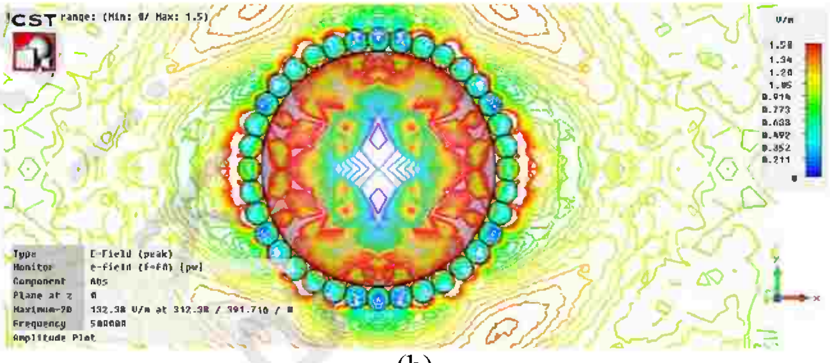

(b)

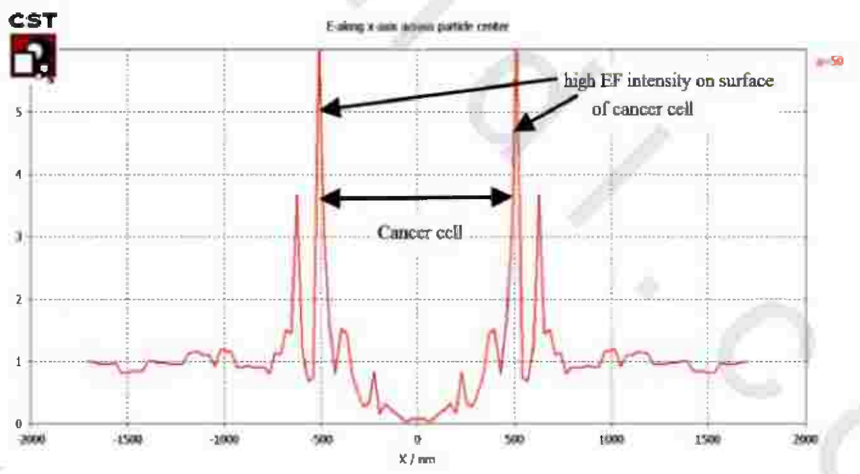

(c)

Figure (217): The EF intensity distribution for 36 GNPs attached to the cancer cell surface. (a) EF intensity. (b) EF intensity contours. (c) 2D EF intensity along X- axis.

From Figure (217) show the EF contour lines on the surface of e 36 GNPs array and on the surface of the cancer cell, it is seen that there high EF intensity on the surfaces of the GNPs Also, there is an area attach to the GNPs which is the electron Cloud area (surface Plasmon area). Moreover, for clear vision we can zoom on this area and rotate the zooming image 90^{o} as shown in fig .218.

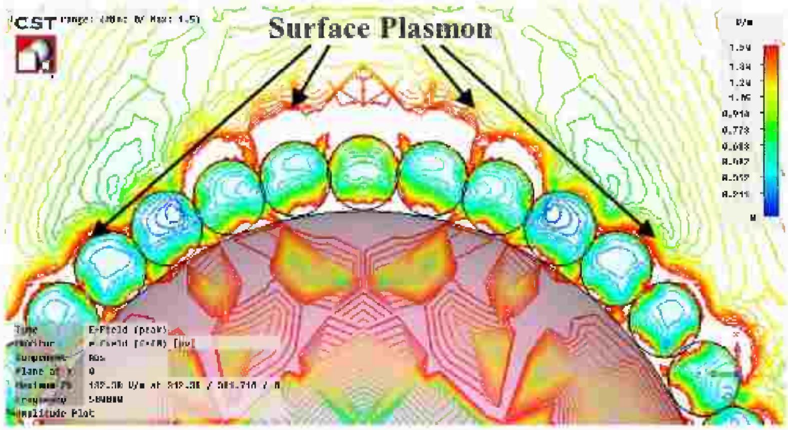

Figure (218): The electron cloud area (surface Plasmon area) on the surface of 36 GNPs (zooming on SP area of Figure (217) (b).

Figure (217) (c) shows the 2D profiles of the EF intensity distribution for the GNPs attached to the cancer cell, it noted that there is two areas of high EF intensity at 20 and -20 nm of X-axis on the edges of the GNP, on the other hand inside the NGP there is a low level of EF intensity.

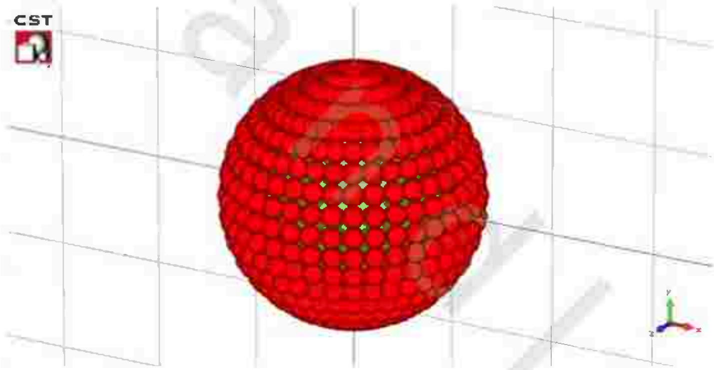

Figure (219): A 1296 Gold nanoparticles attached to the Cancer cell

Figure (219) shows the 3D profiles of the EF intensity distribution or the 1296 GNPs attached to the surface cancer cell, which are illuminated by the incident laser in order to be able of imaging small cancer cells of a 1 µm diameter.